PREPARATION AND CHARACTERIZATION OF POLY(VINYLFERROCENIUM)-SUPPORTED ELECTROCATALYSTS

POLİ(VİNİLFERROSENYUM)-DESTEKLİ ELEKTROKATALİZÖRLERİN HAZIRLANMASI VE KARAKTERİZASYONU

MUTLU SÖNMEZ ÇELEBİ

Submitted to Institute of Sciences of Hacettepe University

as a partial fulfilment to the requirements for the award of the degree of

DOCTOR OF PHILOSOPHY

in

CHEMISTRY

2008

TO MY 'HUGE' FAMILY

PREPARATION AND CHARACTERIZATION OF POLY(VINYLFERROCENIUM)-SUPPORTED ELECTROCATALYSTS

Mutlu Sönmez Çelebi

ABSTRACT

Preparation, characterization and fuel cell performances of two distinct electrocatalyst systems utilizing platinum (Pt) and palladium (Pd) particles supported on poly(viniylferrocenium) (PVF^+) redox polymer was discussed. The work had the innovation of using a redox polymer as a support material for metal particles.

Pt/PVF^+ electrocatalyst system was studied in the first part of the work. K_2PtCl_4 and H_2PtCl_6 were compared as the Pt precursors, and Pt disc electrode and glassy carbon electrode (GCE) were compared for obtaining better catalytic activity towards methanol oxidation. Physical and electrochemical characterization of the electrocatalysts indicated that, obtaining Pt particles from K_2PtCl_4 using Pt disc electrode as the electrode material gave the best results. Fuel cell performances of the Pt/PVF^+ catalysts were tested in a single fuel cell configuration in direct methanol fuel cell (DMFC) and direct hydrazine fuel cell (DHFC) modes under ambient temperature and atmospheric pressure.

Pd/PVF^+ catalysts were prepared using K_2PdCl_4 on GCE as the working electrode. Electrooxidation of hydrazine was used as the test reaction for improving the catalytic activity of the catalyst system. Fuel cell performances of the catalysts were evaluated in DMFC mode under ambient temperature and atmospheric pressure.

Keywords: Pt particles, Pd particles, poly(vinylferrocenium), methanol oxidation, hydrazine oxidation, fuel cell.

Advisor: Prof. Dr. Haluk Özyörük, Hacettepe University, Department of Chemistry, Analytical Chemistry Division

Co-advisor: Prof. Dr. Kadir Pekmez, Hacettepe University, Department of Chemistry, Analytical Chemistry Division

POLİ(VİNİLFERROSENYUM)-DESTEKLİ ELEKTROKATALİZÖRLERİN HAZIRLANMASI VE KARAKTERİZASYONU

Mutlu Sönmez Çelebi

ÖZ

Poli(vinilferrosenyum) (PVF^+) redoks polimeri desteği üzerine tutturulmuş platin (Pt) ve palladyum (Pd) taneciklerinin kullanıldığı iki ayrı elektrokatalizör sisteminin hazırlanması, karakterizasyonu ve yakıt pili performansları tartışılmıştır. Bu çalışma, redoks polimerlerinin metal tanecikleri için destek malzemesi olarak kullanılması yeniliğini getirmektedir.

Öncelikle Pt/PVF^+ elektrokatalizör sistemi çalışılmıştır. Metanol yükseltgenmesine için daha iyi katalitik aktivite elde etmek amacıyla Pt kaynağı olarak K_2PtCl_4 ve H_2PtCl_6, çalışma elektrodu olarak ise Pt disk elektrot ve camsı karbon elektrot (CKE) karşılaştırılmıştır. Pt taneciklerinin K_2PtCl_4 kullanılarak Pt disk elektrot üzerinde elde edilmesinin en iyi sonuçları verdiği, hazırlanan elektrokatalizörlerin fiziksel ve elektrokimyasal karakterizasyonu sonucunda belirlenmiştir. Pt/PVF^+ katalizörlerinin yakıt pili performansları, tek hücre konfigürasyonunda, oda sıcaklığında ve atmosfer basıncında doğrudan metanol yakıtlı yakıt pili (DMYP) ve doğrudan hidrazin yakıt pili (DHYP) şeklinde test edilmiştir.

Pd/PVF^+ katalizörleri, çalışma elektrodu olarak CKE üzerinde K_2PdCl_4 kullanılarak hazırlanmıştır. Katalizör sisteminin katalitik aktivitesinin geliştirilmesi için test reaksiyonu olarak hidrazin elektroyükseltgenmesi kullanılmıştır. Katalizörlerin yakıt pili performansları, oda sıcaklığında ve atmosfer basıncında DHYP şeklinde test edilmiştir.

Anahtar kelimeler: Pt tanecikleri, Pd tanecikleri, poli(vinilferrosenyum), methanol yükseltgenmesi, hidrazin yükseltgenmesi, yakıt pili.

Danışman: Prof. Dr. Haluk Özyörük, Hacettepe Üniversitesi, Kimya Bölümü, Analitik Kimya Anabilim Dalı

Eş-Danışman: Prof. Dr. Kadir Pekmez, Hacettepe Üniversitesi, Kimya Bölümü, Analitik Kimya Anabilim Dalı

ACKNOWLEDGEMENT

I would like to express my special thanks to:

My advisor **Prof. Dr. Haluk Özyörük,** for his invaluable contribution and care through the thesis;

My co-advisor **Prof. Dr. Kadir Pekmez,** for his invaluable guidance and help;

Prof. Dr. Attila Yıldız, for his invaluable suggestions and ideas;

My dear cousin **Res. Ass. Filiz Kuralay,** for her contribution at all levels;

Prof. Dr. Yuda Yürüm and **Dr. Ahu Gümrah Dumanlı** for their undeniable contribution in building up the thesis;

My dear friends **Ayşenur Sağlam** and **Dr. Bora Garipcan** for their help and support;

All members of **Electrochemistry Research Group** for their help;

And my dear husband **Sefa Mustafa Çelebi** and **my huge family,** for their patience, support and invaluable contribution during my whole academic life.

TABLE OF CONTENTS

LIST OF FIGURES

LIST OF SCHEMES

1. INTRODUCTION

Metal nanoparticles have interesting and unique properties compared to the larger corresponding metal particles. Metal particles with nano and uniform sizes have many applications in optics, electronics, magnetic devices and as catalysts, photocatalysts, adsorbents and sensors (Adlim et al., 2004). Generally, the small particle size and high dispersion of metal particles will result in high electrocatalytic activity. However, there exist two factors influencing application of the metal particles, namely stability and reactivity (Guo and Li, 2005). Metal nanoparticles supported on functional polymers have many advantages such as generation of metal nanoparticles with a controlled size and size distribution and influencing the chemical behavior of the metal nanoparticles via interaction with the polymer-bound functional groups (Kralik and Biffis, 2001).

Various metals have been introduced into a conductive polymer matrix by electrochemical deposition methods for applications in catalysis (Gautron et al., 2003). Redox polymers are types of conducting polymers which are characterized by the presence of specific spatially and electrostatically isolated electrochemically active sites. However, use of redox polymers as support materials for metal particles has not been reported recently.

Methanol is one of the most widely studied organic molecules owing to its potential use as an alternative fuel in the near future. The electrooxidation of methanol is a very complex reaction, during which many intermediate and poisoning species are involved. In an acidic medium, the most efficient catalyst for this reaction is platinum (Pt) and its alloys. The electrocatalytic activity of the Pt particles for methanol oxidation is dependent on many factors. Among these, the supporting materials and their surface condition are essential for the Pt catalyst to produce high catalytic activity (Guo and Li, 2004).

Hydrazine is an important high-performance fuel in energy storage and conversion which finds widespread usage in rocket fuels, missile systems, weapons of mass destruction and fuel cells (Nassef et al., 2006; Rao and Trivedi, 2006). Hydrazine is found to be electrocatalytically oxidized on palladium (Pd) based catalysts. Various methods can be used for deposition of Pd nanoparticles (Guo and Li, 2005). Highly dispersed Pd particles formed by electrochemical deposition

constitute a very important state of a noble metal catalyst for heterogeneous catalysis and electrocatalysis (Li et al., 1997).

Because of their high fuel efficiency, fuel cells are considered as the most promising power sources of the next generation, which will replace the internal combustion engine. Direct fuel cell systems, where fuel is directly supplied to the fuel cell without reforming to hydrogen also have great benefits for vehicles and mobile electric appliances (Yamada et al., 2003). Fuel cell technology is becoming applicable for a large variety of technical areas. Currently, some types of fuel cells including direct methanol fuel cells (DMFCs) and direct hydrazine fuel cells (DHFCs) approach commercial feasibility (Wasmus and Küver, 1999).

The DMFC has attracted much attention because of its use of liquid methanol fuel, which is easy to deliver and store. More importantly, liquid fuel can be used at ambient temperature and pressure, which makes the DMFC easy to use with portable electronic devices (Yang et al., 2008).

Since hydrazine is composed of only hydrogen and nitrogen, the anode reaction in a DHFC produces, theoretically, only nitrogen. Therefore, perfect zero emission equal to a pure hydrogen fuel can be realized. Since DHFC does not produce CO-like poisoning species in the direct electrooxidation process, the catalyst poisoning is low in the cell (Yamada et al., 2003).

Preparation, characterization and fuel cell performances of two distinct electrocatalyst systems utilizing Pt and Pd particles supported on poly(vinylferrocenium) (PVF^+), a redox polymer system, was discussed in the present work. In the first part, preparation of Pt/PVF^+ electrocatalyst system was described. Two Pt precursors (K_2PtCl_4 and H_2PtCl_6) and two electrode materials (Pt disc and glassy carbon electrode, GCE) were used in the experiments. Preparation of the catalysts was carried out in two steps:

1. incorporation of Pt complexes into the PVF^+ support,
2. chemical and electrochemical reduction of Pt particles in the polymer matrix.

Electrooxidation of methanol was used as the test reaction for evaluating the catalytic activity of the Pt/PVF^+ system. During preparation of the catalysts, each experimental parameter was optimized according to the oxidation peak current values recorded with 0.5 M CH_3OH solution containing 0.5 M H_2SO_4 as the supporting electrolyte. Physical characterization of the catalysts was carried out using scanning electron microscopy (SEM) and energy dispersive X-ray spectroscopy (EDS) methods; electrochemical characterization was achieved by cyclic voltammetry. Fuel cell performances of Pt/PVF^+ catalysts were tested using a home made single cell in DMFC and DHFC modes.

In the second part of the work, Pd/PVF^+ electrocatalyst was developed on GCE. Pd particles were obtained by one-step deposition of Pd particles into the PVF^+ support. The system showed catalytic activity towards hydrazine oxidation. Optimization of experimental parameters was achieved using oxidation peak current values recorded with 10 mM $N_2H_4{\cdot}H_2SO_4$ containing 0.1 M K_2SO_4. Pd/PVF^+ catalysts were physically characterized by SEM. Finally, fuel cell performance of the system was tested in DHFC mode.

2. REDOX POLYMERS

Redox polymers are types of conducting polymers which are characterized by the presence of specific spatially and electrostatically isolated electrochemically active sites (Yu et al, 2005). Electroactivity in the redox polymer is highly localized, while the electrochemical processes in conjugated polymers lead to a reorganization of the bonds in the molecule itself. Typically, a redox polymer consists of a system where a redox-active transition metal based pendant group is covalently bound to some sort of polymer backbone which may or may not be electroactive (although for synthetic convenience the backbone is frequently formed by the electropolymerization of suitable monomer complexes). A few representative examples are shown in Figure 2.1.

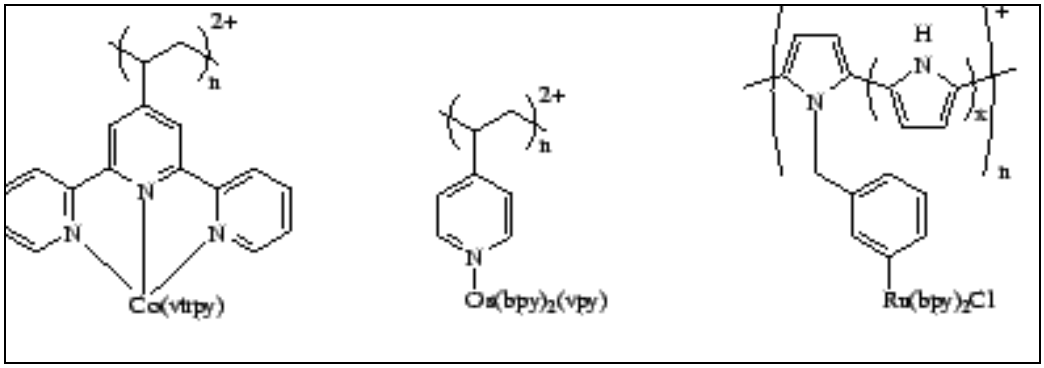

Figure 2.1. Three typical redox polymers

The widespread interest in these polymers has been spurred by their applicability in the area of chemically modified electrodes (Murray, 1984; Abruna, 1988). One goal of coating electrodes with electroactive polymers is the development of new materials with very active catalytic properties. The bulk of the work has been with systems where the polymer itself is inert and serves only as a support for the electrocatalytic metal sites. The electrocatalyst site functions as a mediator, facilitating the transfer of electrons between the electrode and the substrate. Electrocatalysis in general is of great economic importance and the aim of these modified electrodes is to drive electrochemical reactions selectively and/or at modest potentials, and with better control than could be possible by the direct interaction between the substrate and the electrode.

Embedding electrocatalytic transition metal species in a polymer modified electrode matrix is a means to endow the electrode with the chemical, electrochemical, optical, and other properties of the immobilized molecule (Murray, 1984). A number of additional advantages include:

- Control of the reaction rate by the applied potential or current
- Close proximity of electrocatalytic sites to the electrode
- High concentration of active centres despite low amount of material required
- Cooperative effects stemming from the proximity of other catalyst sites
- Easy removal of the catalyst from the substrate.

Unlike the electronically conducting polymers, redox polymers characteristically exhibit conductivity only over a very narrow potential range, with maximum conductivity occurring when the concentrations of the oxidized and reduced forms are equal in the film, *i.e.,* at the formal potential of the redox centers. This leads to a voltammetric profile such as the one shown in Figure 2.2, with the characteristics of a surface bound redox system (or finite linear diffusion).

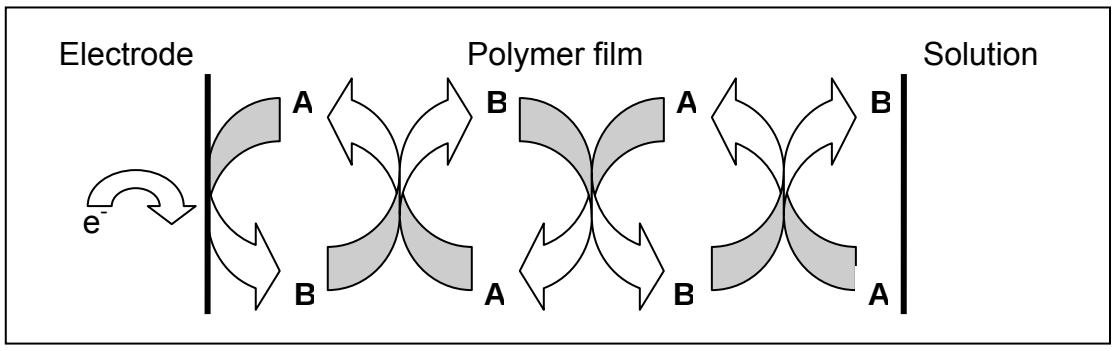

Figure 2.2. Charge propagation by means of quasi-diffusional charge percolation in a redox polymer.

The details of charge transport between the electrode and the supported redox sites are a fundamental consideration. It is commonly held that redox conduction in polymers occurs by the electron hopping process proposed by Kaufman and coworkers (Kaufman and Engler, 1979) whereby electron transfer proceeds as a process of sequential self-exchange steps between adjacent redox groups. The

rate of self exchange R_{SE} and electron transfer processes are connected by the simple relationship:

$$R_{SE} = k_{ET} C_{ox} C_{red}.$$

In the polymer film where the total amount of redox species must be fixed (*i.e.,* $C_{ox} + C_{red} = C_{tot}$) the self-exchange rate will reach a maximum when the concentration of both species is equal, *i.e.,* $C_{ox} = C_{red}$.

Since electroneutrality in the film must be maintained, the generation of charge at the electrode and the motion of the charge throughout the polymer must be accompanied by the ingress and motion of counterions. This is an important consideration since electroactive polymers are really mixed conductors, displaying both electronic and ionic conductivity. Often the ionic contribution may be safely disregarded, in which case the charge transport diffusion may be ascribed entirely to electron diffusion. However this is not always the case and electron hopping rates can be strongly influenced by the nature of the counter ion (Ren and Pickup, 1994). Full characterization should consider both electronic and ionic conductivities of the material.

2.1. Poly(vinylferrocene) (PVF)

Poly(vinylferrocene) (PVF), is a redox polymer, which has long been used as a fundamental conducting polymer system, with the advantages of simple electrochemistry (a reversible one-electron process), high stability (allowing multiple measurements to be made over extended time scale), and the ease of deposition of thin films using a variety of methods (Yu et al, 2005). Chemical structure of neutral form of PVF is presented in Figure 2.3.

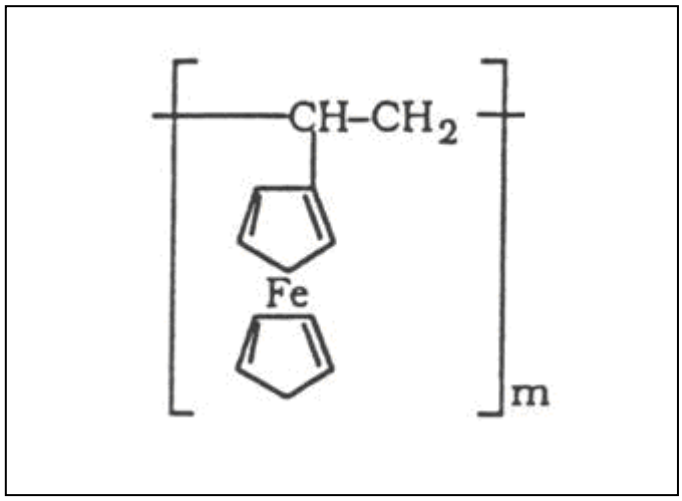

Figure 2.3. Structure of neutral PVF.

Various methods can be used to prepare PVF-coated electrodes (Arrigan, 1994):

Dip coating

The bare electrode is held in a solution of the polymer, which is deposited via an adsorption process.

Droplet evaporation

A small volume (usually a few microliters) of polymer solution is placed on the electrode surface and the solvent is allowed to evaporate. The polymer is confined to the electrode by using it in an electrolyte/solvent in which the polymer is insoluble.

Spin coating

The electrode is set spinning after a drop of the polymer solution is placed on the surface; the result is an even layer of polymer on a surface free of pinholes.

Oxidative deposition

This type of deposition relies on the dependence of polymer solubility on ionic state. PVF oxidizes from methylene chloride to give the less soluble ferrocenium form of the polymer (PVF^+), which precipitates onto the electrode surface to give a PVF^+ modified electrode. It has been stated that the electrodeposited polymer contains both ferrocene (PVF) and ferrocenium (PVF^+) forms of the polymer (Shirota et al., 1984). Structure of electrochemically doped PVF is given in Figure 2.4.

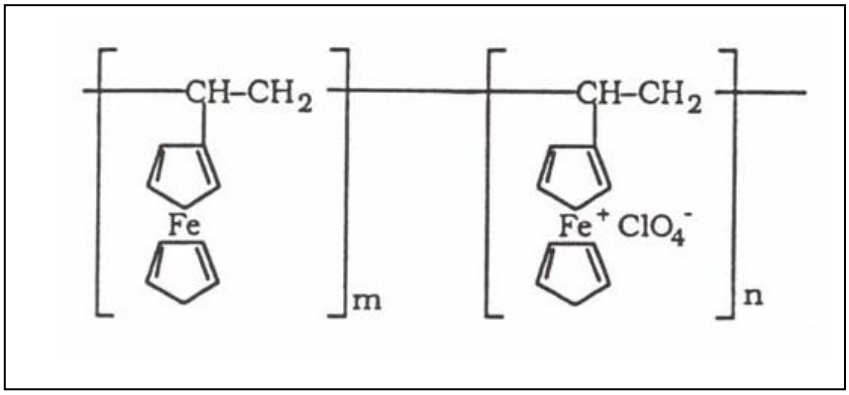

Figure 2.4. Electrochemically doped PVF.

Recently, PVF modified electrodes have been extensively studied in various areas such as electrochemical oxidation and reduction (Gülce et al., 1994), electroanalysis and electrocatalysis (Gülce et al., 1995; Gülce et al., 1997; Kuralay et al., 2007; Sönmez, 2002), and biosensors (Gülce et al., 1995; Gündoğan-Paul et al., 2002; Aydın et al., 2002; Kuralay et al., 2005, Kuralay et al.; 2006; Özer et al., 2007).

3. CATALYSIS BY METAL NANOPARTICLES

Metal nanoparticles are objects of great interest in modern chemistry and materials research, where they find application in such diverse fields as photochemistry, nanoelectronics, optics, and catalysis (Kralik and Biffis, 2001). These particles often possess physical as well as chemical properties, which are distinct both from the bulk phase and from isolated atoms and molecules. Moreover, such unique features of metal nanoparticles appear to be significantly influenced by parameters such as the metal nanoparticle size, the organization of the nanoparticle crystal lattice (i.e. the nature and amount of defects) and the chemical nature of the microenvironment surrounding the nanoparticle. Thus, there is a large potential for the development and application of metal nanoparticles with tailored physical and chemical properties in both catalysis and material science.

Metal nanoparticles supported on functional materials have many advantages over unsupported nanoparticles. In connection with metal nanoparticles as the catalytically active moieties, the use of functional polymers offers some features, namely:

- it allows the generation of metal nanoparticles with a controlled size and size distribution;
- it provides a mean to influence the chemical behavior of the metal nanoparticles through the direct interaction of the metal surface with the polymer-bound functional groups.

The preparation of polymer-supported metal nanoparticles can be carried out along different routes, which are briefly outlined in Scheme 3.1.

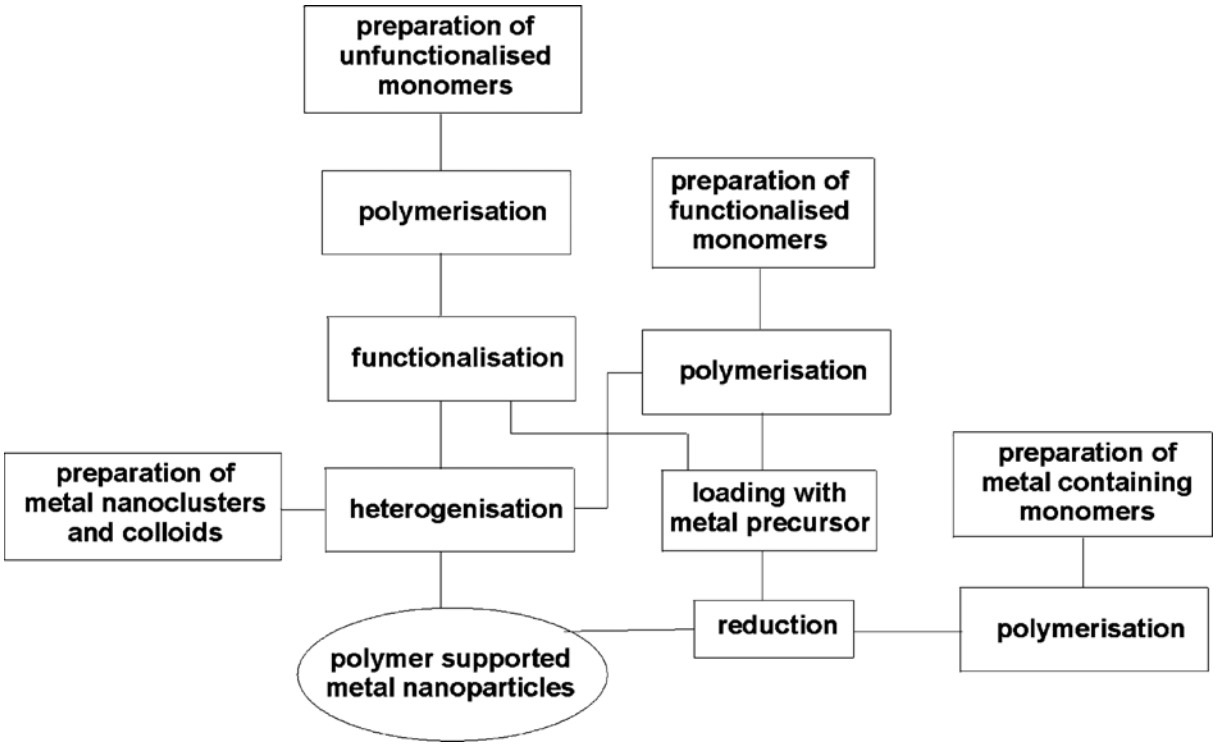

Scheme 3.1. Routes for the preparation of metal nanoparticles supported on functional polymers.

Basically, synthesis of polymer-supported nanoparticles involves three steps:

1. synthesis of a suitably functionalized polymer,
2. loading of the polymer with convenient metal nanoparticle precursor,
3. generation within the polymer of the metal nanoparticles.

The first two steps can be condensed in one upon utilization of metal-containing monomers in the polymer synthesis. Furthermore, the third step can be omitted by directly loading the polymer support with pre-formed metal nanoparticles.

The choice of the nature and amount of functional groups to be built in the polymer is made on the basis of the role that they have to play. Their primary function is to bind metal ions or complexes, which are the most common precursors of the metal nanoparticles. Therefore, the kind of functionality which is most usually built in the polymer support is either an ionic moiety (anionic, e.g. sulphonate or carboxylate or cationic, e.g. tatraalkylammonium) whose counter-ion can be readily exchanged, or a group able to co-ordinate to metal centers (e.g. amino or phosphino). Additionally, since the functional groups determine the compatibility of

the polymer support with different reagents and solvents (a parameter of chief importance for catalyst performance, they have to be chosen according to the requirements of the particular reaction under study. Finally, the functional groups can be also selected in order to influence the catalytic performance of the embedded metal nanoparticles by directly interacting with the metal surface.

For electrochemical deposition of metal particles into polymer supports, several methods have been reported, such as constant potential, double potential step, cyclic potential mode and constant current (Niu et al., 2005).

The final step in the preparation of polymer supported metal nanoparticles is the generation of the metal nanoparticles within the polymer, which is usually accomplished by reduction of the polymer-bound metal precursors. The most frequently employed reducing agents are hydrogen, sodium borohydride, hydrazine, alcohols and formaldehyde. The nanoscale-size controlled generation of metal particles is a challenge to formulation of metal colloid particles, which requires more sophisticated metal precursors, colloid stabilizers and preparation protocols.

The size and size distribution of metal nanoparticles throughout the particles of the support can also depend on other parameters such as the nature and concentration of the reducing agent, the reduction procedure and the metal precursor. Recently, increasing homogeneity of the metal distribution was observed with decreasing metal concentration and increasing concentration of the reductant (Kralik and Biffis, 2001).

A special situation may occur when the polymer-bound metal moiety is difficult to reduce. For example, this is the case of anionic chlorocomplexes present inside a cationic resin. Their reduction requires ligand dissociation in a neutral or basic environment followed by reduction of the metal ion. The reduction can be performed with the following reducing agents:

Hydrazine

$$PdCl_4^{2-} + N_2H_4 + 2\,OH^- \rightarrow Pd + N_2 + 4\,Cl^- + 2\,H_2O \qquad (3.1)$$

Sodium borohydride

$$PdCl_4^{2-} + NaBH_4 \rightarrow Pd + BH_3 + 4\,Cl^- + Na^+ + H^+ \qquad (3.2)$$

Formaldehyde in the presence of carbonates

$$2\,PdCl_4^{2-} + 2\,HCOH + 3\,CO_3^{2-} \rightarrow$$

$$2\,Pd + 3\,CO_2 + 2\,HCOO^- + H_2O + 8\,Cl^- \qquad (3.3)$$

Use of a more strongly basic environment provided by hydroxides or carbonates also enables to use dihydrogen as a reducing agent:

$$PdCl_4^{2-} + H_2 + CO_3^{2-} \rightarrow Pd + CO_2 + H_2O + 4\,Cl^- \qquad (3.4)$$

Characterization of metal catalysts supported on functional polymers can be accomplished by using numerous different techniques. Basically, the properties which need to be evaluated can be divided into two groups:

(i) properties of the support, such as its grain size, morphology, porosity, chemical composition, kind and degree of functionalisation, degree of hydrophilicity/hydrophobicity, etc;

(ii) properties of the supported metal particles, such as their size and size distribution, degree of crystallinity, presence of defects, distribution throughout the support grains, etc.

All these properties may more or less contribute to the overall catalytic activity of the supported catalyst.

Many different methods can be employed for the physical characterization of metal particles supported on functional polymers including scanning electron microscopy (SEM), transmission electron microscopy (TEM), scanning tunneling microscopy (STM), UV-Visible spectroscopy (UV-VIS), infrared spectroscopy (IR), X-Ray diffraction spectroscopy (XRD), X-ray photoelectron spectroscopy (XPS), energy dispersive X-ray spectroscopy (EDS) and nuclear magnetic resonance spectroscopy (NMR) methods.

Cyclic voltammetry can be used for electrochemical characterization of Pt nanoparticles. For this purpose, cyclic voltammogram (CV) of aqueous solution of H_2SO_4 is recorded with the catalyst. The oxidation and reduction peaks observed between 0.00 V and -0.25 V vs. SCE which belong to adsorption and desorption of hydrogen are compared for different catalysts (Figure 3.1). The areas under the hydrogen adsorption/desorption regions are known to be related to both the amount of catalyst applied to the electrode and the catalyst loading on the support (Perez et al, 1998; Shan and Pickup, 2000; Pozio et al., 2002; Ioroi et al., 2002; Chang et al., 2007).

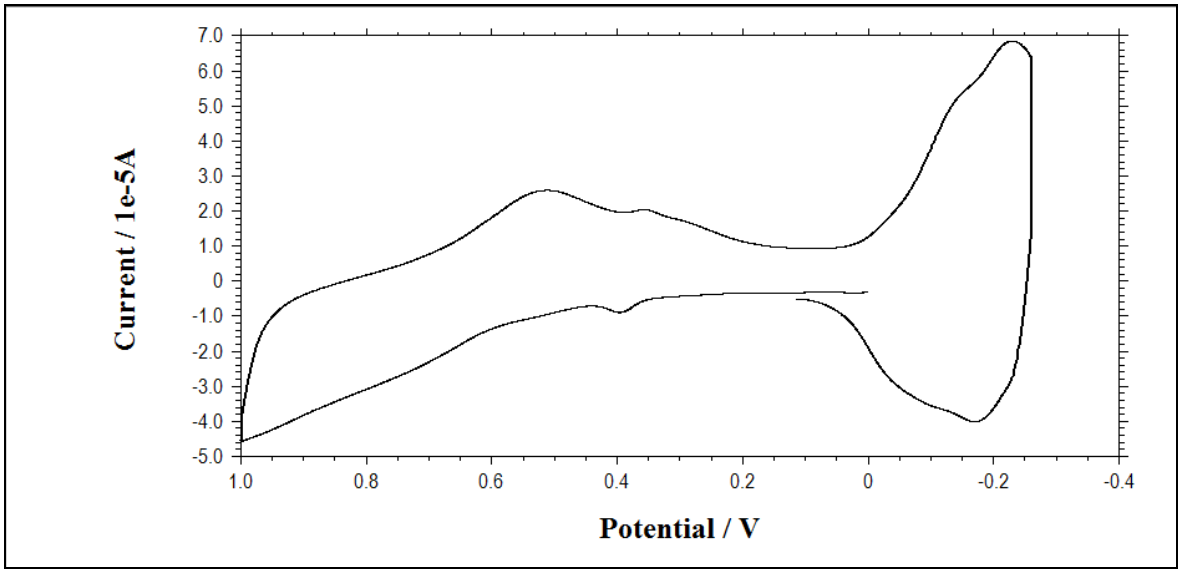

Figure 3.1. CV of 0.5 M H_2SO_4 recorded with Pt/PVF^+ electrocatalyst system.

Numerous studies exist in the literature about metal particles supported on functional polymers for various catalytic reactions. Among these, Pt particles are one of the most widely studied ones. Perez et al. studied electrocatalytic reduction of oxygen on carbon thin porous coating rotating Pt electrodes. Cyclic voltammetry, steady state polarization and impedance spectroscopy techniques were used for characterization of the catalyst. It was reported by the authors that, the mass activity and the specific activity for oxygen reduction was dependent on Pt particle size (Perez et al., 1998).

Surfactant stabilized Pt and Pt alloy electrocatalyst was used for polymer electrolyte fuel cells by Wang and Hsing. Chemical, morphological and crystallographic properties of the electrocatalysts were characterized using surface techniques including XRD, TEM and XPS. It was reported that mono-size, well-dispersed metal colloids could be formed and successfully supported on the carbon black. Moreover, the size of metallic colloids could be manipulated by controlling the synthesis temperature and was independent of the catalyst loading. Electrochemical characterizations showed that in comparison with commercial E-TEK electrocatalysts, surfactant-based Pt/C electrocatalysts possessed similar catalytic activity in terms of oxygen reduction. Also, higher CO tolerance performance could be obtained by the surfactant stabilized Pt,Ru/C electrocatalyst (Wang and Hsing, 2002).

Ioroi and coworkers prepared carbon-supported Pt and molybdenum oxide (Pt/MoO_x) catalysts for use in polymer electrolyte fuel cell (PEFC) anodes and examined their catalytic activity for the oxidation of CO-contaminated H_2 based on the fuel cell performance in PEFC single cell arrangements. Based on the XRDpattern and XPS measurements, of the prepared $Pt/MoO_x/C$ catalysts, it was found that the deposited MoO_x existed as an amorphous oxide phase. This study showed that the addition of MoO_x to Pt/C yielded a desirable improvement of CO-tolerance for the PEFC anode. It was also reported by the authors that the catalyst system was almost comparable to the PtRu(1:1)/C catalyst (Ioroi et al., 2002).

Synthesis and catalytic activity of the transition metal complex catalysts supported on the branched functionalized polysiloxanes grafted on silica was studied. Rh and Pt complex catalysts were immobilized on vinyl-functionalized polysiloxanes having different degree of branching. The attachment of the metal species to the polymer was confirmed by IR and ^1H NMR spectroscopy. The catalytic activity of the complex catalysts was studied in hydrosilylation reaction. Both the Pt and Rh supported systems exhibited good hydroslylation efficiency. The results showed that the catalyst activity depended on the type of the catalyst precursor, the branching degree of polymer support and the content of vinyl ligands (Michalska et al., 2004).

Supported Pt and Pt-Ru nanoparticles were studied as electrocatalysts for low-temperature fuel cells. The support material was high surface area carbon (Vulcan XC-72). The supported Pt and Pt-Ru catalysts were prepared by chemical reduction with formic acid by adding the precursors of the metals (H_2PtCl_6 and $RuCl_3$) to the carbon support impregnated in the formic acid solution at 80 ^oC. Physical characterization of the catalysts was done by XRD and TEM analyses. The catalysts were also electrochemically characterized using cyclic voltammetry. Catalytic activity towards CO and methanol oxidation reactions were achieved with the catalysts (Lizcano-Valbuena et al., 2004).

In another work carried out by Tang et al., size-controlled colloidal Pt nanoparticles were synthesized and their activity for the electrocatalytic oxidation of CO was evaluated. Polyvinylpyrolidone was used as the stabilizing agent and glassy carbon was the support material. H_2PtCl_6 was used as the Pt precursor by reducing with hydrogen. TEM and UV-VIS methods were used for the physical characterization and CV method was used for the electrochemical characterization of the catalysts. The effect of Pt particle size of Pt/GC catalyst electrode on the electrocatalytic oxidation of CO has been investigated. It was recorded that a higher potential was needed for the oxidation of absorbed CO with a decrease of the Pt particle size for particles larger than 1 nm. For particle sizes smaller than 1 nm, the potential remained constant while the activity decreased with decreasing the size (Tang et al., 2005).

Saha and coworkers used multiwalled carbon nanotubes (CNTs) as the support material for obtaining high loading and monodispersed Pt nanoparticles. Composite electrodes consisting of Pt nanoparticles-supported on multiwalled CNTs were grown directly on carbon paper (Pt/CNTs/carbon paper). TEM, XPS and cyclic voltammetry methods were used for the physical and electrochemical characterization of the catalysts. The Pt/CNT/carbon paper composite electrodes were compared with standard Pt/C electrode and were found to exhibit higher electrocatalytic activity for methanol oxidation reaction and higher single cell performance in a H_2/O_2 fuel cell (Saha et al., 2008).

Pt-Pd particles were prepared in a water-in-oil microemulsion of water/polyethyleneglyycol-dodecylether/*n*-heptane by Solla-Gullon et al. the bimetallic nanoparticles were obtained by reduction of H_2PtCl_6 and K_2PdCl_4 with hydrazine. XPS, AAS, UV-VIS and CV were used for characterization of the nanoparticles. CO adsorption-oxidation and dissociative adsorption of formic acid and methanol were used as test reactions to check the electrocatalytic behavior of the bimetallic nanoparticles. The electrochemical adsorption behavior and electrocatalytic properties of the particles were under the control of their composition and of their size (Solla-Gullon et al., 2003).

Synthesis of chitosan-stabilized Pt and Pd nanoparticles (chi-Pt and chi-Pd) were studied by Adlim and coworkers. The finest and well-dispersed particles of chi-Pt and chi-Pd were obtained when methanol or $NaBH_4$ were used as the reducing agents. Physical characterization of the catalysts was done using UV-VIS and TEM methods. Catalytic activity of the Pt and Pd catalysts were tested with hydrogenation of cyclooctane and octane. The catalytic activity of chi-Pt was higher than chi-Pd for both the hydrogenations (Adlim et al., 2004).

Hasik et al. prepared polyaniline (PANI)-supported Pd catalysts. Pd metal was incorporated into PANI in the polyemeraldine base form via its treatment with $PdCl_2$ aqueous solutions containing various amounts of HCl. Fourier transform IR, Raman, electron spectroscopy for chemical analysis (ESCA) and UV-VIS methods were used for the characterization of the catalyst. PANI was doped in all the cases, but the oxidation level of Pd introduced into the polymer matrix depended upon the acidity of the $PdCl_2$ solution. After the reaction in highly acidic solutions Pd^{2+} was exclusively present in the matrix, whereas upon PANI contact with the solutions of low acidity, partial reduction of Pd^{2+} to Pd^0 with simultaneous oxidation of the polymer took place. PANI-Pd systems were active in the catalytic hydrogenation of 2-ethylanthraquinone and their activity depended on preparation conditions (Hasik et al., 1997).

Polypyrrole (PPy) was also used as a support material for the preparation of Cu and Pd particles, for application in heterogeneous catalysis. Catalysts were characterized by TEM coupled with EDS and XRD. Their activity and selectivity were determined in the reduction of nitrate and intermediate nitrite in water. In nitrite reduction, the catalysts demonstrated a better activity and a higher selectivity towards nitrogen formation than their Pd/Al_2O_3 counterpart. On the other hand, the bimetallic catalyst tested for nitrate reduction showed an activity similar to the one of a classical $Pd\text{-}Cu/Al_2O_3$ catalyst, but no intermediate nitrite was observed (Gautron et al., 2003).

A similar study was carried out by Hasik et al. in order to synthesize PPy-Pd systems prepared in $PdCl_2$ aqueous solutions. PPy-Pd systems were prepared by stirring the polymer powder at room temperature in the $PdCl_2$ aqueous solutions containing HCl and/or KCl for 72 h. Characterization of the catalysts were carried out using UV-VIS, elemental analysis, XPS, FTIR, XRD and SEM methods. It has been found that different chemical reactions took place in various $PdCl_2$ solutions depending on the acidity of the medium (Hasik et al., 2003).

In another work carried out by Aoki and coworkers, Pd spherical particles 0.23 μm in diameter were synthesized by reducing palladium acetate with hydrazine in the presence of surfactant. UV-VIS and SEM methods were used for the characterization of Pd particles. The colloidal suspension of the particles was found to be electrochemically active, exhibiting the oxidation wave of Pd metal and the reduction wave of palladium acetate. The particles worked as a catalyst for the reduction of methylene blue by hydrazine. The rate constant was the first order, and was proportional to the surface area of the Pd particles, as predicted for a surface catalytic reaction (Aokoi et al., 2007).

3.1. Electrocatalytic Oxidation of Methanol

From the different small organic molecules, methanol is the one being most intensively investigated at present, because, it is expected that the traditional systems for energy generation would be replaced by fuel cells in a medium long term. DMFCs are one of the most developed fuel cells using methanol directly as combustible (Iwasita, 2002; Calvillo et al., 2007).

The thermodynamic potential for methanol oxidation to CO_2, lies very close to the equilibrium potential of hydrogen:

$$CH_3OH + H_2O \rightarrow CO_2 + 6\,H^+ + 6\,e^- \qquad E^0 = 0.02\ V \qquad (3.5)$$

However, compared with hydrogen oxidation, this reaction is by several orders of magnitude slower.

The basic mechanism for methanol oxidation can be summarized in terms of two basic functionalities (Hamnett, 1997):

(a) electrosorption of methanol onto the substrate,
(b) addition of oxygen to adsorbed carbon-containing intermediates to generate CO_2.

The total oxidation process, in principle, can be formulated as follows:

$$CH_3OH \rightarrow \text{(adsopbed intermediates)} \begin{cases} \nearrow\ CO_{ad} \rightarrow CO_2 \\ \searrow\ HCHO, HCOOH \rightarrow CO_2 \end{cases}$$

Very few electrode materials are capable of adsorption of methanol; in acid solution only Pt and Pt-based catalysts have been found both to show sensible activity and stability, and almost all mechanistic studies have concentrated on these materials.

On a pure Pt electrode, complete oxidation of methanol takes place via two processes occurring in separate potential regions:

- The first process, involving adsorption of methanol molecules, requires several neighboring places at the surface. Since methanol is not able to displace adsorbed H atoms, adsorption can only begin at potentials where enough Pt sites become free from H, i.e. near 0.2 V vs. reversible hydrogen electrode (RHE) for a polycrystalline Pt electrode.
- The second process requires dissociation of water, which is the oxygen donor of the reaction. On pure Pt electrode, a strong interaction of water with the catalyst surface is only possible at potentials above 0.40 V-0.45 V vs. RHE.

Thus, on a pure Pt catalyst, methanol oxidation to CO_2 cannot begin below 0.45 V. However, the adsorbate layer does not exhibit a good reactivity below approximately 0.70 V vs. RHE, i.e. a high rate of oxidation at pure Pt occurs at potentials without technological interest.

To solve the problems associated with the use of pure Pt catalysts for methanol oxidation, incorporation of Pt particles into suitable support materials such as conducting polymers, which exhibit enhanced electrocatalytic activities has been widely studied (Niu et al., 2005). The increase in the catalytic activity may be due to the decrease in the poisoning effect, which is caused by highly dispersed metal particles and the synergistic effects of conducting polymer and metal particles.

Binary and ternary catalysts were also proposed for methanol oxidation, most of them based in modifications of Pt with some other metal. This metal must fulfil the requirement of forming O-containing surface species at low potentials. There are, of course, several practical factors limiting the choice of the metal. Many O-adsorbing metals can produce negative effects, e.g. inhibit methanol adsorption or may be not sufficiently stable for long-term use, as required for a fuel cell. At present, there is a general consensus that PtRu offers the most promising results (Iwasita, 2002).

Methanol oxidation on supported Pt catalysts has been the matter of a number of papers. Effect of Pt deposition modes on electrocatalytic behavior of Pt-modified polyaniline electrode for methanol oxidation was studied by Niu and coworkers. Electrodeposition methods including constant potential, cyclic potential and double potential step, have been applied to characterize the performance of different electrodeposition modes. Variables related to reaction kinetics, such as mass transport of species, concentration of methanol and acidity of solution, were investigated and reaction mechanism was discussed. SEM method was used for examining the polyaniline films. The electrocatalytic activity of the catalyst was related to the distribution and state of Pt particles incorporated in polyaniline film matrix and the synergistic effects between the dispersed Pt particles and the polyaniline film. The authors reported that methanol adsorption would mainly control the rate of the overall oxidation reaction, and the reaction was determined as first-order with respect to methanol (Niu et al., 2005).

Effect of deposition potential and temperature on electrooxidation of methanol on Pt doped polyaniline (PANI) electrodes was studies by Fıçıcıoğlu and Kadırgan. Pt was deposited onto the PANI films from H_2PtCl_6 in H_2SO_4 at constant potentials. The amount of deposited Pt was evaluated from the cathodic charge consumed during electrodeposition, assuming that Pt^{4+} to Pt^0 reduction was 100% efficient. Activation energy values were determined by studying the oxidation of methanol between 20 ^oC and 45 ^oC and compared with similar studies. It was also reported that the electrochemical deposition potential offered a control over the properties of crystalline structure and grain morphology of the Pt on the surface (Fıçıcıoğlu and Kadırgan, 1997).

High dispersion and electrocatalytic properties of Pt nanoparticles on single-walled carbon nanotube (SWNT) bundles were studied by Guo and Li. Pt nanoparticles were electrochemically dispersed on SWNT bundles by electroreduction of the Pt(IV) complex formed on the SWNT surface. The structure and elemental composition of the resulting Pt/SWNT composite were characterized by TEM, XRD and EDS methods. The electrocatalytic properties of the Pt/SWNT electrode for methanol oxidation have been investigated by CV. The authors reported a high electrocatalytic activity and excellent stability of the electrode which was attributed

to the high dispersion of Pt nanoparticles and the particular properties of the SWNT suppots (Guo and Li, 2004).

In another study carried out by Chang et al., Pt nano-cluster thin film (PtNCF) was formed on glassy carbon and applied for methanol oxidation. Through the reduction of $PtCl_4^{2-}$ by ascorbic acid in the presence of glassy carbon (GC) substrate, a Pt thin continuous film composed of small nano-clusters which had a further agglomerated nanostructure of small grains could be attached on the GC surface. The electrocatalytic performance of PtNCF per Pt amount was superior to that of Pt black on GC. The authors also reported that, in spite of the continuous nanostructures, nano-grains of PtNCF worked efficiently for methanol oxidation reaction (Chang et al., 2007).

Calvillo and coworkers used Pt supported on functionalized ordered mesoporous carbon (OMC) as electrocatalyst for DMFCs. The electrocatalysts were prepared by reduction of H_2PtCl_6 with $NaBH_4$. The same procedure was also employed with commercial carbon (Vulcan XC-72) as support for comparison. Physical and electrochemical characterization of the catalyst was accomplished by TEM and XRD and cyclic voltammetry methods. It was reported that, Pt supported materials were well dispersed over the OMC support and its catalytic performance towards methanol oxidation improved when compared with Vulcan XC-72 (Calvillo et al., 2007).

Nano-composites comprised of PtRu alloy nanoparticles and an electronically conducting polymer for the anode electrode in DMFC were prepared by Choi et al. two conducting polymers of poly(N-vinyl carbazole) and poly(9-(4-vinyl-phenyl)carbazole) were used for the nano-composite electrodes. Structural analyses were carried out using FT-NMR, AC Impedance, XRD, TEM and SEM methods. Electrocatalytic activities were investigated by voltammetry and chronoamperometry in a 2 M CH_3OH/0.5 M H_2SO_4 solution and the data were compared with a carbon supported PtRu electrode. Electrochemical measurements and DMFC-unit cell tests indicated that the nano-composites could be useful in a DMFC, but its performance would be slightly lower than that of a carbon-supported electrode (Choi et al., 2003).

3.2. Electrocatalytic Oxidation of Hydrazine

Hydrazine finds widespread usage in rocket fuels, missile systems, weapons of mass destruction and fuel cells. In industrial applications, is also used as catalyst, emulsifier, corrosion inhibitor and reducing agent. It is also used as an oxygen scavenger in industry and has found wide application as an antioxidant, photographic developer and an insecticide (Nassef et al., 2006). Having a high theoretical electromotive force (1.56V); electrooxidation of hydrazine gains attraction for use as a high-performance fuel in energy storage and conversion. Another advantage of using hydrazine as a fuel is that, since hydrazine is composed of only hydrogen and nitrogen, DHFCs do not exhaust environmentally loading materials such as CO_2 (Yamada et al., 2003).

It is known that, hydrazine can be efficiently electrooxidized on supported Pd particles. Li et al. developed a method of electrodepositing highly dispersed nano Pd particles on GCE. K_2PdCl_4 was used as the Pd precursor and Pd complexes formed on the GCE surface were reduced to Pd^0 by electrochemical potential scanning. STM and XPS methods were used for the characterization of the catalysts. The Pd particles obtained were in nanometer scale and repotted to exhibit high catalytic activity towards hydrazine oxidation (Li et al., 1997).

Li et al also studied nanometer-size Pd particles supported on highly orientated pyroytic graphite (HOPG) using in situ STM method. XPS and CV methods were also used for the characterization of the supported Pd particles. Pd particles were electroreduced from the surface complexes of Pd(IV) which were obtained from K_2PdCl_4. Pd particles deposited on the HOPG support were highly disperse and in the nanometer range of size. According to the experimental results, the particles obtained in this way exhibited a high electrocatalytic activity towards the electrooxidation of hydrazine and hydroxylamine (Li et al, 1997).

Guo and Li studied electrochemical synthesis of Pd nanoparticles on functional multi-walled carbon nanotube (MWNT) surfaces. Pd nanoparticles were electrocrystallized on 4-aminobenzene monolayer-grafted MWNTs by a potential-step method. The structure and nature of the resulting Pd/MWNT composite were characterized by TEM and XRD. The results showed that the electrochemically synthesized Pd nanoparticles were homogenously dispersed and well separated

from one another on the modified MWNT surfaces. The mean diameter of Pd nanoparticles were about 1-3 nm. The electrocatalytic properties of the Pd/MWNT electrode for oxidation of hydrazine were investigated by CV and excellent electrocatalytic activity was reported. This was attributed to the small particle size and high dispersion of Pd particles (Guo and Li, 2004).

Guo and Li also studied high dispersion and electrocatalytic properties of Pd nanoparticles on SWNTs. Pd nanoparticles were electrochemically dispersed on SWNTs by electroreduction of octahedral Pd(IV) complex formed on the SWNT surface. The structure and nature of the resulting Pd-SWNT composites were characterized by TEM and XRD. The electrocatalytic properties of the Pd/SWNT electrode for hydrazine oxidation have been investigated by CV and high electrocatalytic activity was observed owing to the high dispersion of Pd catalysts and the particular properties of SWNT supports (Guo and Li, 2005).

Rao and Trivedi described a one-pot method to synthesize Pd nanoparticles incorporated polypyrrole films (Pd–Ppy). The films were homogeneous with Pd particles and were peeled from the electrode surface as free standing films. Novelty of this procedure was that the Pd particles were prepared and stabilized in presence of the surface-active dopant, dodecylbenzene sulphonic acid sodium salt (NaDBSA), and were incorporated in to the polymer matrix along with dopant during the growth of the film. It was observed that the incorporation of Pd was uniform and homogeneous. An unprecedented catalytic activity by these Pd–Ppy composite layers in enhancing the rate of polymer deposition was observed. The films also electrocatalyzed the oxidation of hydrazine more effectively than did the pure Ppy films (Rao and Trivedi, 2006).

Dong et al. studied high dispersion and electrocatalytic activity of Pd/titanium dioxide nanotubes (Pd/TiO_2-NTs) catalysts for hydrazine oxidation. Pd particles were obtained from palladium chloride solution by a simple reduction method on TiO_2-NTs support. The structure and morphology of the resulting catalysts were characterized by TEM and XRD methods. The authors reported that Pd particles with a size range from 6 to 13 nm were well-dispersed on the surface of TiO_2-NTs. The electrocatalytic properties of the catalysts were also investigated by cyclic voltammetry towards hydrazine oxidation. Compared to that of pure Pd particles

and Pd/TiO_2 particles, Pd/TiO_2-NTs catalysts showed much higher electrochemical activity. This result was attributed to the uniform dispersion of Pd nanoparticles on TiO_2-NTs, smaller particle size and unique properties of TiO_2-NTs support. The oxidation of hydrazine was reported as an irreversible process, which was probably controlled by diffusion process of hydrazine (Dong et al., 2008).

4. FUEL CELLS

Fuel cells are devices which convert chemical energy directly to electrical energy (www.fuelcellknowledge.org). During the operation of a fuel cell, hydrogen and oxygen are combined to produce electricity, with water and heat as its by-product. As long as fuel is supplied, the fuel cell will continue to generate power. Since the conversion of the fuel to energy takes place via an electrochemical process, not combustion, the process is clean, quiet and highly efficient – two to three times more efficient than fuel burning (www.fuelcells.org).

A fuel cell consists of two electrodes sandwiched around an electrolyte. Oxygen passes over one electrode and hydrogen over the other, generating electricity, water and heat. Schematic representation of a fuel cell is given in Figure 4.1.

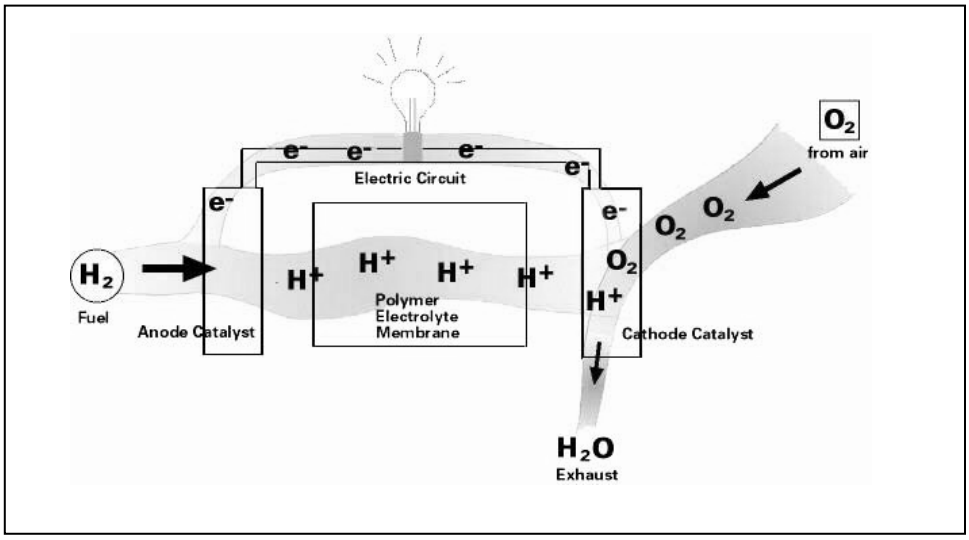

Figure 4.1. Schematic representation of a fuel cell.

Hydrogen fuel is fed into the anode of the fuel cell. Oxygen (or air) enters the fuel cell through the cathode. Encouraged by a catalyst, the hydrogen atom splits into a proton and an electron, which take different paths to the cathode. The proton passes through the electrolyte. The electrons create a separate current that can be utilized before they return to the cathode, to be reunited with the hydrogen and oxygen in a molecule of water.

A fuel cell system which includes a fuel reformer can utilize the hydrogen from any hydrocarbon fuel - from natural gas to methanol, and even gasoline. Since the fuel cell relies on chemistry and not combustion, emissions from this type of a system would still be much smaller than emissions from the cleanest fuel combustion processes.

The fuel cell was first demonstrated in 1839 by William Grove. Unfortunately development of viable technology for exploitation of the principle has been slow, primarily due to the incompatibility of the required material properties. Inevitably the first uses were space and military applications, in which cost is of secondary importance to performance.

With increasing understanding of fuel cell and relevant materials science, driven by these specialist applications, there have been a number of false dawns when fuel cells have been proclaimed the solution to all of our energy needs, only to realize that there are inherent limitations on particular technologies applications. This roller coaster road to development has however generated a wide range of fuel cell systems with one or more suitable for virtually every power application imaginable.

Fuel cell technologies can be classified in many ways, for example by temperature, fuel type, oxidizer type, or charge carrier. According to a common classification by electrolyte type; polymer electrolyte (PEFC), alkaline electrolyte (AFC), phosphoric acid electrolyte (PAFC), molten carbonate electrolyte (MCFC) and solid oxide electrolyte (SOFC) fuel cells are the most common fuel cell types.

No other energy generating technology offers carries the combination of benefits that fuel cells offer. These benefits include:

Low to zero emissions

A fuel cell running on pure hydrogen is a zero-emission power source. Some stationary fuel cells use natural gas or hydrocarbons as a hydrogen feedstock, but even those produce far less emissions than conventional power plants.

Fuel cell vehicles are the least polluting of all vehicles that consume fuel directly. Fuel cell vehicles operating on hydrogen stored on-board produce zero pollution in

the conventional sense. Neither conventional pollutants nor green house gases are emitted. The only byproducts are water and heat. The simple reaction that takes place inside the fuel cell is highly efficient. Even if the hydrogen is produced from fossil fuels, fuel cell vehicles can reduce emissions of carbon dioxide, a global warming concern, by more than half. Fuel cells used as auxiliary power units (APUs) to power air conditioners and accessories in over-the-road trucks could reduce emissions by up to 45% from long haul vehicles, and deliver economic benefits to the truck owner in lower fuel use.

Fuel cells are also very quiet, which reduces noise pollution.

High efficiency

Because they make energy electrochemically, and do not burn fuel, fuel cells are fundamentally more efficient than combustion systems. When the fuel cell is sited near the point of use, its waste heat can be captured for beneficial purposes (cogeneration). In large-scale building systems, these fuel cell cogeneration systems can reduce facility energy service costs by 20% to 40% compared to conventional energy service.

- Fuel cell power generation systems in operation today achieve 40% to 50% fuel-to-electricity efficiency utilizing hydrocarbon fuels.
- Systems fueled by hydrogen can consistently provide more than 50% efficiency. Even more efficient systems are under development.
- In combination with a turbine, electrical efficiencies can exceed 60%.
- When waste heat is put to use for heating and cooling, fuel utilization can exceed 85%.
- Fuel cell passenger vehicles are expected to be up to three times more efficient than internal combustion engines, which now operate at 10 to 16% efficiency.

High reliability/high quality power

Most fuel cells run on hydrogen and will continue to generate power as long as fuel is supplied. The fuel cell doesn't care where the hydrogen comes from, so a fuel cell system that includes a "fuel reformer" can generate hydrogen from

diverse, domestic resources including fossil fuels, such as natural gas and coal; alcohol fuels, such as methanol or ethanol; from hydrogen compounds containing no carbon, such as ammonia or borohydride; or from biomass, methane, landfill gas or anaerobic digester gas from wastewater treatment plants. Hydrogen can also be produced from electricity from conventional, nuclear or renewable sources such as solar or wind. Fuel cells offer clean, high quality power, crucial to an economy that depends on increasingly sensitive computers, medical equipment and machines.

Lightweight/long-lasting battery alternative

Fuel cells are being developed for portable electronic devices such as laptops, cellular phones, etc. Fuel cells are providing e a much longer operating life than a battery would, in a package of lighter or equal weight per unit of power output. The fuel cell doesn't require recharging; a liquid, solid, or gaseous fuel canister could be replaced in a moment. Fuel cells also have an environmental advantage over batteries, since certain kinds of batteries require special disposal treatment. Fuel cells provide a much higher power density, packing more power in a smaller space.

Using a liquid fuel in fuel cells has advantages over gasses because liquid fuels typically feature higher volumetric and gravimetric energy densities, and are easier to transport, store and handle. A variety of liquids have been proposed as fuels for direct fuelled fuel cells, including methanol, ethanol, hydrazine, formaldehyde and forming acid. However the intended application as a customer friendly fuel sets additional constraints such as cost, availability, safety, and corrosivity. Ethanol and other C_2 compounds, which would fulfil most of the requirements, present difficulties in that the C-C bond is hard to split electrochemically, resulting in variety of undesirable reaction products such as ethyl acetate and acetaldehyde. As a result, methanol is considered to be the most promising candidate for direct-fuelled fuel cells apart from hydrogen (Urban et al., 2001).

4.1. Direct Methanol Fuel Cells (DMFC)

The technology behind Direct Methanol Fuel Cells (DMFC) is still in the early stages of development, but it has been successfully demonstrated powering mobile phones and laptop computers—potential target end uses in future years (www.fctec.com).

DMFC is shown schematically in Figure 4.2 (www.dtienergy.com). It consists of an anode at which methanol is electrooxidized to CO_2 through the reaction:

$$CH_3OH + H_2O \rightarrow CO_2 + 6\,H^+ + 6\,e^- \qquad (4.1)$$

and a cathode at which oxygen (usually as air) is reduced to water or steam (Hamnett, 1997).

$$3/2\,O_2 + 6\,e^- + 6\,H^+ \rightarrow 3\,H_2O \qquad (4.2)$$

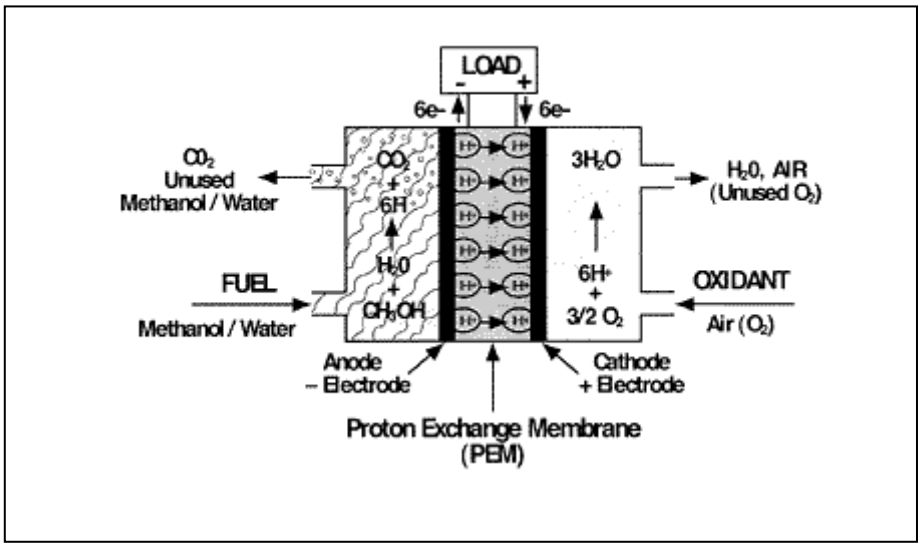

Figure 4.2. Schematic representation of a DMFC.

During the operation of DMFCs, at zero current a certain voltage can be measured between the both electrodes (anode and cathode) (Urban et al., 2001). If a current is drawn, this voltage diminishes due to

1. activation losses at the catalyst,
2. limited transport of the reactants to the catalysts,
3. Ohmic losses of the electrodes and the electrolyte.

DMFCs have been tested in a temperature range from about 50 ºC-120 ºC. This low operating temperature and no requirement for a fuel reformer make the DMFC an excellent candidate for very small to mid-sized applications, such as cellular phones and other consumer products, up to automobile power plants.

The methanol crossover is an important issue during the operation of DMFCs. Wang et al. (Wang et al., 1996) found that methanol is oxidized heterogeneously in the presence of oxygen and a suitable catalyst leading to a so-called 'mixed potential' effect, and that the cathode is additionally poisoned by methanol. The effect responsible for cathode performance decay was also used to diminish anode poisoning: oxygen oxidizes adsorbed species derived from methanol heterogeneously. However, part of the anode performance gain is compensated by the fact that also at the anode a mixed potential is established.

Two options do exist to overcome cathode performance losses due to methanol crossover: (I) polymer electrolyte membranes have to be used which allow less methanol permeation, or, (ii) a cathode catalyst has to be found which neither catalyzes the heterogeneous oxidation of methanol. The first approach seems to be more promising, since perspectives of the second approach concerning cathode catalyst cost, performance and long-term stability are yet uncertain. Furthermore, approach (ii) does not solve the problem of a significant loss of fuel due to crossover (Wasmus and Küver, 1999).

Various studies were carried out in order to improve the performances of DMFCs. Jung and coworkers investigated the performance of a DMFC based on a polymer electrolyte membrane electrolyte. Pt-Ru/C (60 wt.%) and Pt/C (60 wt.%) catalysts were employed for methanol oxidation and oxygen reduction, respectively. Cell performances were evaluated over the range of 60-120 ^{o}C. The cell fabricated with Nafion® 112 membranes with a current density of 230 mA cm^{-2} at 0.55 V was obtained from 2.5 M methanol (Jung et al., 1998).

Motokawa et al. designed a micro DMFC with an active area of 0.018 cm^{2}. The methanol anode and oxidant cathode were prepared by electroplating either Pt-Ru or Pt and Pt, respectively, onto Ti/Au electrodes. The cell was operated at ambient temperature and atmospheric pressure using

2.0 M CH_3OH/0.5 M H_2SO_4/H_2O as the fuel and O_2-sat./0.5 M H_2SO_4 as the oxidant. The open circuit voltage (OCV) was 300 mV for Pt cell and 400 mV for Pt-Ru cell. The maximum power density was 0.44 mW cm^{-2} at 3 mA cm^{-2} at Pt electrode. With Pt-Ru anode, the maximum power density reached 0.78 mW cm^{-2} at 3.6 mA cm^{-2} (Motokawa et al., 2004).

In a study carried out by Serov and coworkers, RuSe/C catalysts were used as cathode for oxygen reduction in DMFCs. The anode catalyst was PtRu black and the membrane was Nafion® 112. Polarization curves were obtained using a homemade single cell with a working area of 10 cm^2. Methanol solution (1 M) was fed to the anode side while dry air was fed to the cathode sideunder atmospheric pressure. The single cell operated at 80 ^oC gave a performance of 62 mW cm^{-2} using 80 wt.% RuSe/C in the cathode with an OCV around 0.77 V (Serov et al., 2008).

Yang et al. studied electrochemical performance of an air-breathing DMFC using poly(vinyl alcohol)/hydroxyapatite composite polymer membrane. The cell was comprised of the air cathode electrode with MnO_2/BP2000 catalyst inks and the PtRu Ti-anode electrode. At ambient temperature and pressure, the maximum power density of the cell in 8 M KOH + 2 M CH_3OH solution was about 11.48 mW cm^{-2} (Yang et al., 2008).

The effects of two different microporous layer preparation methods, including a heated-spraying method and a scrapping method, on the performance of a DMFC were investigated by Lin et al. The catalyst for the anode was unsupported Pt/Ru black and the catalyst for the cathode was Pt black. Performance of the fuel cell was tested using a single cell with a working area of 5 cm^2. A solution of 2 M aqueous CH_3OH was fed to the anode side. Air was supplied to the cathode side at a flow rate of 670 mL min^{-1} under ambient pressure. The maximum power densities of the two cells were up to 46.32 and 34.2 mW cm^{-2} when the operating temperatures were 35 ^oC and 55 ^oC, respectively (Lin et al., 2008).

4.2. Direct Hydrazine Fuel Cells (DHFC)

Hydrazine fuel cells are ideal in that they do not exhaust environmentally loading materials such as CO_2 and can generate high voltage as a direct fuel system

(Yamada et al., 2003). Since hydrazine is composed of only hydrogen and nitrogen, the anode reaction produces, theoretically, only nitrogen. Therefore, perfect zero emission equal to a pure hydrogen fuel can be realized. Since DHFC does not produce CO-like poisoning species in the direct electrooxidation process, the overvoltage by the catalyst poisoning is low in the cell.

In DHFCs, the theoretical electromotive force is as high as 1.56 V, and highly efficient high power density is expected:

$$N_2H_5^+ \rightarrow N_2 + 5\,H^+ + 5\,e^- \quad \text{(in acid solutions)} \qquad (4.3)$$

$$N_2H_4 + 4\,OH^- \rightarrow N_2 + 4\,H_2O + 4\,e^- \quad \text{(in alkaline solutions)} \qquad (4.4)$$

Hydrazine has excellent handling characteristics, relative stability under normal conditions, and clean decomposition products. It is not very safe above 150 ^oC, but is technically stable to about 250 ^oC. Hydrazine is reactive and highly soluble in the electrolyte, yielding high current densities. However; because of its hazardous effects, care should be taken while working with hydrazine (www.asi.org).

In 2003, collaboration of Daihatsu Motor Co. Ltd. and National Institute of Advanced Industrial Science and Technology resulted in a series of studies about DHFCs. In the first study, Yamada and coworkers investigated a polymer electrolyte membrane (PEM) type DHFC. Hydrazine generated a higher cell voltage than methanol in direct-liquid-fueled fuel cell using PEM as the electrolyte. At a current density of 40 mA cm^{-2} or less, DHFC generated over 1 V (Yamada et al., 2003).

In the second study, potential application of anion-exchange membrane for hydrazine fuel cell electrolyte was investigated. The prepared MEA, with an electrode area of 10 cm^2, was inserted into a single cell to measure the cell performance. A sufficient amount of 2 M aqueous solution of hydrazine hydrate ($N_2H_4 \cdot H_2O$) was supplied to the anode at a flow rate of 2 ml min^{-1} and argon gas humidified at 60 ^oC was supplied to the cathode at a flow rate of 200 ml min^{-1}. The

cell temperature was controlled at 60 ^{o}C. When DHFC performances were compared, anion-exchange membrane was found superior to the cation-exchange membrane (Yamada et al., 2003).

In the third study, effect of anode electrocatalyst for DHFC using proton exchange membrane was reported. Four kinds of unsupported powder catalyst, Pt, Rh, Pd and ruthenium oxide were tested. The high open-circuit voltages over 1V were observed for DHFC using Pt and Pd. The Pd electrode was found to have a similar trend to the Pt electrode in the dependence of cell voltage on current density. Using Pd, the cell voltage was lower than using Pt and decreased more rapidly with increasing the current density in the low-current density region below 40 mA cm^{-2}. The open-circuit voltage of the cell using Rh was 0.8 V, the lowest value of all four electrodes. However, the cell using Rh gave the lowest cell-voltage loss with increase of current density and the highest cell voltage at current densities over 70 mA cm^{-2}. The poorest performance was obtained in the cell using Ru electrocatalyst. The open-circuit voltage was low and the cell voltage showed the lowest value at almost all current densities (Yamada et al., 2003).

In 2007, Daihatsu Motor Co. Ltd. announced the development of fundamental technology for a fuel cell system using hydrazine (N_2H_4) as a fuel. According to the report announced by the company, the new fuel cell achieved a maximum output density of 0.50 mW cm^{-2}, which is on par with that of the existing fuel cell (PEFC) using hydrogen as a fuel. The system used hydrazine hydrate (N_2H_4, H_2O) in the form of a 5% by mass aqueous solution. Hydrazine hydrate and oxygen were supplied to the fuel and air electrodes, respectively. The Ni and Co catalysts were used for the fuel and air electrodes, respectively.

To ensure safe use of hydrazine, Daihatsu unveiled a technology to use hydrazine hydrate after solidification. To enhance safety, the company proposed a system in which hydrazine hydrate is normally stored in a fixed state, and only the required quantity is liquefied to be supplied for the fuel cell. Specifically, hydrazone obtained by bonding hydrazine with a polymer having a carbonyl group (C=O) and stored can be reliquefied and returned to hydrazine hydrate by hydrolysis when used as a fuel. When it is used in a vehicle, the polymer with a carbonyl group is provided as a fuel tank (http://techon.nikkeibp.co.jp).

5. EXPERIMENTAL TECHNIQUES

5.1. Controlled Potential Electrolysis with Coulometry

In controlled potential electrolysis technique, the potential of the working electrode is measured against a suitable reference electrode. The potential impressed across the working electrode and its counter electrode can then be adjusted to the level that will impart the desired potential to the cathode or anode with respect to the reference electrode.

The potential difference between the reference electrode and the cathode is measured with an electronic voltmeter. The potential applied between the working electrode and its counter electrode is controlled with a voltage divider so that the cathode potential is maintained at a level suitable for the separation.

During the electrolysis process, relatively high initial potentials can be applied to give high currents. As the electrolysis progresses, however, a lowering of the applied potential is required this decrease, in turn, diminishes the current. Completion of the electrolysis will be indicated by the approach of the current to zero. The changes that occur in a typical constant-cathode-potential electrolysis are depicted in Figure 5.1.

Coulometry encompasses a group of analytical methods that involve measuring the quantity of electricity needed to convert the analyte quantitatively to a different oxidation state. The quantity of electricity or charge is measured in units of the coulomb (C) and the faraday (F). The coulomb is the quantity of charge that is transported in one second by a constant current of one ampere. The faraday is the charge in coulombs associated with one mole of electrons.

Controlled potential electrolysis with coulometry (or potentiostatic colulometry) involves maintaining the potential of the working electrode at a constant level such that quantitative oxidation or reduction of the analyte occurs without involvement of less reactive species in the sample or solvent. Here the current is initially high but decreases rapidly and approaches to zero as the analyte is removed from the solution (see Figure 5.1).

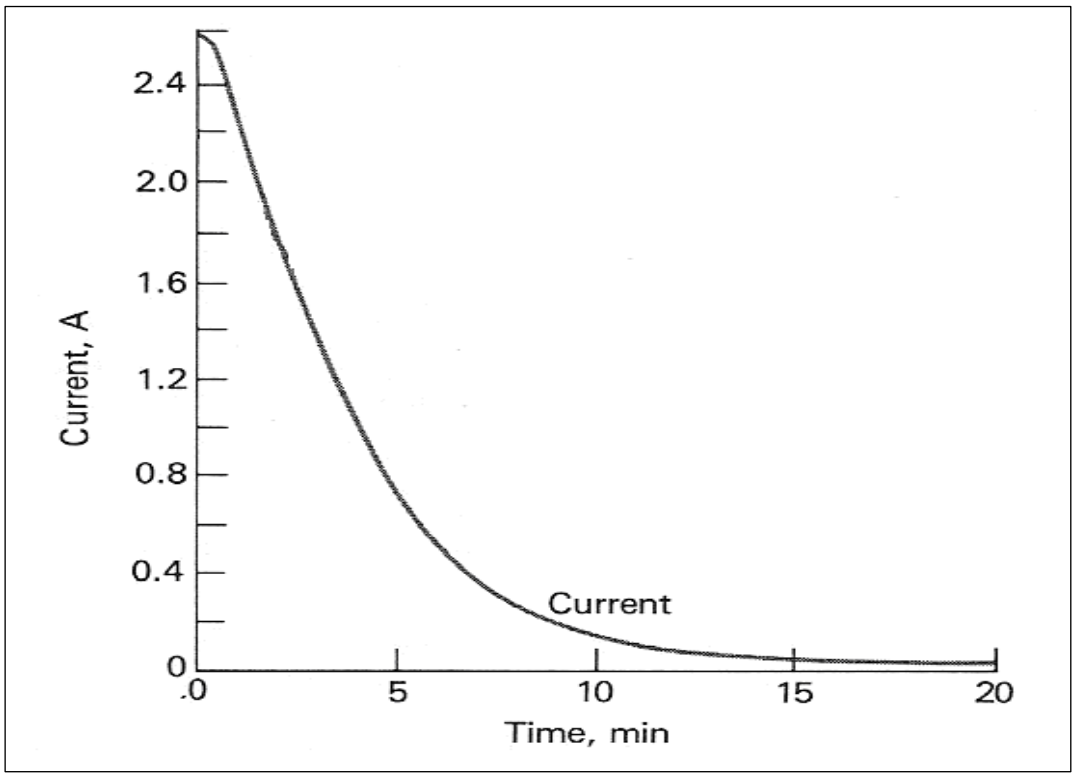

Figure 5.1. Change in current during a controlled-cathode-potential electrolysis.

5.2. Cyclic Voltammetry

A simple potential wave form that is often used in electrochemical experiments is the linear wave form i.e., the potential is continuously changed as a linear function of time. The rate of change of potential with time is referred to as the scan rate (*v*). In cyclic voltammetry the potential range is scanned in one direction, starting at the initial potential then finishing at the final potential and then the direction of the potential is reversed at the end of the first scan. Thus, the waveform is usually of the form of an isosceles triangle. This has the advantage that the product of the electron transfer reaction that occurred in the forward scan can be probed again in the reverse scan. In addition, it is a powerful tool for the determination of formal redox potentials, detection of chemical reactions that precede or follow the electrochemical reaction and evaluation of electron transfer kinetics.

Cyclic voltammetry is mainly used for studying the reversibility of electrode process and for kinetic observations. The voltage cycle illustrated in Figure 5.2 ensures that the reaction products formed at the potential E_{pc} on the cathodic path are reoxidized at E_{pa} in the complete anodic sweep.

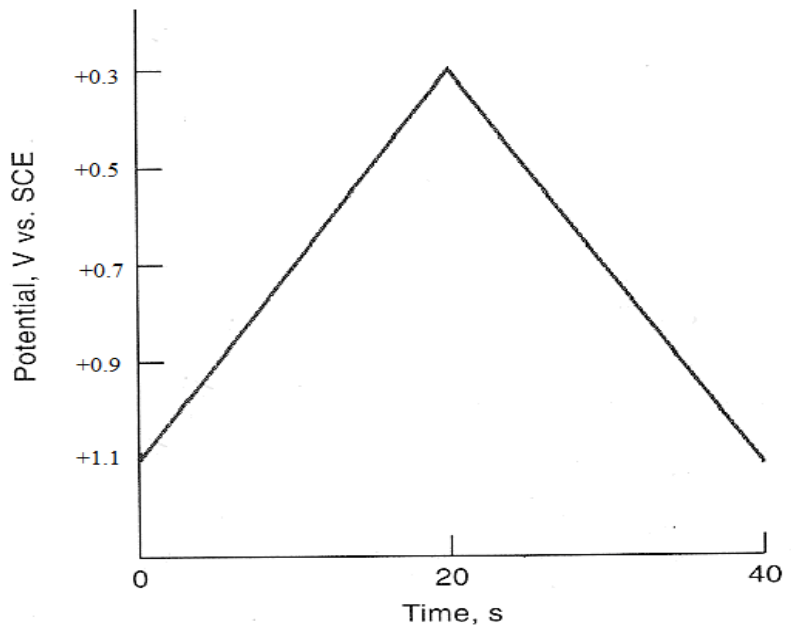

Figure 5.2. Variation of potential with time in cyclic voltammetry.

For a reversible system, the peak current is expressed with Randles-Sevcik equation:

$$i_p = k\, n^{3/2}\, A\, D^{1/2}\, C\, v^{1/2} \qquad (5.1)$$

where;
- i_p : peak current in amperes
- n : number of transferred electrons in the electrode reaction
- A : area of the working electrode in cm^2
- D : diffusion coefficient in $cm^2\ s^{-1}$
- C : concentration of the electroactive species in mol cm^{-3}
- v : potential scanning rate in V s^{-1}
- k : Randles-Sevcik constant (2.69×10^5).

A typical cyclic voltammogram (CV) is presented in Figure 5.3. It is known that for a reversible redox process:

$$\Delta E_p = E_{pc} - E_{pa} = (59 / n)\ mV \qquad (5.2)$$

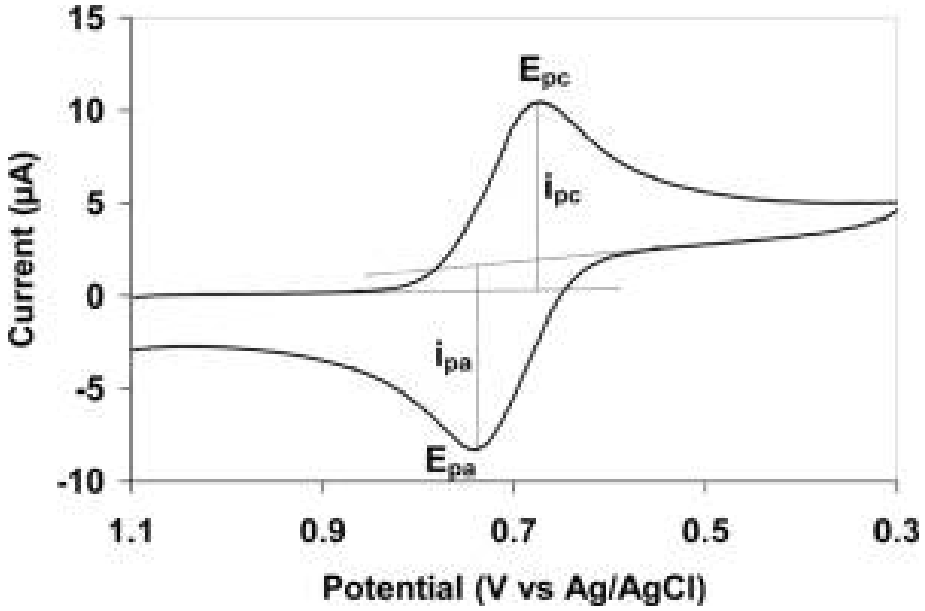

Figure 5.3. Cyclic voltammogram of a reversible electrode reaction (http://en.wikipedia.org/wiki/Image:Cyclovoltammogram.jpg).

The position of the current peak in this case being independent of the voltage scan rate. The two peaks have equal heights. With increasing irreversibility, ΔE_p becomes greater. For quasi-reversible processes and for slow change of voltage, the difference is about (60/n) mV, but it becomes greater for a faster sweep. For totally irreversibly processes, the reduction product is not reoxidized, so the anodic current peak is not seen.

Cyclic voltammetry gives information on the redox behaviour of electrochemically active species and on the kinetics of electrode reactions as well as offering the possibility of identifying reactive intermediates or subsequent products. Cyclic voltammetry, while not use for routine quantitative analysis, has become an important tool for the study of mechanism and rates of oxidation-reduction processes, particularly in organic and metal-organic systems. Often CVs will reveal the presence of intermediates in oxidation-reduction reactions.

5.3. Scanning Electron Microscopy

In many fields of chemistry, material science, geology, and biology, detailed knowledge of the physical nature and chemical composition of the surfaces of solids on a submicrometer scale is of great importance. Currently, such knowledge can be obtained by scanning electron microscopy (SEM).

In obtaining an electronic microscopic image, the surface of a solid sample is swept in a raster pattern with a finely focused beam of electrons. A raster is a scanning pattern in which an electron beam is (1) swept across a surface in a straight line, (2) returned to its starting position, and (3) shifted downward by a standard increment. This process is repeated until a desired area of the surface has been scanned. Several types of signals are produces from a surface when it is scanned with an energetic beam of electrons. These signals include backscattered, secondary, and Auger electrons; X-ray fluorescence; and other protons of various energies. All of these signals have been used for surface studies, but the two most common are backscattered and secondary electrons, which serve as the basis of scanning electron microscopy.

For obtaining SEM images of solids, samples that conduct electricity are the easiest to study, because the unimpeded flow of electrons to ground minimizes artifacts associated with the buildup of charge. In addition, samples that are good conductors of electricity are usually also good conductors of heat, which minimizes the likelihood of their thermal degradation. A variety of techniques have been developed for obtaining SEM images of non-conducting samples, but the most common approaches involve coating the surface of the sample with a thin metallic film produced by sputtering or by vacuum evaporation. A representative SEM image of $PVF^{+}ClO_4^{-}$ film is given in Figure 5.5.

Figure 5.4 is a schematic of a scanning electron microscope.

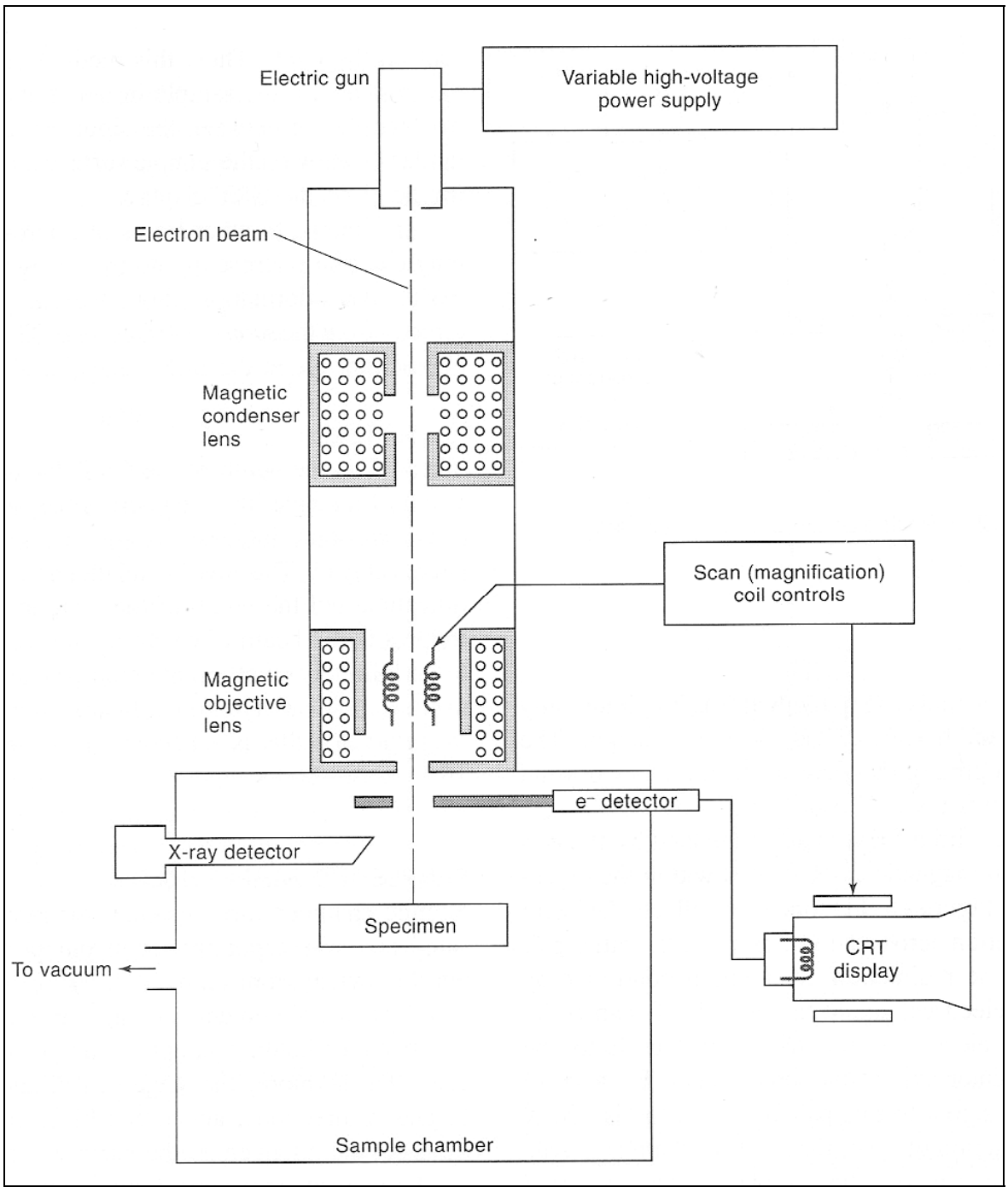

Figure 5.4. Schematic of a scanning electron microscope.

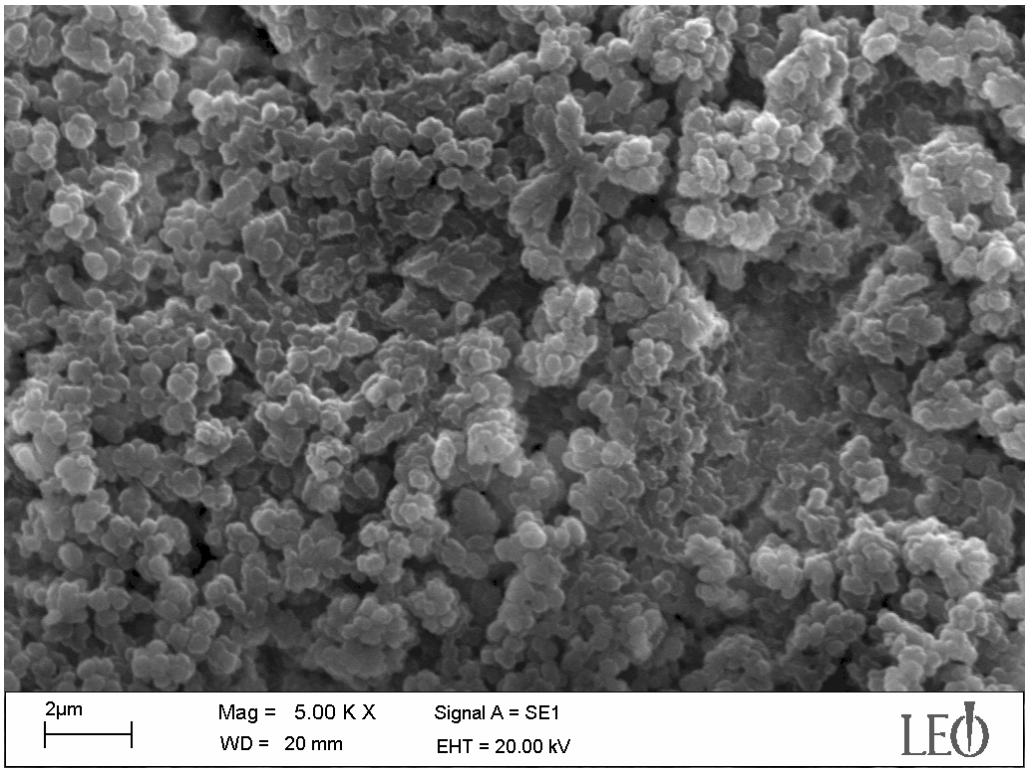

Figure 5.5. SEM image of $PVF^{+}ClO_4^{-}$ film.

5.4. Energy Dispersive X-Ray Spectroscopy

Energy dispersive X-ray spectroscopy (EDS) is a chemical microanalysis technique performed in conjunction with a SEM. The technique utilizes X-rays that are emitted from the sample during bombardment by the electron beam to characterize the elemental composition of the analyzed volume. Features or phases as small as about 1µm can be analyzed.

When the sample is bombarded by the electron beam of the SEM, electrons are ejected from the atoms comprising the sample's surface. A resulting electron vacancy is filled by an electron from a higher shell, and an X-ray is emitted to balance the energy difference between the two electrons.

The EDS X-ray detector measures the number of emitted X-rays versus their energy. The energy of the X-ray is characteristic of the element from which the X-ray was emitted. A spectrum of the energy versus relative counts of the detected X-rays is obtained and evaluated for qualitative and quantitative determinations of the elements present in the sampled volume.

A typical EDS spectrum is presented in Figure 5.6.

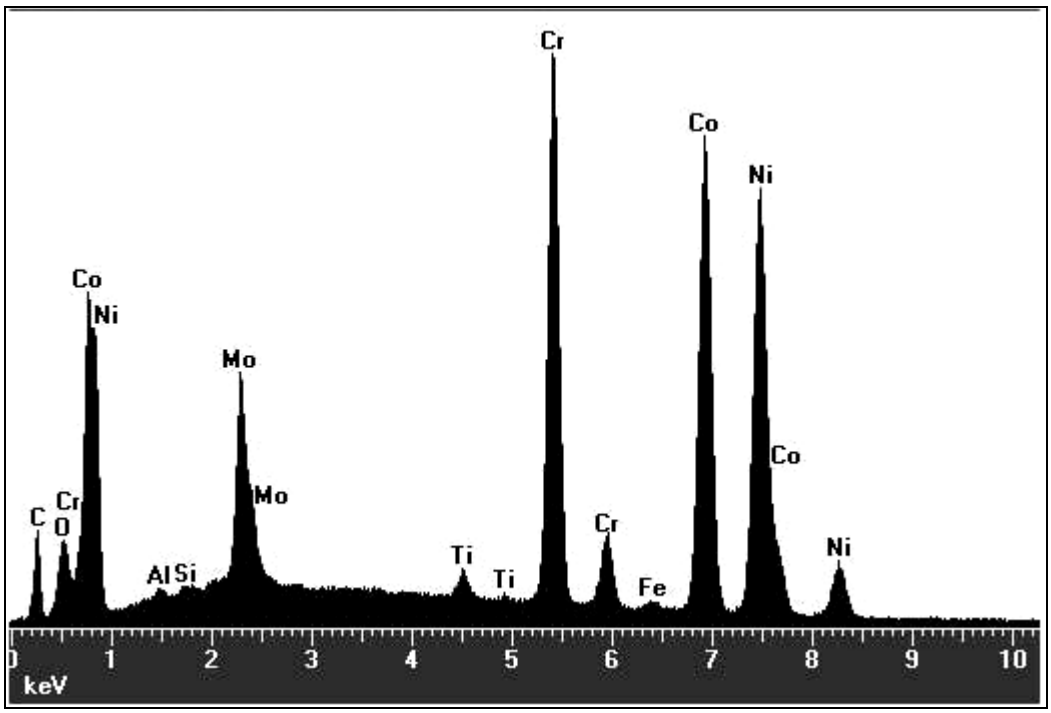

Figure 5.6. Typical EDS spectrum for a corrosion resistant alloy (http://www.mee-inc.com/eds.html).

6. EXPERIMENTAL

6.1. Electronic Equipment

The potential-controlled coulometric and cyclic voltammetric studies were carried out with CH Instruments System, Model 608B. This system was connected to a personnel computer.

Temperature controlled experiments were carried out with PolyScience® digital temperature controller.

The catalyst system was examined using a Gemini scanning electron microscope equipped with Leo 32 Supra 35VP field emission scanning system and electron dispersive spectrometer was used for images and analysis respectively.

6.2. Electrochemical Cell

Electrochemical measurements were carried out in a special electrochemical cell which has five necks (Figure 6.1). Three of them belong to the electrodes which are used as working, reference and counter electrode. The others are used to nitrogen inlet and outlet.

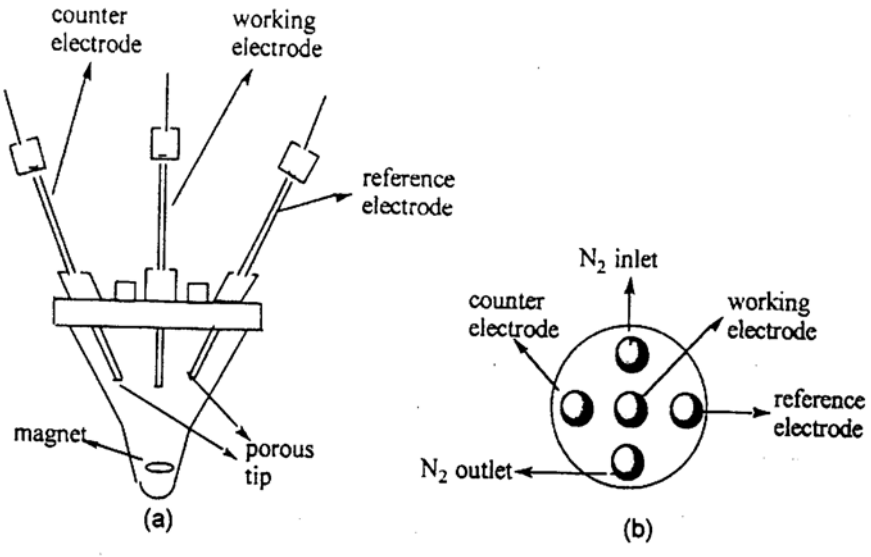

Figure 6.1 An electrochemical cell: a) cross-sectional view, b) top view of the cell.

Before electrochemical experiments, the cell was washed with basic $KMnO_4$, concentrated HCl, acidic $K_2Cr_2O_7$, distilled water and alcohol. Then it was dried at 100 ^oC. After this washing and drying procedure, it was ready to use for electrochemical experiments.

In electrochemical studies, it is very important to remove O_2 from working cell in order to investigate electrochemical behavior of any substance correctly. For that reason, all electrochemical experiments were carried out under very pure nitrogen atmosphere by bubbling nitrogen gas for at least 20 minutes (BOS, 99.99%).

6.3. Electrodes

In electrochemical studies, a platinum (Pt) disc electrode (A = $7.85x10^{-3}$ cm^2) and a glassy carbon electrode (GCE) (A = 0.2827 cm^2) were used as the working electrodes. Before each experiment, the electrodes were polished with alumina (5.0 μm), then rinsed with triple distilled water, cleaned in ultrasonic bath and dried. In the methylene chloride medium, a Ag/AgCl electrode was used as the reference electrode. This electrode was prepared by anodic electrolysis of a silver electrode in 0.1 M HCl solution for 3 hours at +2.1 V with a current density of 2 mA cm^{-2}. The electrode was immersed in a separate compartment containing methylene chloride/0.1 M TBAP solution with a saturated amount of AgCl. In the electrochemical experiments that were carried out in methylene chloride medium, a Pt wire in separate compartment containing methylene chloride/0.1 M TBAP solution was used as the counter electrode. In aqueous medium, a saturated calomel electrode (SCE) was used as the reference electrode and a Pt wire electrode with a surface area of 2 cm^2 in spiral form was used as the counter electrode.

6.4. Reagents and Preparation of Solutions

PVF was synthesized according to the procedure described by Aso et al. (Aso et al., 1969). Vinylferrocene was purchased from Aldrich. 2,2'-Azo-bis(2-methyl-propionitrile) (AIBN) was obtained from Alfa. Tetra-n-butyl ammonium perchlorate (TBAP) was synthesized by the reaction of tetra-n-butyl ammonium hydroxide (40% aqueous solution, Merck) with perchloric acid (BDH) and recrystallized from the 1:9 mixture of water and ethyl alcohol

(Merk), by volume, several times. It was then dried at 120 ^{o}C under vacuum for 12 h. This salt was always kept under nitrogen atmosphere.

Methylene chloride (HPLC grade, Riedel de Häen), methanol (Riedel de Häen) H_2SO_4 (Merck) and K_2SO_4 (Analar, BDH) were used as received. K_2PtCl_4 and K_2PdCl_4 were obtained from Merck and $H_2PtCl_6 \cdot H_2O$ was obtained from Aldrich. Hydrazine solution was prepared from hydrazinium sulfate salt ($N_2 \cdot H_4 \cdot H_2SO_4$, BDH).

6.5. Single Cell Tests

Nafion® membrane (NE 450, Aldrich) was used in the DMFC and DHFC constructions. The anode materials were PVF^+-supported Pt and Pd catalyst systems. Pt black coated Pt electrode was used as the cathode material. Fuel cell performances were tested using a home made single cell with a working area of 1 cm^2 (Figure 6.2). All fuel cell tests were carried out at ambient temperature and atmospheric pressure.

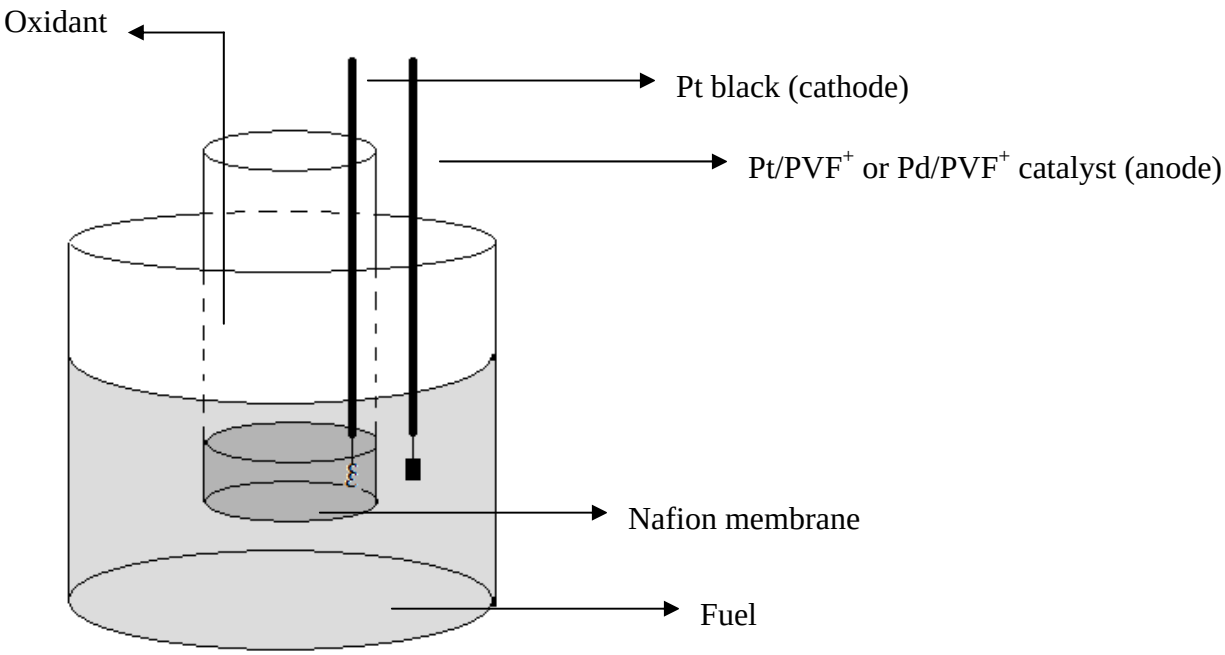

Figure 6.2. Schematic representation of the home made single cell.

7. RESULTS AND DISCUSSION

7.1. Electrodeposition of PVF^+

In all experiments, oxidized form of PVF (PVF^+) was electrodeposited onto the working electrode by the electrooxidation of 1.0 mg mL^{-1} solution of PVF in methylene chloride containing 0.1 M TBAP at +0.7 V vs. Ag/AgCl. The thicknesses of the polymer films were controlled by the charge passed during the electroprecipitation of oxidized form of the polymer onto the electrode surface. This charge was considered as an indication of polymer film thickness. CV of 1.0 mC $PVF^+ClO_4^-$ film recorded in 0.1 M NaCl solution is given in Figure 7.1.

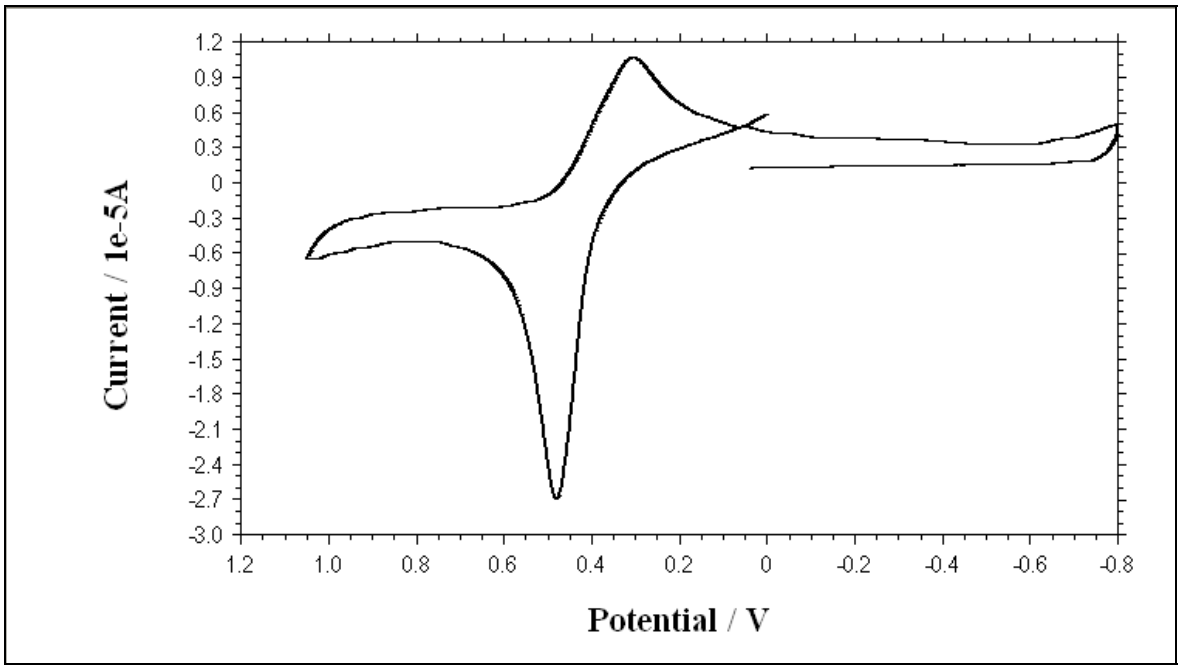

Figure 7.1. CV of $PVF^+ClO_4^-$ coated Pt disc electrode corresponding to a film thickness of 1.0 mC recorded in 0.1 M NaCl solution. Scan rate: 100 mV s^{-1}.

7.2. Pt/PVF^+ Electrocatalyst System

7.2.1. K_2PtCl_4 as the Pt precursor

Aqueous solution of K_2PtCl_4 was used as the Pt precursor in order to obtain Pt particles in the polymer matrix. In aqueous solution, two extensive but slow reactions of $PtCl_4^{2-}$ complex is given (Cotton and Wilkinson, 1972; Lederer and Leipzig-Pagani, 1997):

$PtCl_4^{2-} + H_2O \leftrightarrow PtCl_3(H_2O)^- + Cl^-$ $K = 1.34x10^{-2}$ M (at 25°C) (7.1)

$PtCl_3(H_2O)^- + H_2O \leftrightarrow PtCl_2(H_2O)_2 + Cl^-$ $K = 1.1x10^{-3}$ M (at 25°C) (7.2)

Polycyclic voltammogram of 2 mM K_2PtCl_4 solution is given in Figure 7.2 for 30 cycles recorded with PVF^+ coated Pt disc electrode. In the voltammogram, oxidation and reduction of the polymer are observed at +0.49 V and +0.26 V vs. SCE respectively. The remaining oxidation and reduction peaks belong to the Pt complex species.

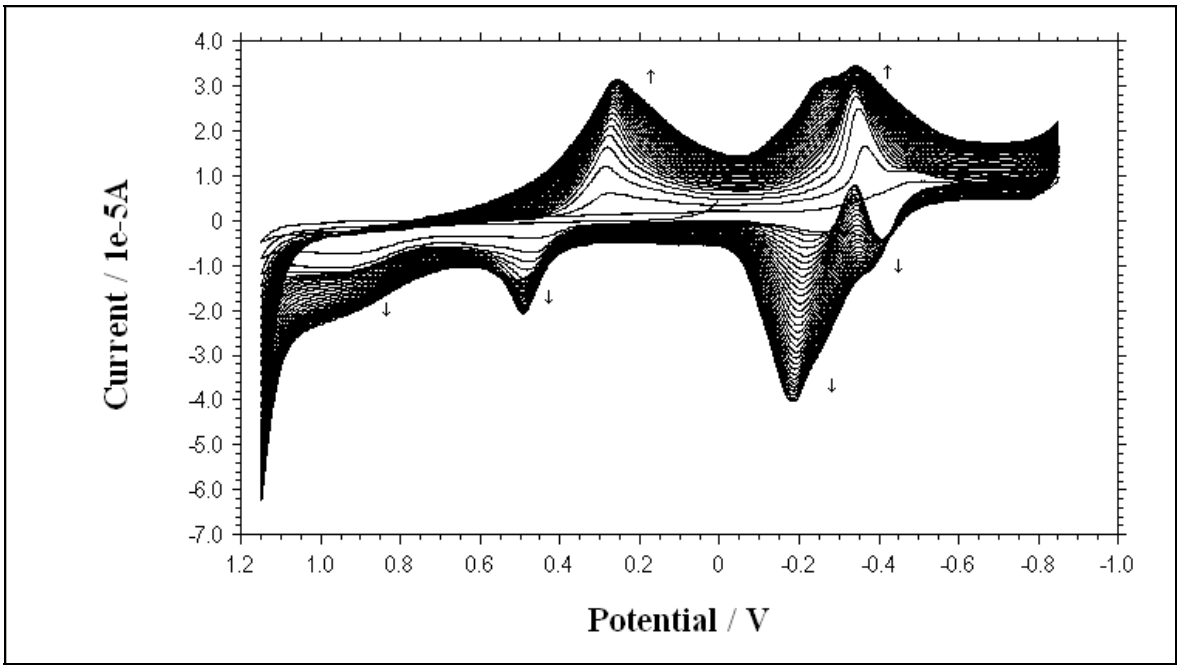

Figure 7.2. Polycyclic voltammogram of 2 mM K_2PtCl_4 solution recorded with PVF^+ coated Pt disc electrode. Scan rate: 100 mV s^{-1}.

During preparation of the Pt/PVF^+ system, Pt particles were incorporated into the polymer matrix via cyclic voltammetric scans in aqueous 2 mM K_2PtCl_4 solution without supporting electrolyte. In this step, Pt is in complex form and does not show catalytic activity. Two separate methods were used for reduction of Pt complexes. In the first method, polymer coated electrode containing Pt complex was immersed in 0.1 M $N_2H_4 \cdot H_2SO_4$ solution stirred continuously at open circuit. In the second method, Pt particles were electrochemically reduced in 0.5 M H_2SO_4 solution. After reduction of Pt particles, the Pt/PVF^+ system showed catalytic activity towards methanol oxidation. Constant potential electrolysis was also

studied for immobilization of Pt particles; however, unsuccessful results were obtained.

Steps for preparation of the catalyst are represented schematically in Scheme 7.1.

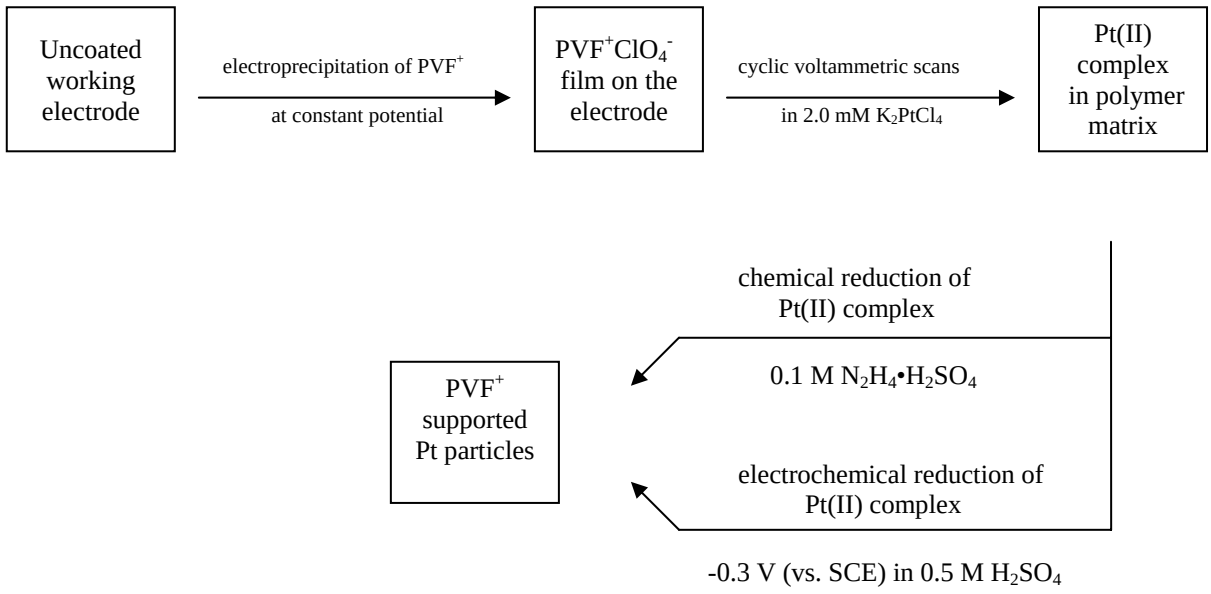

Scheme 7.1. Schematic procedure for the preparation of PVF^+ supported Pt particles using K_2PtCl_4.

In order to evaluate the effect of PVF^+ support on the performance of the catalyst, oxidation of methanol was recorded with and without use of PVF^+ during the preparation of the catalyst (Figure 7.3). In the CV shown in Figure 7.3.a, Pt particles were deposited directly onto the uncoated Pt disc electrode by cyclic voltammetric scans in K_2PtCl_4 solution. The CV shown in Figure 7.3.b was recorded with the PVF^+ supported electrocatalyst which was prepared according to the procedure described in Scheme 7.1. Two peaks of methanol oxidation were observed at the potentials +0.56 V and +0.52 V vs. SCE respectively from curve b in the figure. The shape of the CV and the peak potential values are consistent with the data in the literature (Fıçıcıoğlu and Kadırgan, 1997; Niu et al., 2005; Selvaraj and Alagar, 2007; Cao et al., 2007; Sivakumar, 2007; Pang et al., 2008). The onset potential of methanol oxidation was observed at 0.30 V which is in agreement with other work cited. Presence of the polymer support in the catalyst

greatly enhanced the oxidation peak current of methanol. This enhancement can be attributed to three effects: (1) as being a positively charged polymer matrix, the negatively charged Pt complexes can be more easily immobilized into the polymer, (2) as being a redox polymer, poly(vinylferrocene) acts as a mediator and increases the catalytic activity of the Pt/PVF^{+} catalyst, and, (3) as being in a porous structure, the polymer supplies an appropriate matrix for the Pt particles.

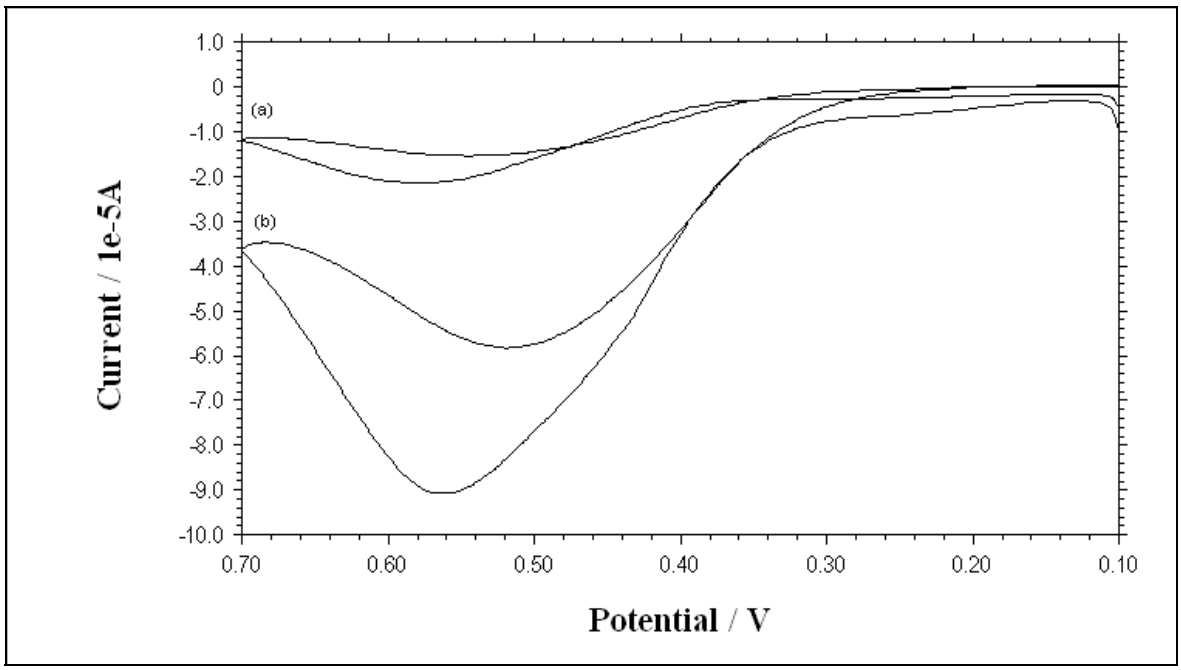

Figure 7.3. CVs of 0.5 M CH_3OH solution containing 0.5 M H_2SO_4 recorded with (a) Pt black on uncoated Pt disc electrode and (b) Pt/PVF^{+} catalyst on Pt disc electrode. Scan rate: 5 mV s^{-1}.

7.2.1.1. Pt disc as the working electrode

Pt disc was used as the first electrode material. Figure 7.4 shows cyclic voltammetric behavior of 0.5 M CH_3OH solution containing 0.5 M H_2SO_4 recorded with uncoated Pt disc electrode. As seen in the figure, bulk Pt does not show catalytic activity towards oxidation of methanol.

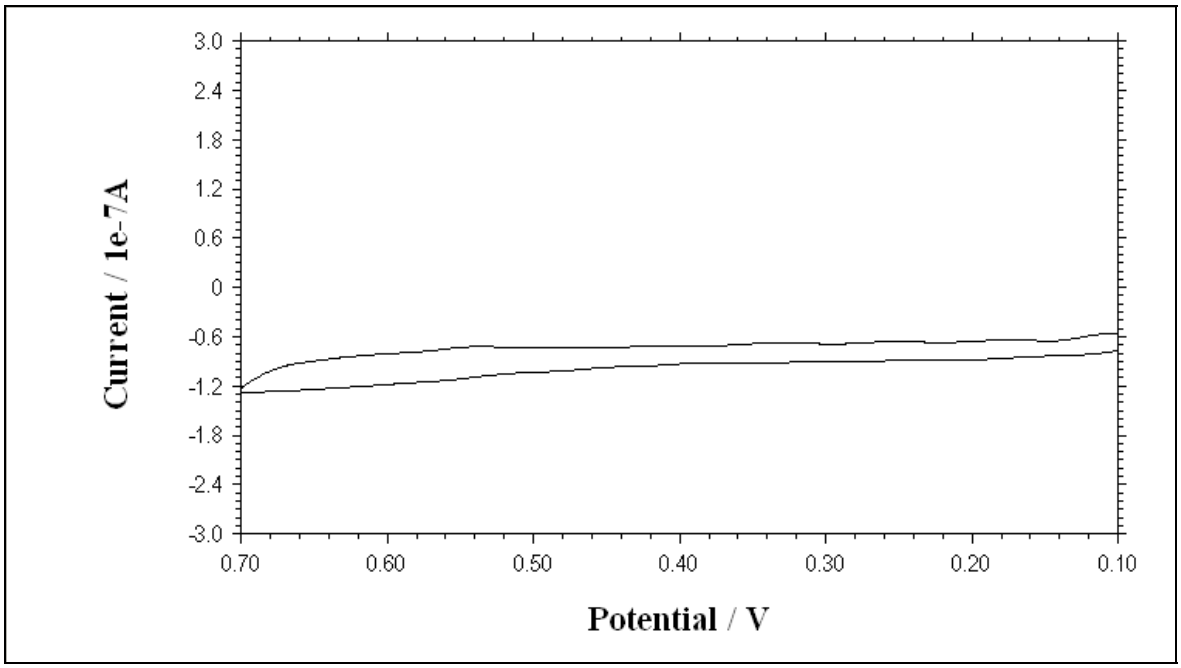

Figure 7.4. CV of 0.5 M CH_3OH solution containing 0.5 M H_2SO_4 recorded with uncoated Pt disc electrode. Scan rate: 5 mV s^{-1}.

After electrodeposition of PVF^+ onto the electrode surface, Pt particles were incorporated into the polymer matrix via cyclic voltammetric scans in aqueous 2 mM K_2PtCl_4 solution without supporting electrolyte. In Figure 7.5, CVs of the film before and after incorporation of $PtCl_4^{2-}$ are given in 0.1 M NaCl solution. Oxidation and reduction peaks of Pt complex species are observed at potentials +0.86 V, -0.21 V, -0.69 V and -0.67 V vs. SCE (Figure 7.5.b). It can be concluded that Pt complex species can be successfully immobilized in the polymer matrix by cyclic voltammetric scans.

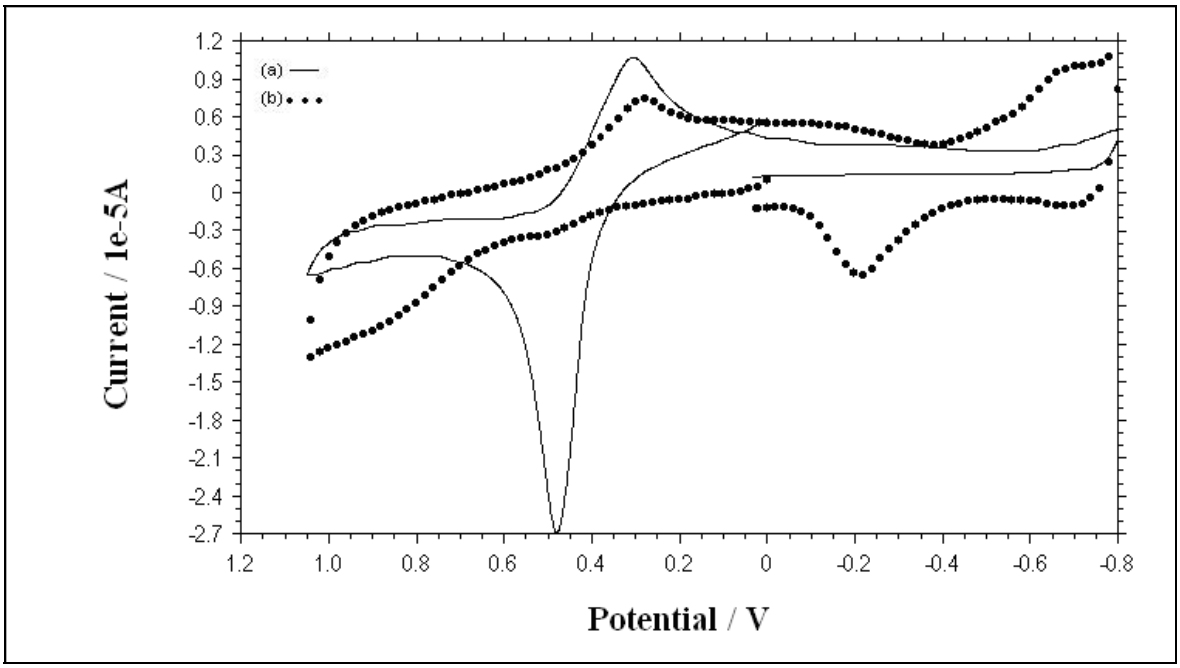

Figure 7.5. CVs of $PVF^+ClO_4^-$ film (a) before incorporation of $PtCl_4^{2-}$, (b) after incorporation of $PtCl_4^{2-}$ in 0.1 M NaCl solution. Scan rate: 100 mV s^{-1}.

Two separate methods were used for reduction of Pt particles. In the first method, polymer coated electrode containing Pt complex was immersed in 0.1 M $N_2H_4 \cdot H_2SO_4$ solution stirred continuously at open circuit. In the second method, Pt particles were electrochemically reduced in 0.5 M H_2SO_4 solution. Figure 7.6 shows CVs of the Pt/PVF^+ electrocatalysts prepared by (a) chemical reduction and (b) electrochemical reduction. The peaks except oxidation and reduction of the polymer at +0.36 V and +0.49 V vs. SCE and the oxidation peak at +0.26 V vs. SCE belong to the Pt particles. The oxidation peak at +0.26 V (Figure 7.6.a) is not observed after the first cycle. This peak belongs to the irreversible electrocatalytic oxidation of the adsorbed $N_2H_4 \cdot H_2SO_4$ during chemical reduction on Pt/PVF^+ catalyst.

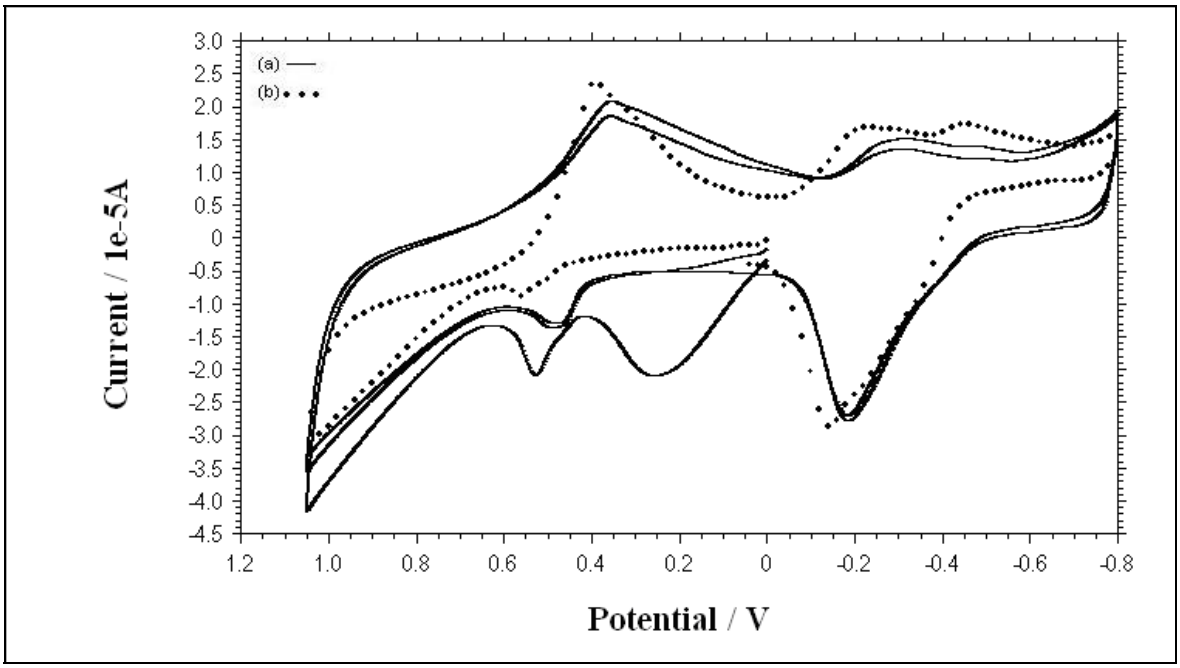

Figure 7.6. CVs of Pt/PVF^+ catalysts prepared by (a) chemical reduction, (b) electrochemical reduction in 0.1 M NaCl solution. Scan rate: 100 mV s^{-1}.

Optimization of experimental parameters

Each experimental parameter was optimized according to the oxidation peak current values at +0.56 V vs. SCE recorded with 0.5 M CH_3OH solution containing 0.5 M H_2SO_4 as the supporting electrolyte. The other parameters were kept constant.

Polymer film thickness

Effect of polymer film thickness was studied by the charge passed during the electroprecipitation of oxidized form of the polymer onto the electrode surface. A charge of $1x10^{-3}$ C corresponded to $1.32x10^{-6}$ moles of the oxidized PVF per cm^2 (dry thickness of ~300 μm, which corresponds to about $3x10^5$ layers) (Peerce and Bard, 1980). The other experimental conditions were 30 cyclic voltammetric scans in 2 mM K_2PtCl_4 solution, 60 min reduction time in 0.1 M $N_2H_4 \cdot H_2SO_4$ solution at ambient temperature. A polymer film thickness corresponding to a charge of 0.8 mC gave the maximum oxidation peak current for methanol (Figure 7.7).

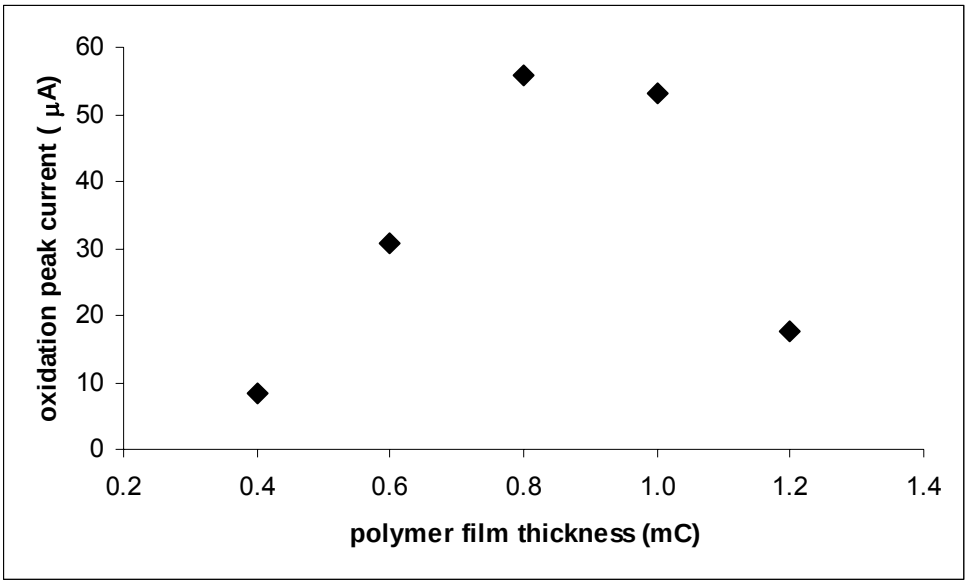

Figure 7.7. Effect of polymer film thickness on oxidation peak current of methanol (30 cyclic voltammetric scans, 60 min chemical reduction time, ambient reduction temperature).

Number of cyclic voltammetric scans in K_2PtCl_4 solution

Number of cyclic voltammetric scans in K_2PtCl_4 solution was the most important parameter as it directly influenced the number of Pt particles immobilized into the polymer matrix. Effect of number of cyclic voltammetric scans on oxidation peak current of methanol was studied for 5 to 45 cycles. The other parameters were kept constant as 0.8 mC polymer film thickness and 60 min reduction time in 0.1 M $N_2H_4 \cdot H_2SO_4$ solution at ambient temperature. As seen in Figure 7.8, the oxidation peak current of methanol increased until 30 cycles and decreased afterwards.

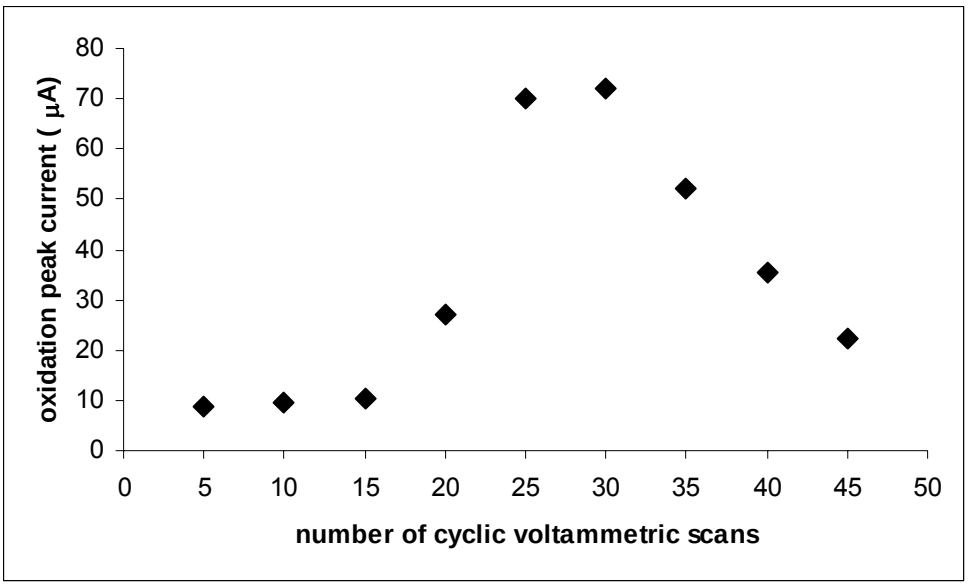

Figure 7.8. Effect of number of cyclic voltammetric scans on oxidation peak current of methanol (0.8 mC polymer film thickness, 60 min chemical reduction time, ambient reduction temperature).

Chemical reduction time

Chemical reduction of Pt particles was done using 0.1 M $N_2H_4 \cdot H_2SO_4$ solution for 15 to 90 min. The other experimental conditions were 0.8 mC polymer film thickness, 30 cyclic voltammetric scans in K_2PtCl_4 solution and ambient reduction temperature. As it can be seen from Figure 7.9, oxidation peak current increased until 60 min, and remained almost constant after this time. So, 60 min reduction in $N_2H_4 \cdot H_2SO_4$ solution was optimum for electrooxidation of methanol.

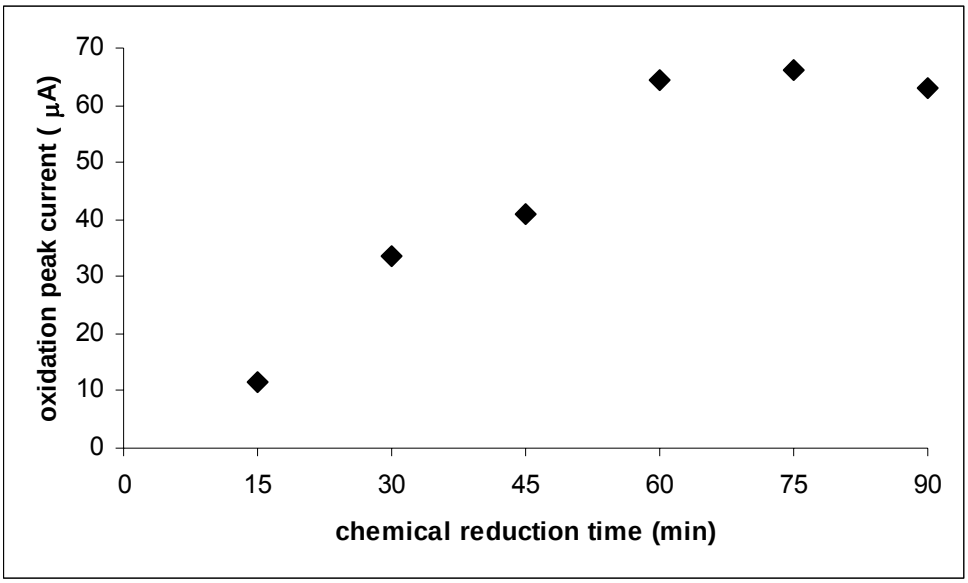

Figure 7.9. Effect of chemical reduction time in 0.1 M $N_2H_4 \cdot H_2SO_4$ solution on oxidation peak current of methanol (0.8 mC polymer film thickness, 30 cyclic voltammetric scans, ambient reduction temperature).

Chemical reduction temperature

Effect of chemical reduction time was studied between 25 ^{o}C and 75 ^{o}C. Oxidation peak current reached a maximum at 40 ^{o}C and decreased at higher temperatures (Figure 7.10).

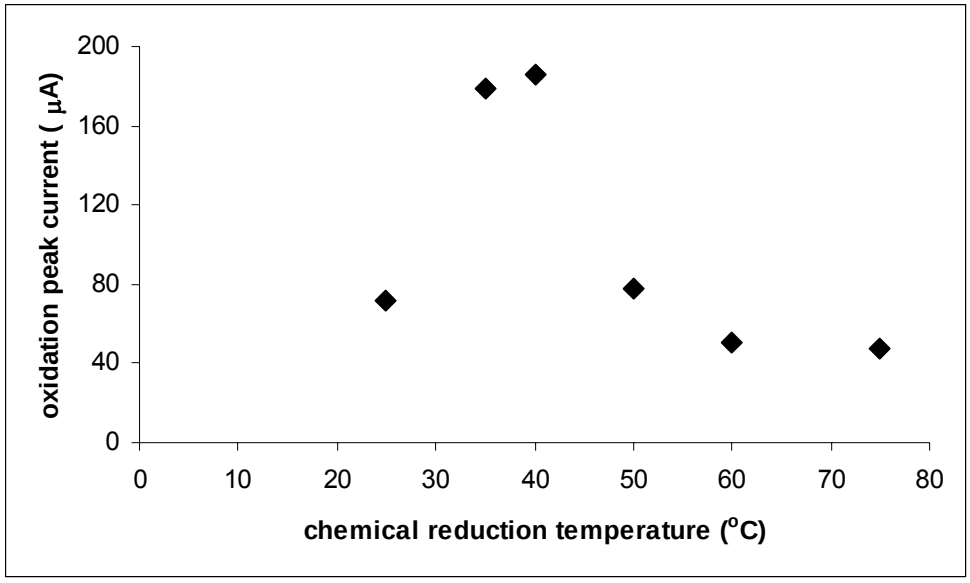

Figure 7.10. Effect of chemical reduction temperature in 0.1 M $N_2H_4 \cdot H_2SO_4$ solution on oxidation peak current of methanol (0.8 mC polymer film thickness, 30 cyclic voltammetric scans, 60 min reduction time).

Electrochemical reduction potential

Electrochemical reduction of Pt particles was also studied and compared with chemical reduction. For this purpose, Pt particles were reduced in 0.5 M H_2SO_4 solution which was stirred continuously. Experimental conditions were 0.8 mC polymer film thickness, 30 cyclic voltammetric scans in K_2PtCl_4 solution, 15 min electrochemical reduction at ambient temperature. Oxidation peak current of methanol vs. reduction potential is presented in Figure 7.11 between potentials -0.20 V to -0.40 V vs. SCE. Maximum oxidation peak current was obtained at -0.30 V vs. SCE.

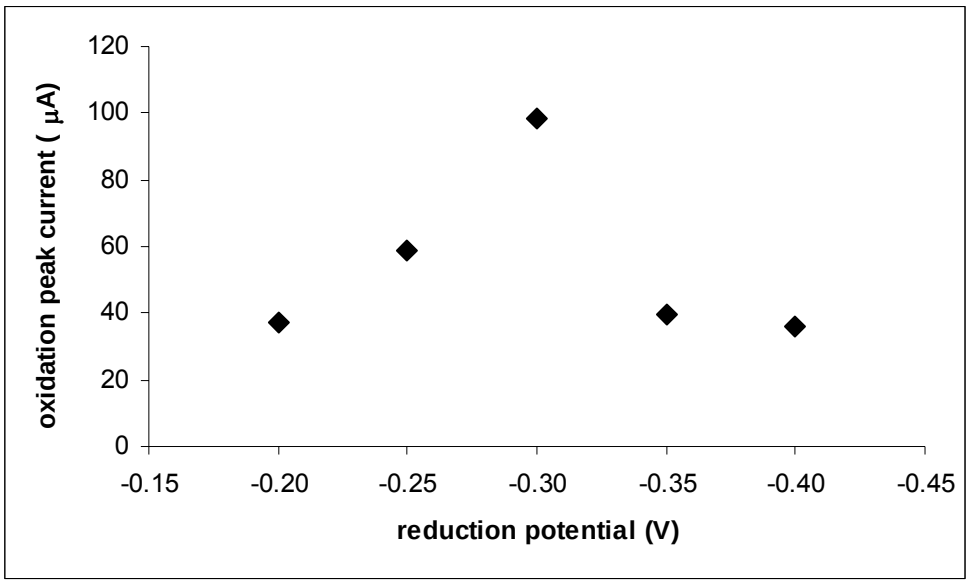

Figure 7.11. Effect of electrochemical reduction potential on oxidation peak current of methanol (0.8 mC polymer film thickness, 30 cyclic voltammetric scans, 15 min electrochemical reduction at ambient temperature).

Electrochemical reduction time

In order to evaluate optimum electrochemical reduction time, Pt particles were electrochemically reduced for 5 to 25 min at -0.3 V vs. SCE in 0.5 M H_2SO_4 solution. Maximum oxidation peak current was obtained for 15 min reduction time (Figure 7.12).

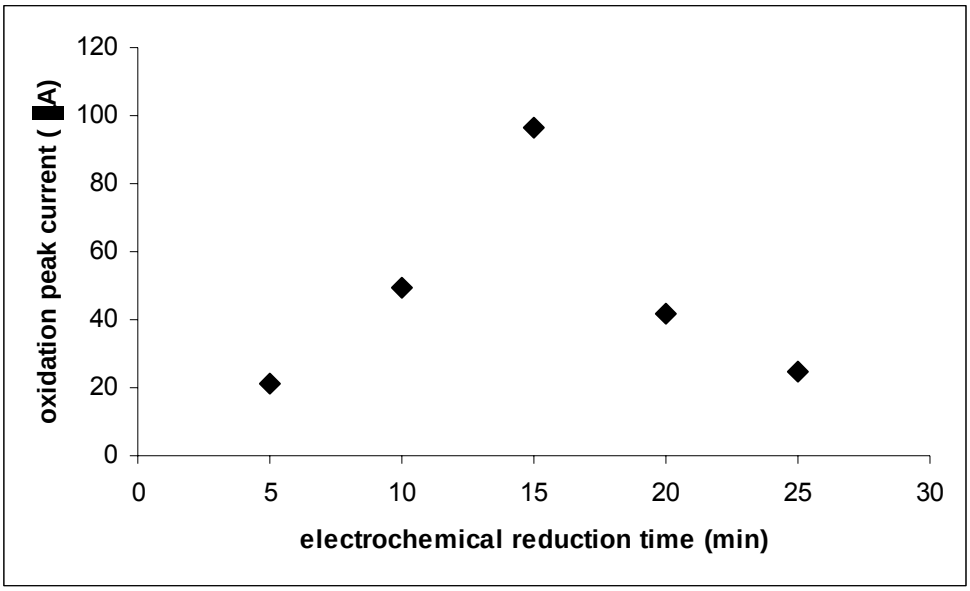

Figure 7.12. Effect of electrochemical reduction time on oxidation peak current of methanol (0.8 mC polymer film thickness, 30 cyclic voltammetric scans, -0.30 V electrochemical reduction potential vs. SCE, ambient temperature).

Comparison of chemical and electrochemical reduction methods

In Figure 7.13, comparison of the two reduction methods is presented. It is known that Pt adsorbs a monoatomic H layer and this allows for the evaluation of the electrochemically active surface area of electrodes. However, Pt is also known to absorb molecular hydrogen which is one of the products in the electrochemical reduction of Pt particles. This property of Pt metal is a disadvantage in electrodeposition processes leading to high internal stress in the deposits (Rao and Trivedi, 2005). Consistent with this property, the electrocatalyst system prepared by reduction in $N_2H_4 \cdot H_2SO_4$ solution gives higher oxidation peak current and chemical reduction is more convenient for obtaining Pt particles on PVF^+.

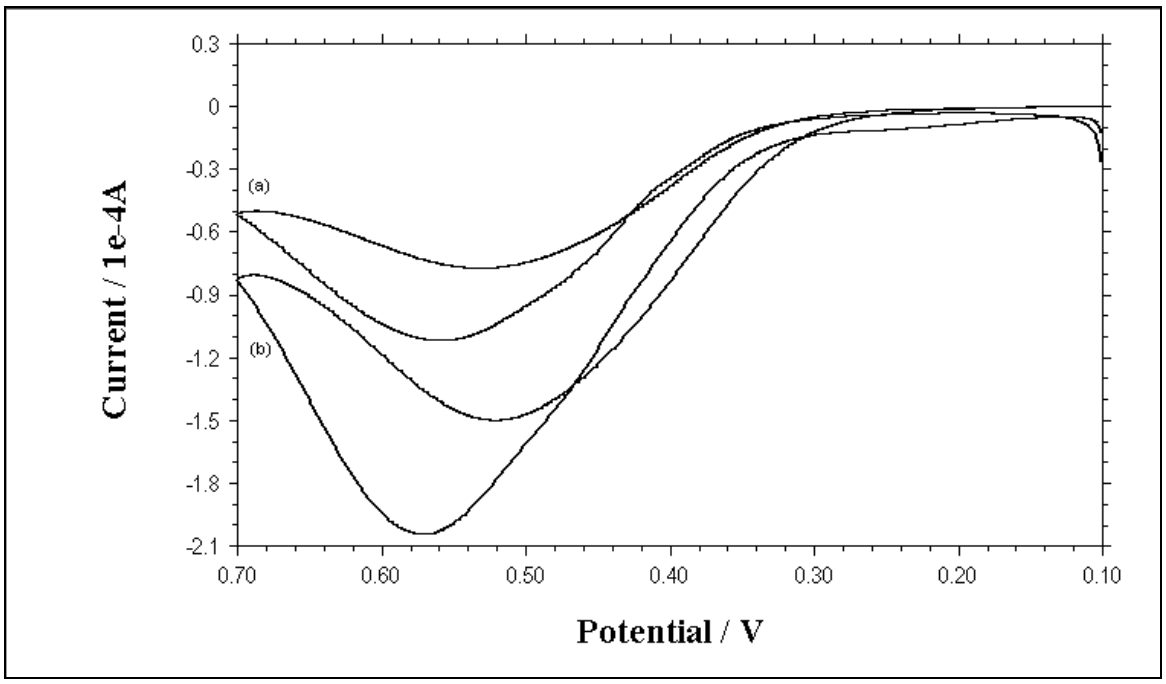

Figure 7.13. CVs of 0.5 M CH_3OH solution containing 0.5 M H_2SO_4 recorded with Pt/PVF^+ catalysts prepared by (a) electrochemical reduction, (b) chemical reduction. Scan rate: 5 mV s^{-1}.

Electrochemical characterization of the catalyst

Cyclic voltammetric behavior of 0.5 M H_2SO_4 solution was recorded using (a) uncoated Pt disc electrode, (b) PVF^+ coated Pt disc electrode, (c) electrochemically reduced Pt particles on PVF^+ and (d) chemically reduced Pt particles on PVF^+. The CVs are presented in Figure 7.14. In the voltammograms, oxidation of Pt was observed in the region 0.00 V – +1.00 V vs. SCE. The oxidation and reduction peaks observed at +0.48 V and +0.32 V are related to electrochemical oxidation and reduction of the polymer, respectively. Between 0.00 V and -0.25 V vs. SCE, oxidation and reduction behavior of weakly and strongly adsorbed hydrogen on Pt/PVF^+ catalyst was observed. This redox behavior in H_2SO_4 solution is typical for Pt nanoparticles (Perez et al., 1998; Pozio et al., 2002; Ioroi et al., 2002; Chang et al., 2007).

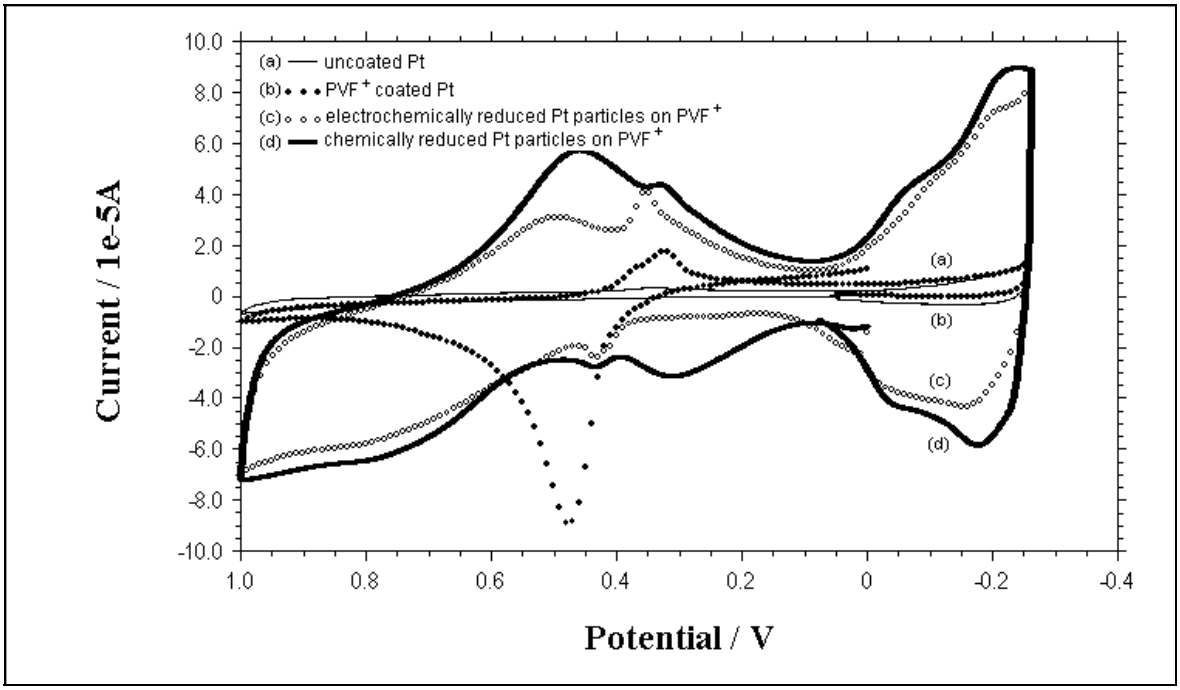

Figure 7.14. CVs of 0.5 M H_2SO_4 solution recorded with (a) uncoated Pt disc electrode, (b) PVF^+ coated Pt disc electrode, (c) electrochemically reduced Pt particles on PVF^+, and (d) chemically reduced Pt particles on PVF^+. Scan rate: 100 mV s^{-1}.

Figure 7.15 shows CVs of 0.5 M H_2SO_4 solution recorded with Pt/PVF^+ catalysts having different amounts of Pt. The amount of Pt was controlled by the number of cyclic voltammetric scans in K_2PtCl_4 solution during catalyst preparation. As we expected, the oxidation and reduction peak current values of hydrogen recorded with the catalyst having optimum amount of Pt (corresponding to 30 cycles in K_2PtCl_4 in Figure 7.8) were considerably high with respect to the others.

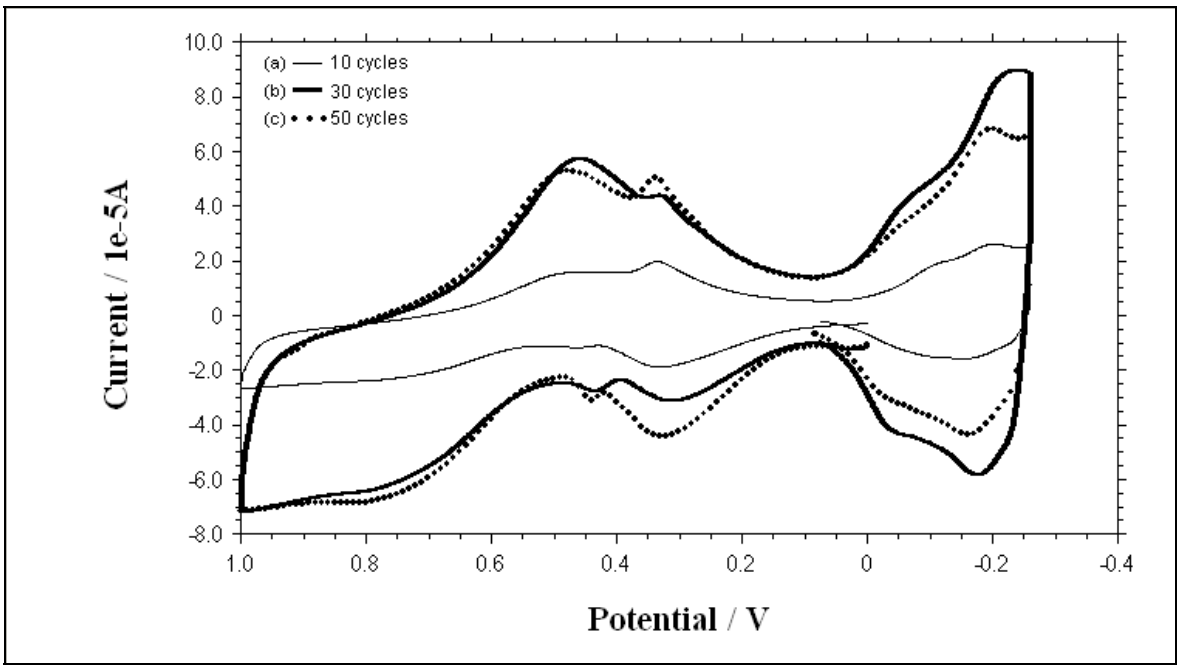

Figure 7.15. CVs of 0.5 M H_2SO_4 solution recorded with Pt/PVF^+ catalysts with Pt loadings corresponding to (a)10 (b)30 (c)50 cycles in K_2PtCl_4 solution (0.8 mC polymeric film thickness, 60 min reduction time in $N_2H_4 \cdot H_2SO_4$ solution). Scan rate: 100 mV s^{-1}.

7.2.1.2. GCE as the working electrode

GCE was used as the second electrode material. Figure 7.16 shows cyclic voltammetric behavior of 0.5 M CH_3OH solution containing 0.5 M H_2SO_4 recorded with Pt/PVF^+ catalyst on GCE.

Two peaks of methanol oxidation were observed at the potentials +0.61 V and +0.57 V vs. SCE respectively. The onset potential of methanol oxidation was observed at +0.40 V. If the two electrode materials are compared, it can be concluded that Pt disc electrode gives better results by means of potential values.

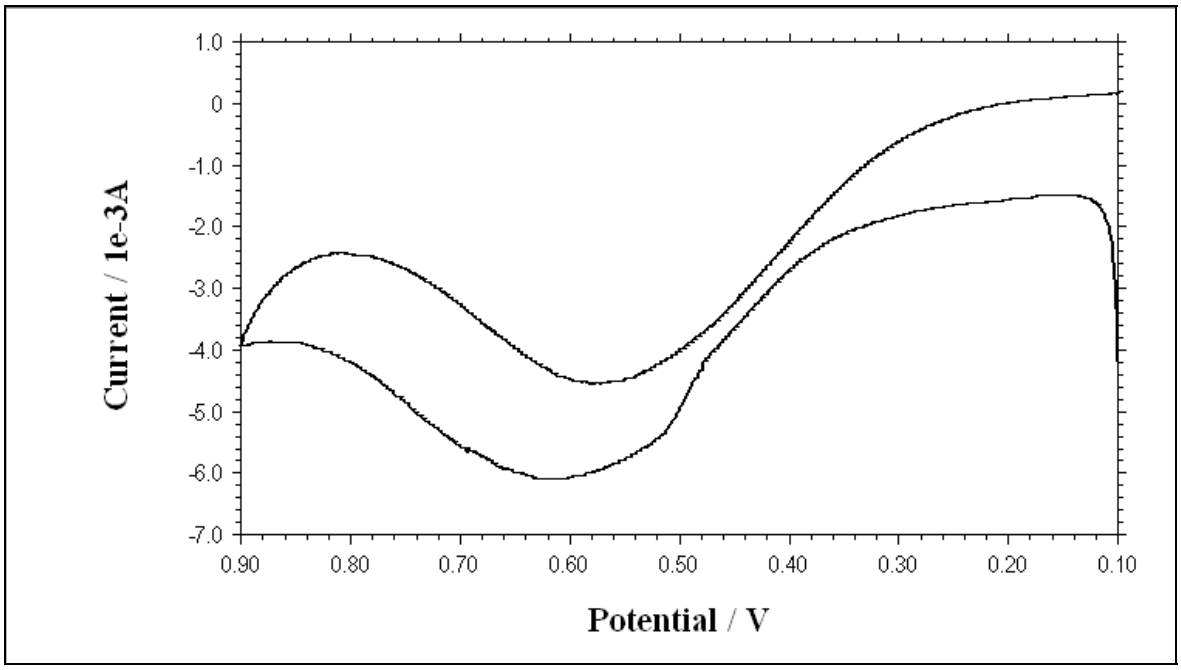

Figure 7.16. CV of 0.5 M CH_3OH solution containing 0.5 M H_2SO_4 recorded with Pt/PVF^+ catalyst on GCE. Scan rate: 5 mV s^{-1}.

Optimization of experimental parameters

Similar to the studies with Pt disc electrode, experimental parameters were optimized according to the oxidation peak current values at +0.61 V vs. SCE recorded with 0.5 M CH_3OH solution containing 0.5 M H_2SO_4 as the supporting electrolyte keeping the other parameters constant.

Polymer film thickness

Effect of polymer film thickness was studied between 30 mC and 70 mC (Figure 7.17). The other experimental conditions were 50 cyclic voltammetric scans in 2 mM K_2PtCl_4 solution, 60 min reduction time in 0.1 M $N_2H_4 \cdot H_2SO_4$ solution at 40 ^oC. Polymer film thickness corresponding to a charge of 50 mC gave the maximum oxidation peak current for methanol.

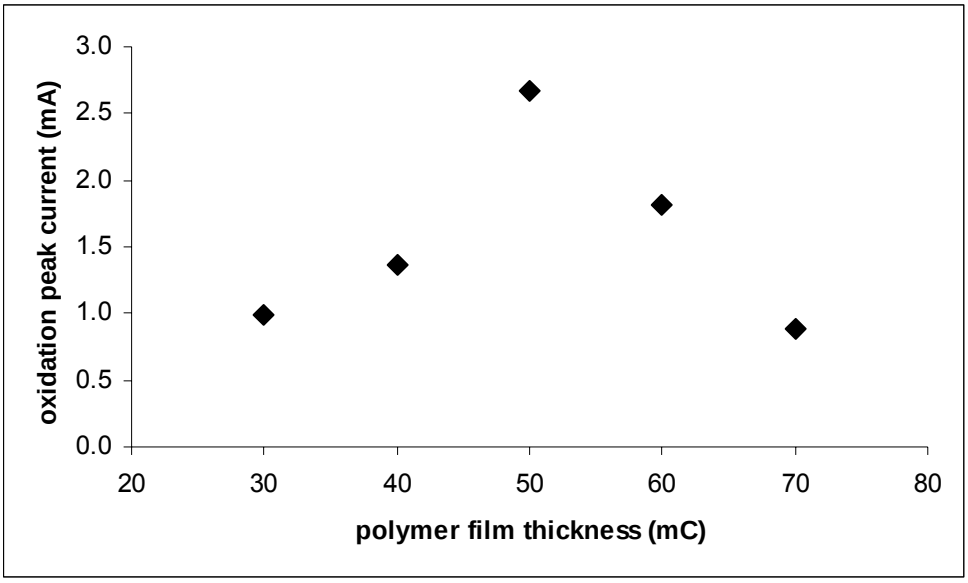

Figure 7.17. Effect of polymer film thickness on oxidation peak current of methanol (50 cyclic voltammetric scans, 60 min chemical reduction time, 40 ^oC reduction temperature).

Number of cyclic voltammetric scans in K_2PtCl_4 solution

Effect of number of cyclic voltammetric scans on oxidation peak current of methanol was studied for 30 to 90 cycles. The other parameters were kept constant as 50 mC polymer film thickness and 60 min reduction time in 0.1 M $N_2H_4 \cdot H_2SO_4$ solution at 40 ^oC. As seen in Figure 7.18, optimum number of cyclic voltammetric scans was determined as 70.

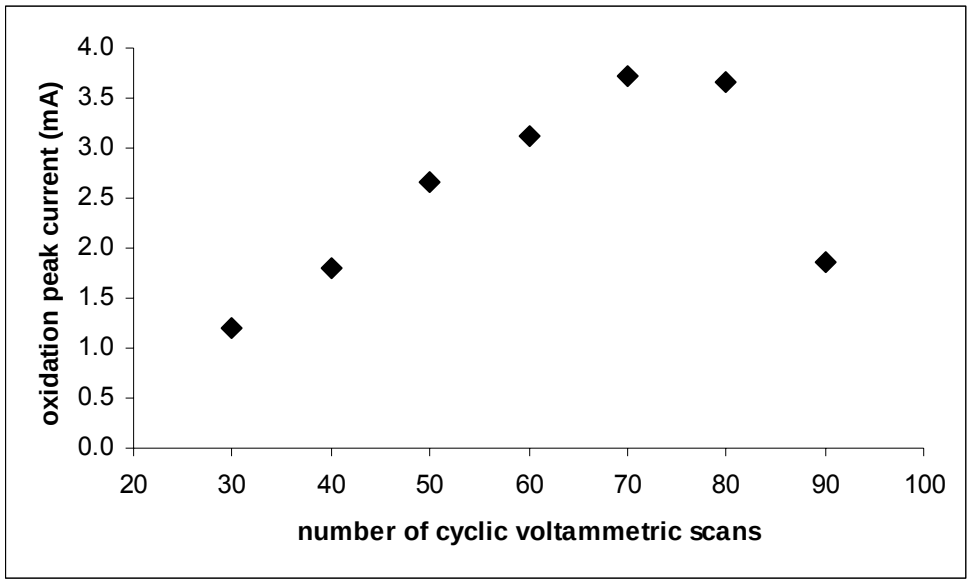

Figure 7.18. Effect of number of cyclic voltammetric scans on oxidation peak current of methanol (50 mC polymer film thickness, 60 min chemical reduction time, 40 ^oC reduction temperature).

Chemical reduction time

Chemical reduction of Pt particles was done using 0.1 M $N_2H_4 \cdot H_2SO_4$ solution for 15 to 90 min at 40 ^oC (Figure 7.19). The other experimental conditions were 50 mC polymer film thickness and 70 cyclic voltammetric scans in K_2PtCl_4 solution. Similar to the Pt disc electrode, oxidation peak current increased until 60 min, and remained nearly constant after this time.

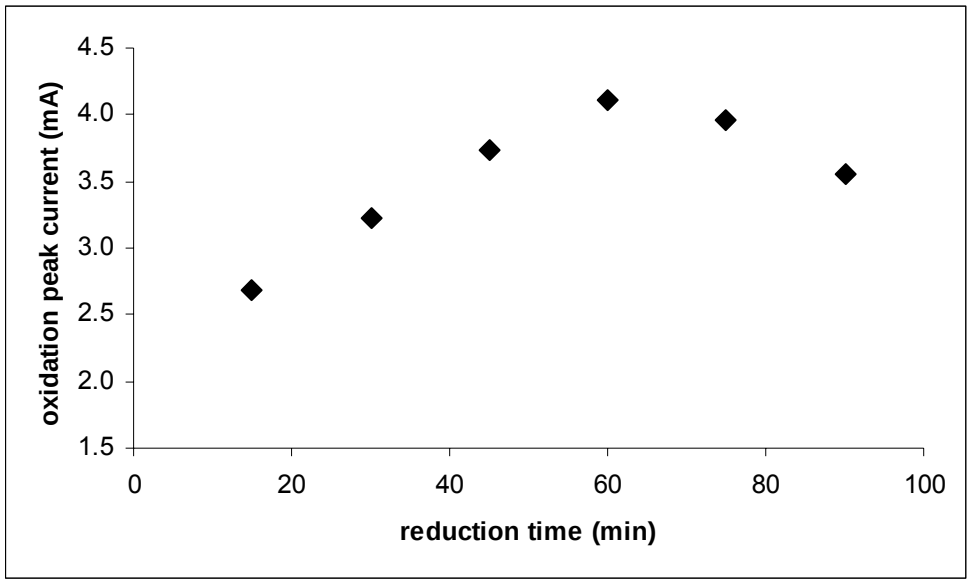

Figure 7.19. Effect of chemical reduction time in 0.1 M $N_2H_4 \cdot H_2SO_4$ solution on oxidation peak current of methanol (50 mC polymer film thickness, 70 cyclic voltammetric scans, 40 ^oC reduction temperature).

Electrochemical reduction time

In order to evaluate optimum electrochemical reduction time, Pt particles were electrochemically reduced for 5 to 25 min at -0.3 V vs. SCE in 0.5 M H_2SO_4 solution. Maximum oxidation peak current was obtained for 15 min (Figure 7.20).

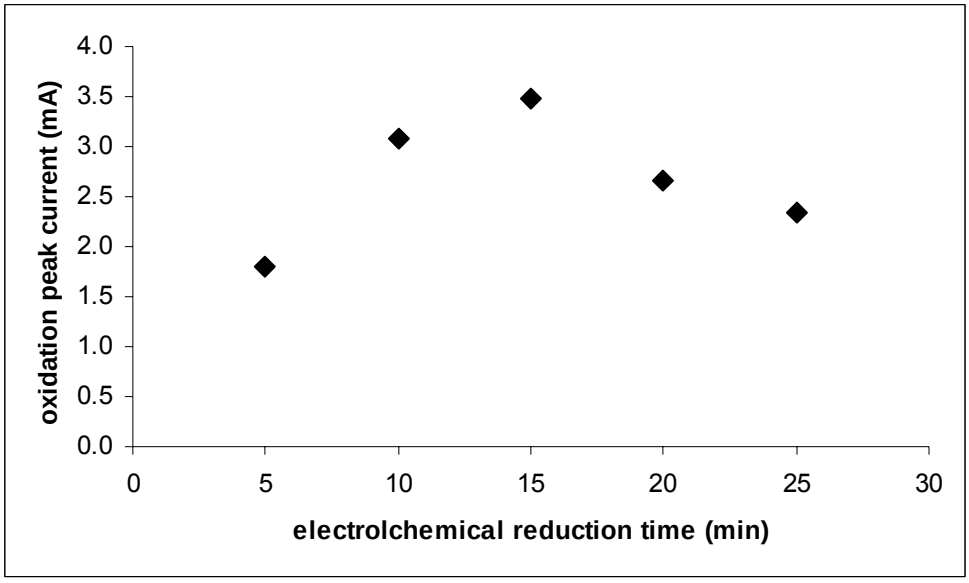

Figure 7.20. Effect of electrochemical reduction time on oxidation peak current of methanol (50 mC polymer film thickness, 70 cyclic voltammetric scans, -0.30 V electrochemical reduction potential vs. SCE, ambient temperature).

Comparison of chemical and electrochemical reduction methods

In Figure 7.21, comparison of the two reduction methods is presented. As expected, the electrocatalyst system prepared by reduction in hydrazine solution gave higher oxidation peak current with respect to electrochemical reduction.

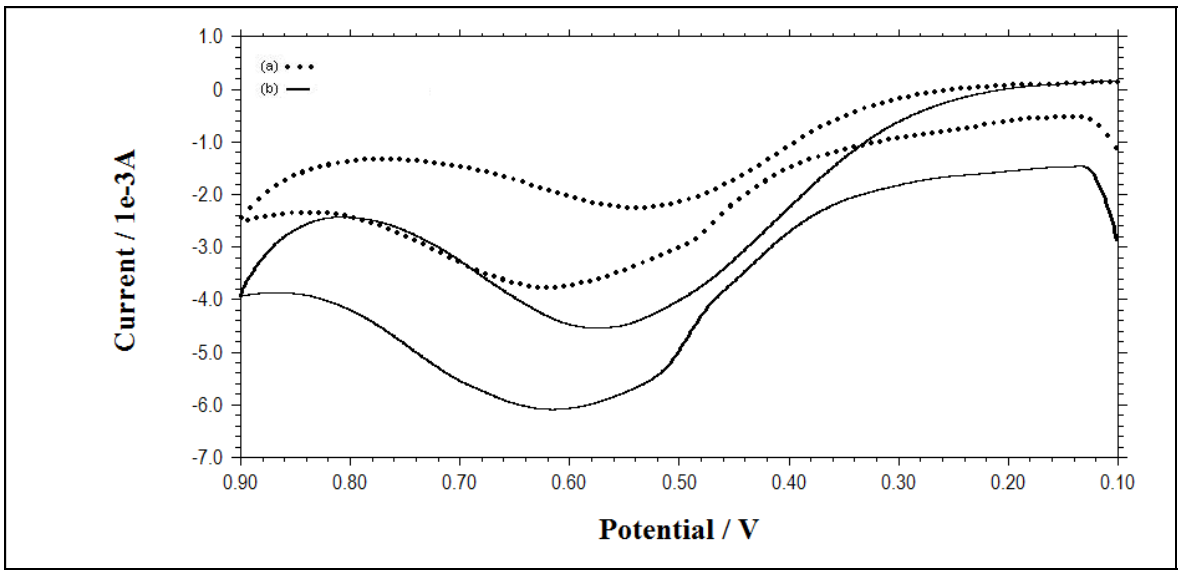

Figure 7.21. CVs of 0.5 M CH_3OH solution containing 0.5 M H_2SO_4 recorded with Pt/PVF^+ catalysts on GCE prepared by (a) electrochemical reduction, (b) chemical reduction. Scan rate: 5 mV s^{-1}.

Electrochemical characterization of the catalyst

Cyclic voltemmetric behavior of Pt/PVF^+ system on GCE in 0.5 M H_2SO_4 solution was recorded with (a) electrochemically reduced Pt particles in the polymer matrix and (b) chemically reduced Pt particles in the polymer matrix (Figure 7.22). However, oxidation and reduction behavior of weakly and strongly adsorbed hydrogen between 0.00 V and -0.25 V vs. SCE was not observed. According to the data, it was concluded that using Pt disc electrode instead of GCE was more convenient for preparation of Pt/PVF^+ catalysts.

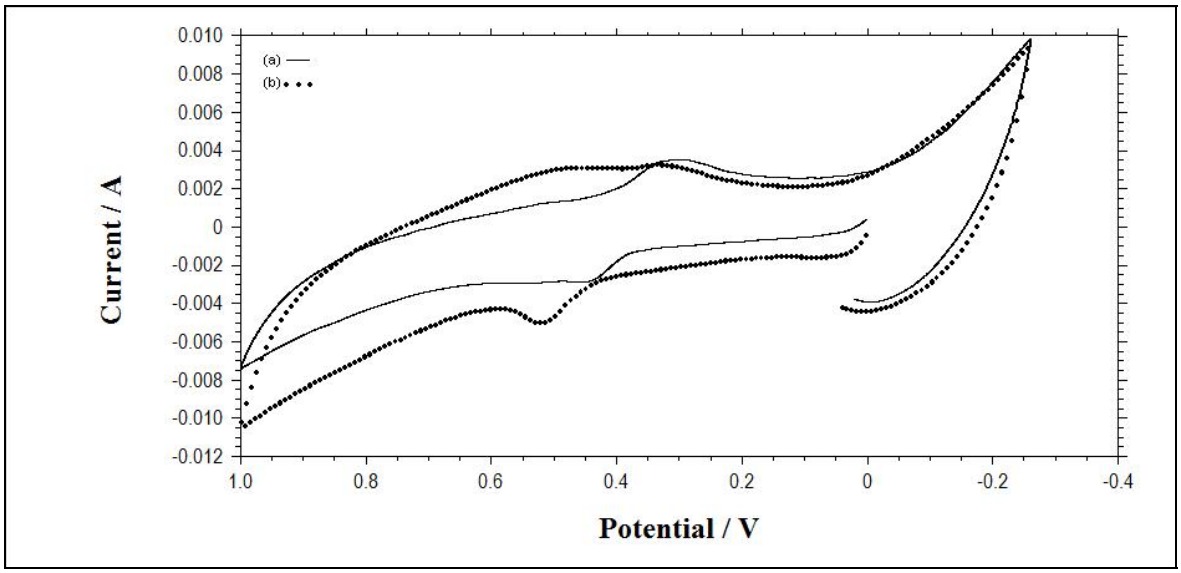

Figure 7.22. CVs of 0.5 M H_2SO_4 solution recorded with Pt/PVF^+ system on GCE prepared by (a) electrochemical reduction (b) chemical reduction.
Scan rate: 100 mV s^{-1}.

7.2.1.3. SEM images and EDS of Pt/PVF^+ catalysts prepared using K_2PtCl_4

Pt/PVF^+ catalysts were characterized by SEM method using Pt foil electrodes (3mmx3mm). SEM images $PVF^+ClO_4^-$ film having a thickness corresponding to 30 mC is given in Figure 7.23 in two different scales.

SEM images of Pt/PVF^+ catalysts prepared by chemical reduction and electrochemical reduction are represented in Figures 7.24 and 7.25 respectively. It can be concluded that Pt particles that were obtained by chemical reduction are at the nanoscale and well dispersed over the polymer film. However, the particles obtained by electrochemical reduction are not regularly dispersed and spherical.

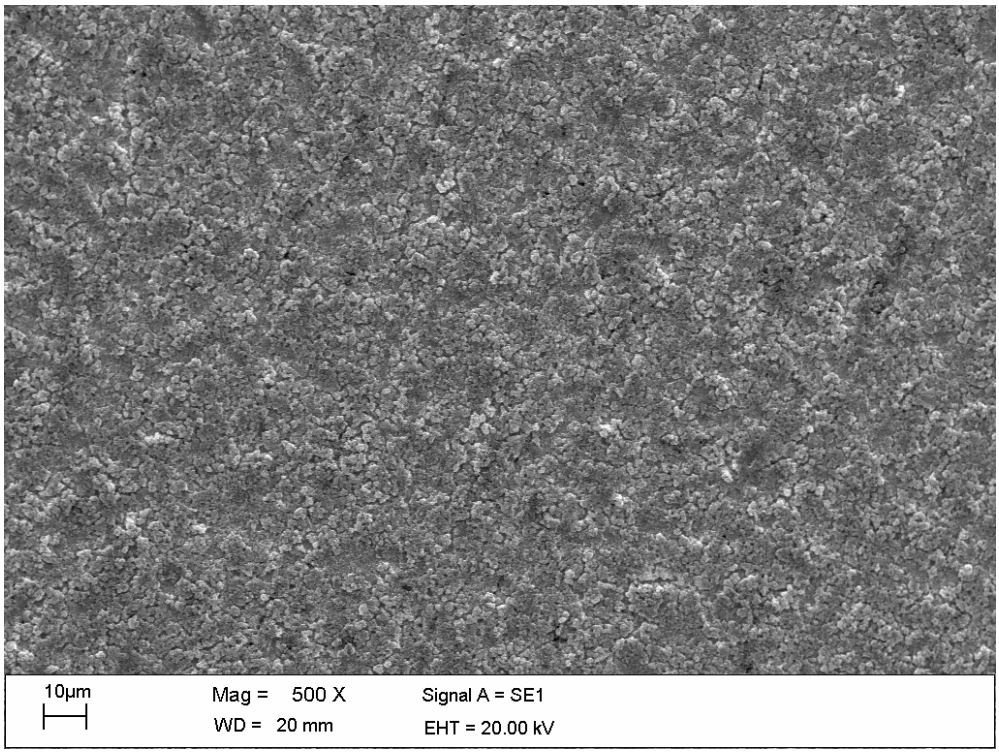

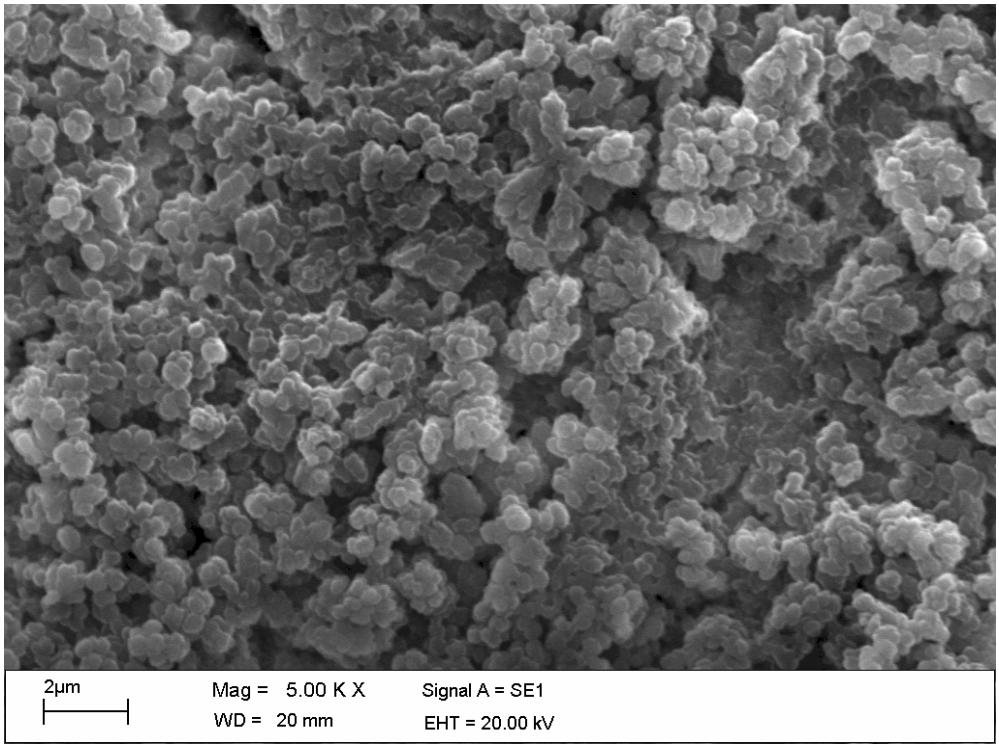

Figure 7.23. SEM images of $PVF^{+}ClO_4^{-}$ film on Pt foil electrode.

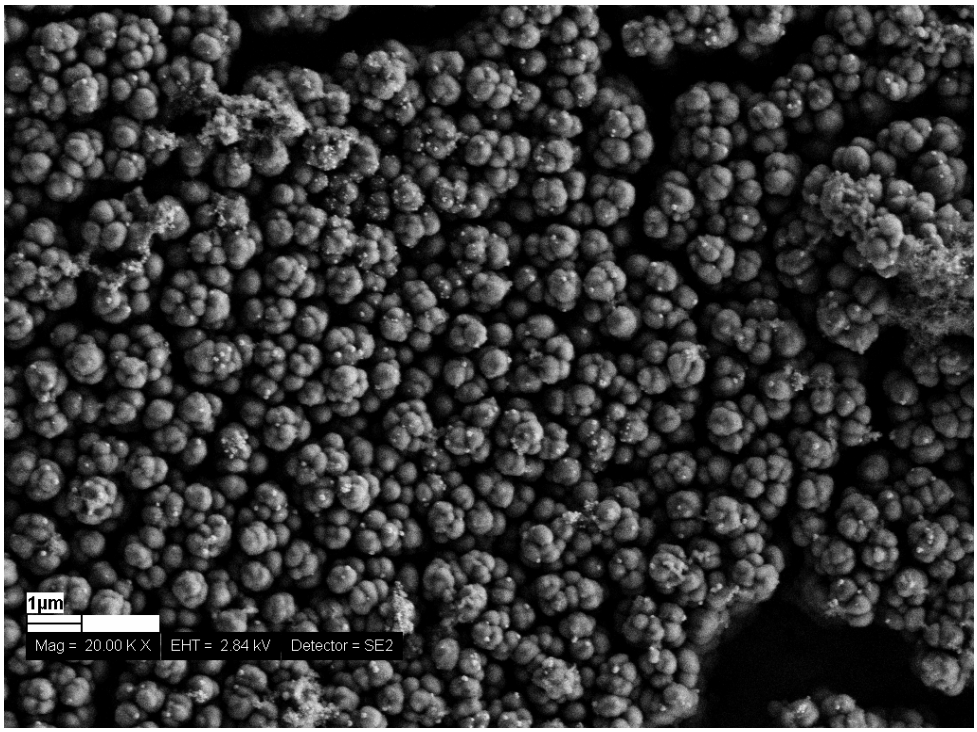

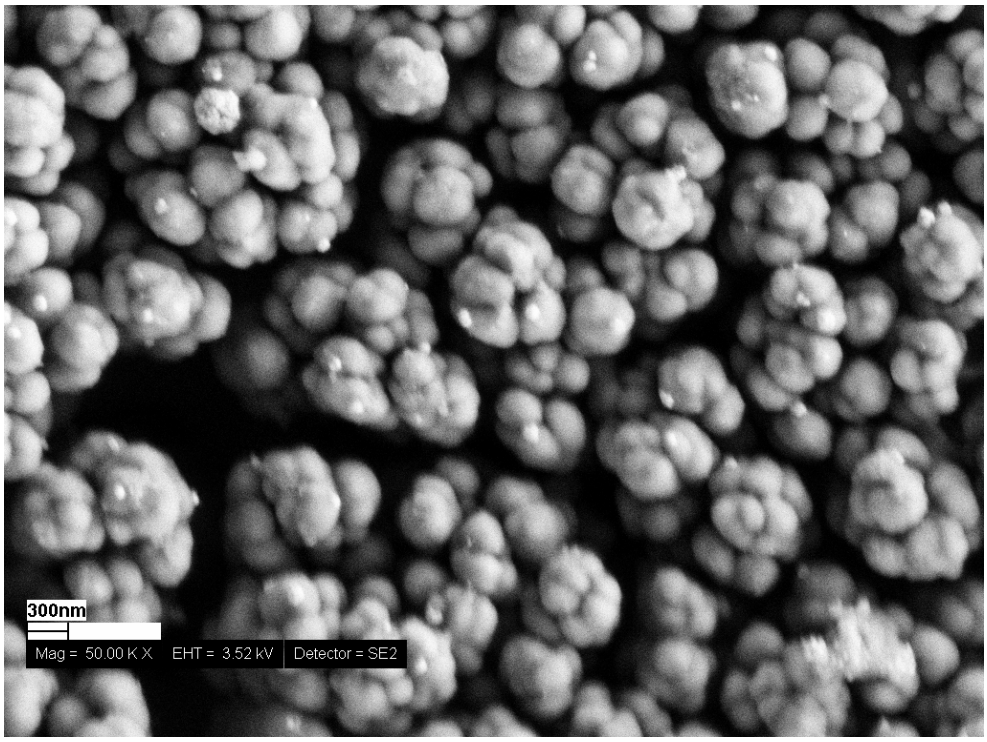

Figure 7.24. SEM images of Pt/PVF^{+} catalyst prepared by chemical reduction (30 mC polymer film thickness, 75 cyclic voltammetric scans, 60 min chemical reduction time, 40 ^{o}C reduction temperature).

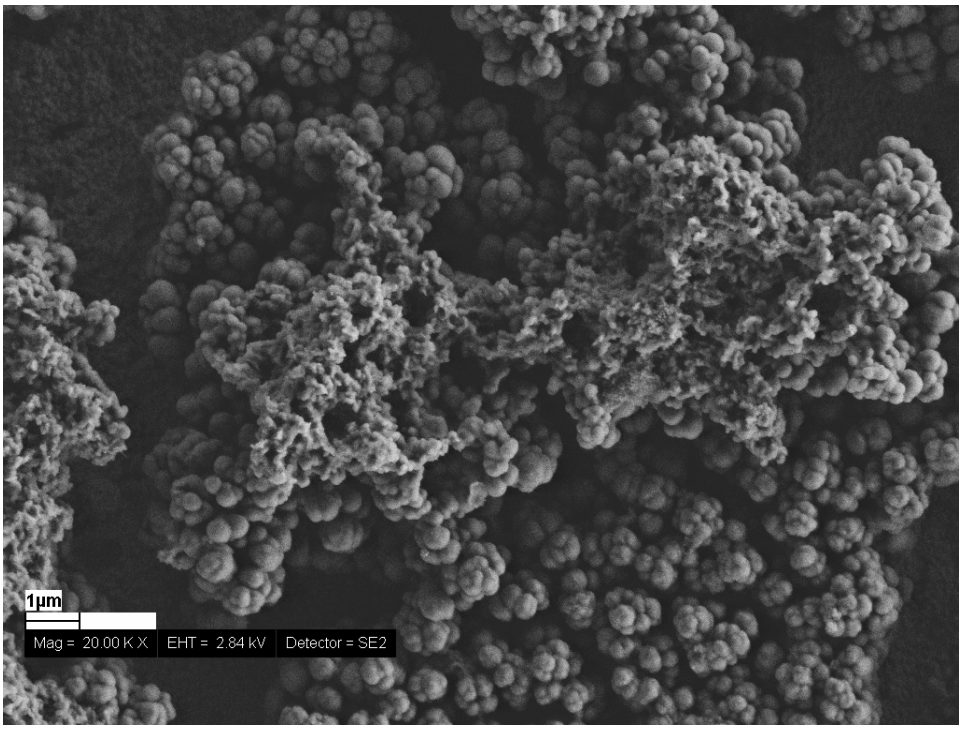

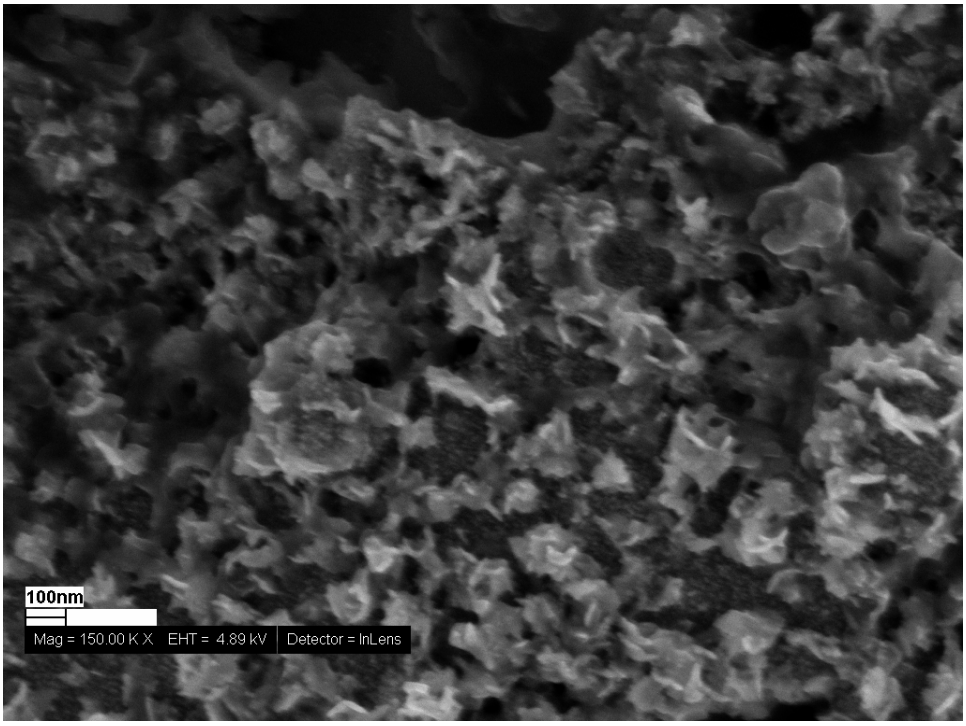

Figure 7.25. SEM images of Pt/PVF^{+} catalyst prepared by electrochemical reduction (30 mC polymer film thickness, 75 cyclic voltammetric scans, -0.3 V reduction potential, 15 min electrochemical reduction time, ambient reduction temperature).

EDS of the Pt/PVF^+ system is shown in Figure 7.26. The electrocatalyst was prepared on GCE (r = 0.3 cm) to avoid Pt peaks coming from the electrode material. The spectrum indicated that C, Fe and Pt were the major elements. While the C atoms come both from the electrode material and the polymer support, Fe atoms come from the ferrocenium groups of PVF^+ support and Pt atoms come from the Pt particles obtained by reduction of the $PtCl_4^{2-}$ complex. Quantitative analysis indicated that the ratio of Fe atoms to Pt atoms was 10:1.

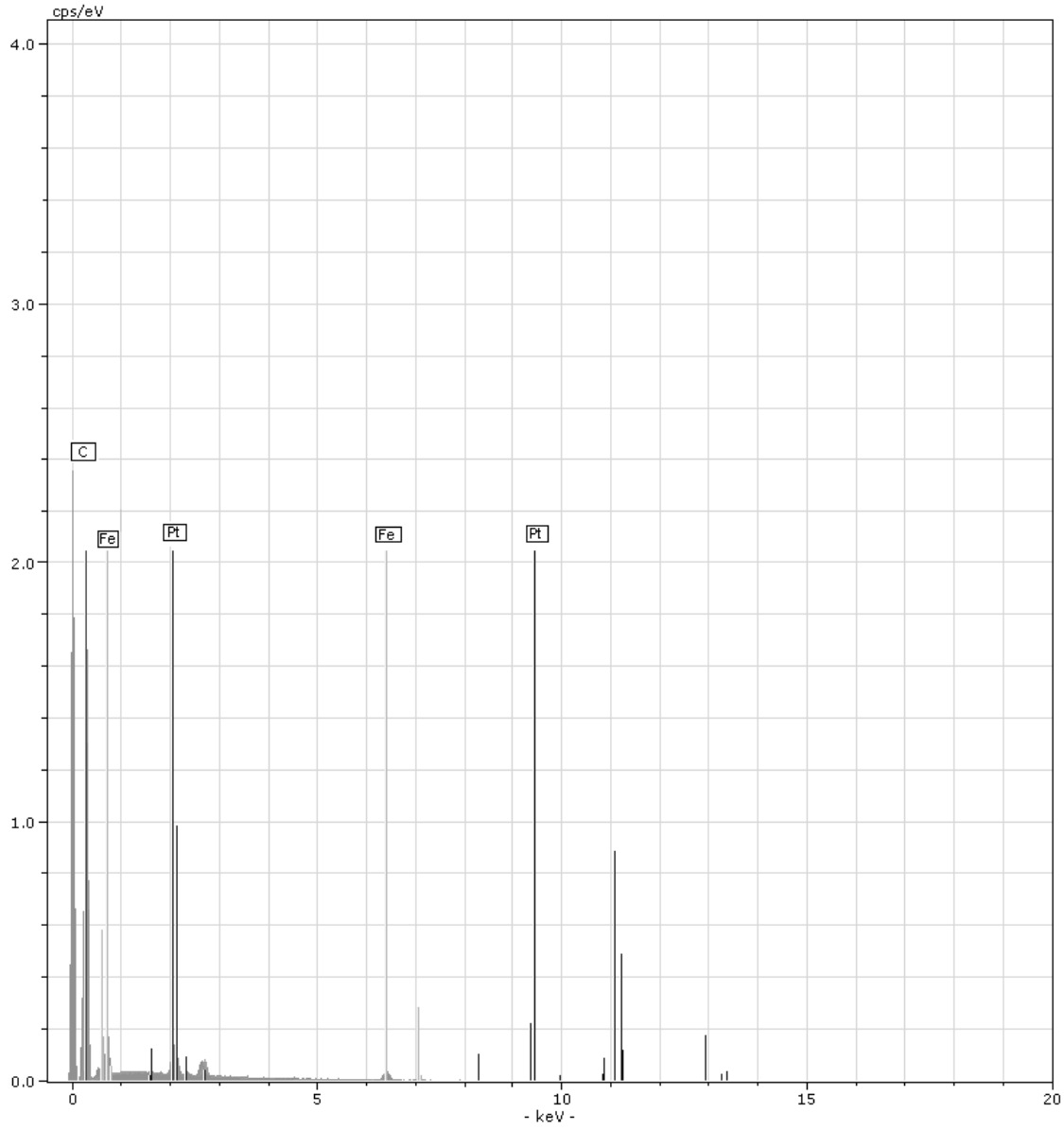

Figure 7.26 EDS of Pt/PVF^+ catalyst system prepared on GCE.

7.2.1.4. Fuel cell performances of Pt/PVF^+ catalysts prepared using K_2PtCl_4

DMFC mode

Pt/PVF^+ catalyst system prepared using K_2PtCl_4 was first tested in a single fuel cell configuration in DMFC mode at ambient temperature and atmospheric pressure. Experimental conditions during preparation of the catalyst were 100 mC polymer film thickness, 70 cyclic voltammetric scans, 60 min chemical reduction time and 40 ^oC reduction temperature. 2 M CH_3OH solution containing 0.5 M H_2SO_4 was used as the fuel and 0.5 M H_2SO_4 solution saturated with pure O_2 gas was used as the oxidant. The OCV was 680 mV for the system and the maximum power density was 0.310 mW cm^{-2} at 0.63 mA cm^{-2}. Current/voltage diagram for the fuel cell is given in Figure 7.27.

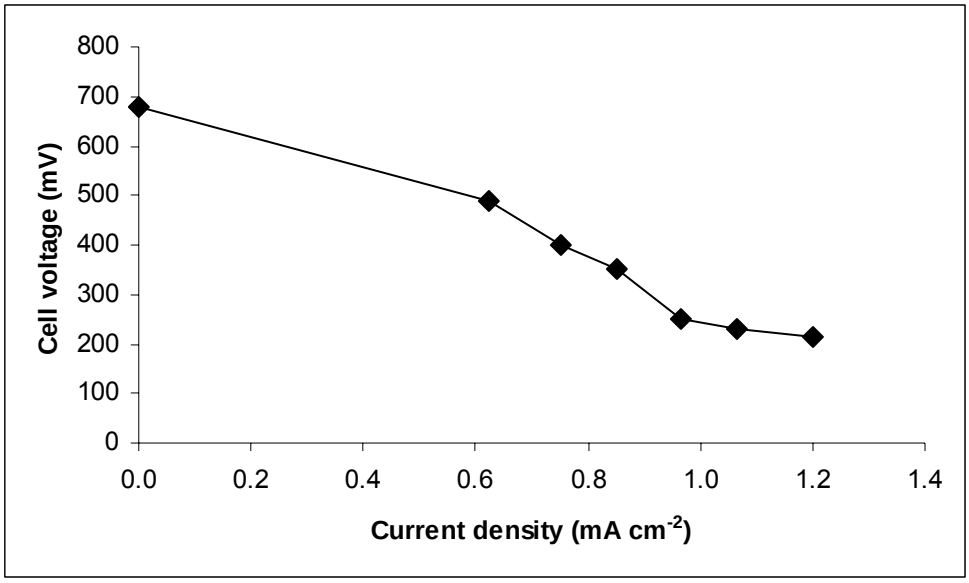

Figure 7.27 Current / voltage diagram for single DMFC using Pt/PVF^+ catalyst as anode and Pt black as cathode at ambient temperature and atmospheric pressure.

Additionally, PVF^+ support was compared with carbon support using the single fuel cell configuration in DMFC mode. For this purpose, C supported Pt particles were prepared at the same conditions using GCE as the support material. Despite the fact that C support is more conductive than the PVF^+ support, the OCV of the fuel cell using the C supported Pt particles as the anode catalyst was lower (540 mV).

DHFC mode

Pt/PVF^+ catalyst system was also tested in a single DHFC configuration at ambient temperature and atmospheric pressure using the same preparation conditions. Saturated aqueous solution of $NH_2{\cdot}NH_2{\cdot}H_2SO_4$ containing 0.1 M K_2SO_4 was used as the fuel and 0.1 M K_2SO_4 solution saturated with pure O_2 gas was used as the oxidant. The OCV was 190 mV for the system and the maximum power density was 0.224 mW cm^{-2} at 2.8 mA cm^{-2}. Current/voltage diagram for the cell is given in Figure 7.28.

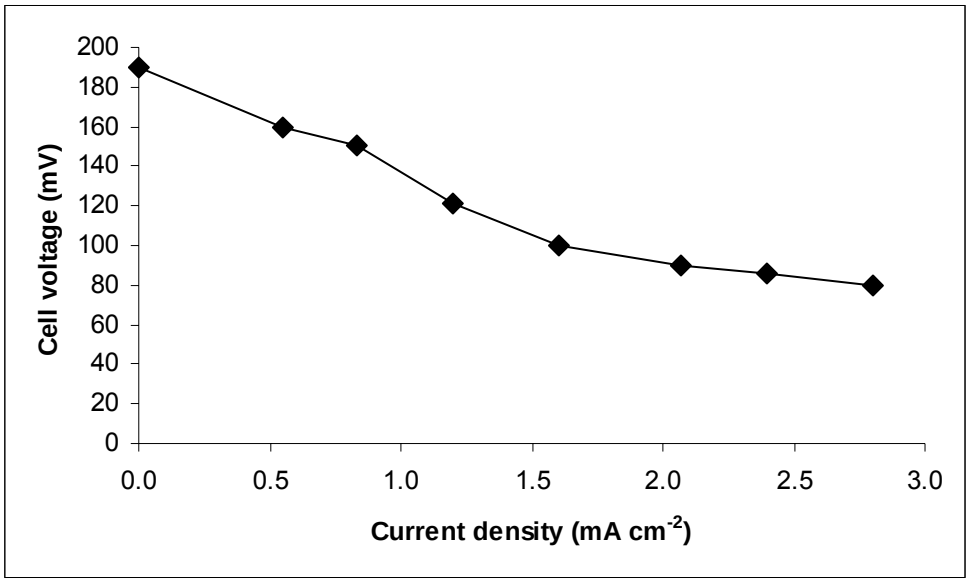

Figure 7.28 Current / voltage diagram for single DHFC using Pt/PVF^+ catalyst as anode and Pt black as cathode at ambient temperature and atmospheric pressure.

7.2.2. H_2PtCl_6 as the Pt precursor

Aqueous solution of $H_2PtCl_6 \cdot H_2O$ was also used as the Pt precursor in order to obtain Pt particles in the polymer matrix. Polycyclic voltammogram of 3 mM $H_2PtCl_6 \cdot H_2O$ solution containing 0.5 M H_2SO_4 is given in Figure 7.29 for 50 cycles recorded with polymer coated GCE. After incorporation of Pt complex into the polymer matrix, oxidation and reduction peaks of Pt particles at -0.047 V and -0.35 V vs. SCE observed in the CV of 0.1 M NaCl solution indicate the existence of the Pt species in the polymer matrix (Figure 7.30).

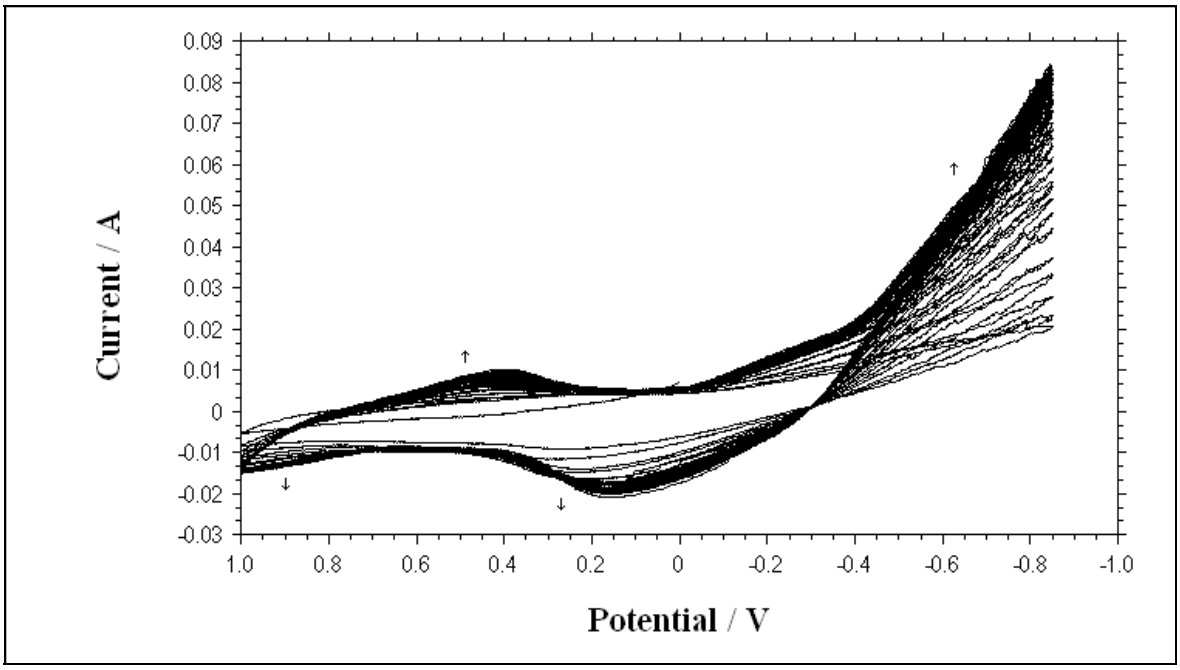

Figure 7.29. Polycyclic voltammogram of 3 mM $H_2PtCl_6 \cdot H_2O$ solution containing 0.5 M H_2SO_4 recorded with PVF^+ coated GCE. Scan rate: 100 mV s^{-1}.

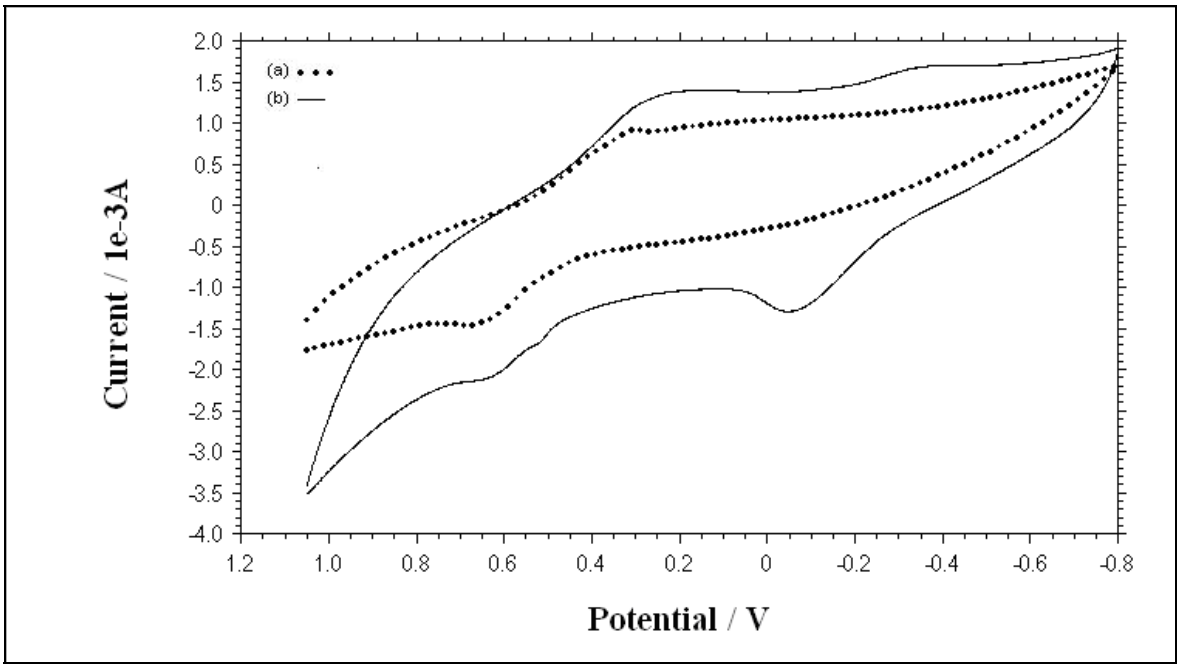

Figure 7.30. CVs of 0.1 M NaCl solution recorded with PVF^+ coated GCE (a)before, and (b) after incorporation of $PtCl_6^{2-}$ complex. Scan rate: 100 mV s^{-1}.

In this part of the study, unlike the case in K_2PtCl_4 studies, immobilization of Pt particles from H_2PtCl_6 was performed by both cyclic voltammetric scans and constant potential electrolysis. After this step, Pt particles were reduced by chemical and electrochemical reduction methods. Preparation of Pt/PVF^+ catalysts using H_2PtCl_6 was studied by Pt disc electrode and GCE. However, no successful results were obtained by Pt electrode. So, GCE was used the electrode material.

Steps for preparation of the catalyst are represented schematically in Scheme 7.2.

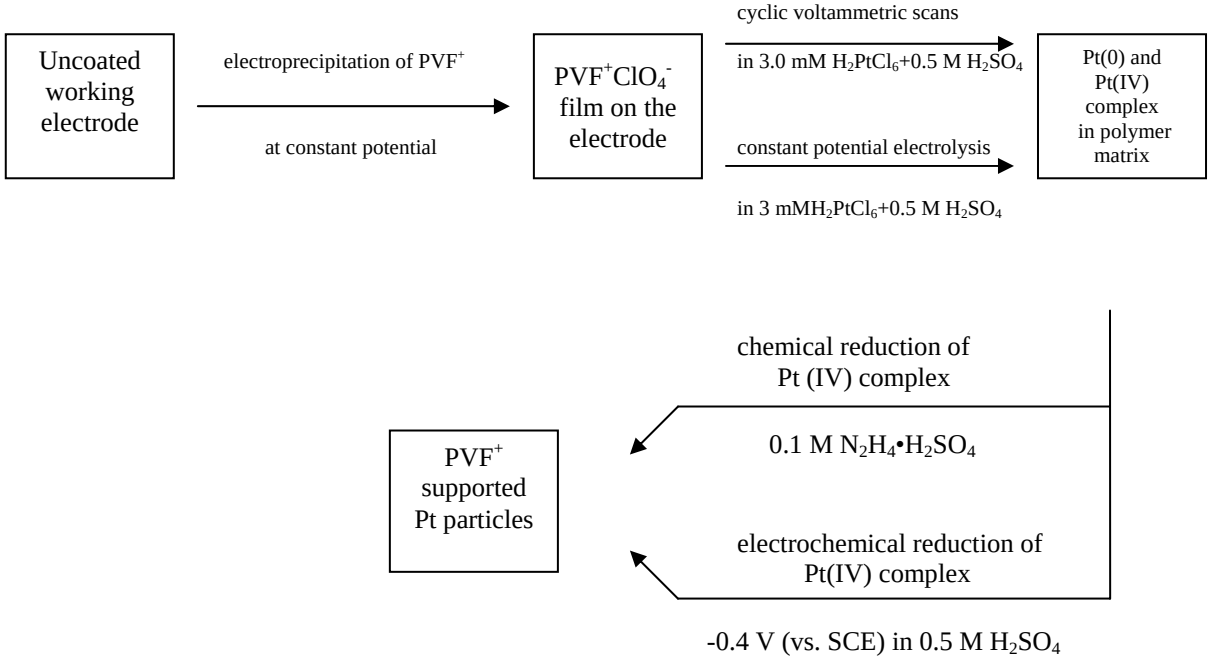

Scheme 7.2. Schematic procedure for the preparation of PVF^+ supported Pt particles using H_2PtCl_6.

7.2.2.1. Immobilization of Pt particles by cyclic voltammetric scans

Optimization of experimental parameters

Experimental parameters were optimized according to the oxidation peak current values at +0.84 V vs. SCE recorded with 0.5 M CH_3OH solution containing 0.5 M H_2SO_4 as the supporting electrolyte keeping the other parameters constant.

Cathodic potential limit

Cathodic potential limit during cyclic voltammetric scans was an important parameter because, at cathodic potentials, H_2 gas was evolved on the electrode surface. When large amounts of H_2 gas were formed under uncontrolled conditions, the film was ruptured and it was unable to keep the catalyst on the electrode surface. Effect of cathodic potential limit during cyclic voltammetric scans was studied up to -1.15 V vs. SCE, and maximum oxidation peak current was observed at -0.85 V cathodic potential limit for methanol oxidation (Figure 7.31).

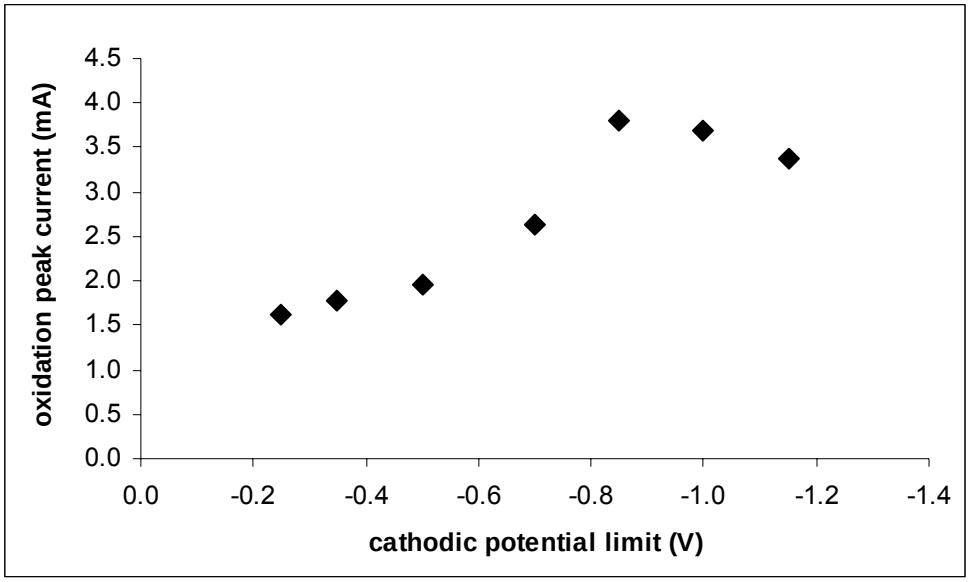

Figure 7.31. Effect of cathodic potential limit during cyclic voltammetric scans (50 mC polymer film thickness, 50 cyclic voltammetric scans, 60 min chemical reduction at ambient temperature).

Polymer film thickness

Effect of polymer film thickness was studied between 10 mC and 140 mC. Best results were obtained when the polymer film had a thickness corresponding to 70 mC (Figure 7.32).

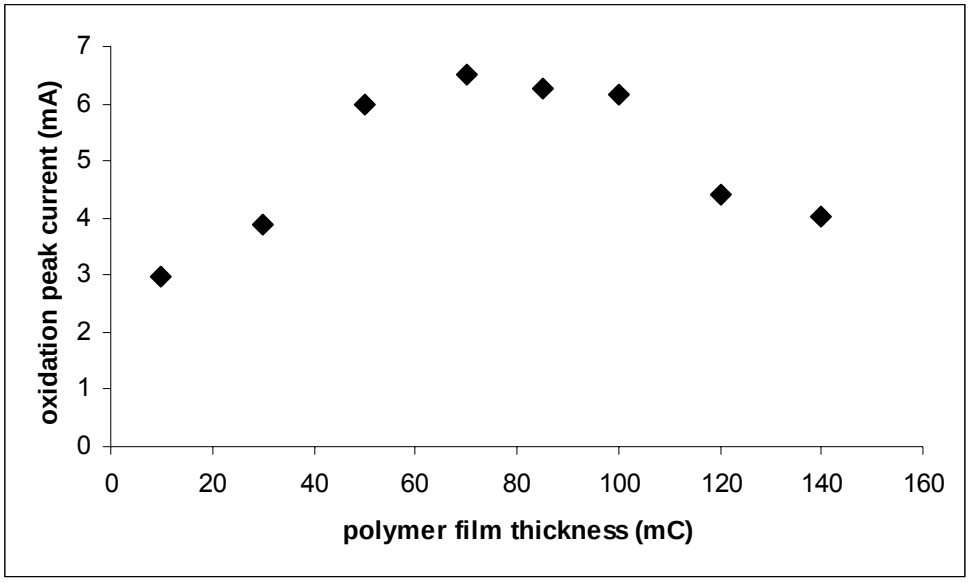

Figure 7.32. Effect of polymer film thickness on oxidation peak current of methanol (50 cyclic voltammetric scans, 60 min chemical reduction time, ambient reduction temperature).

Number of cyclic voltammetric scans in H_2PtCl_6 solution

Effect of number of cyclic voltammetric scans in 3 mM $H_2PtCl_6 \cdot H_2O$ solution containing 0.5 M H_2SO_4 on oxidation peak current of methanol was studied while the other experimental parameters were kept constant as 70 mC polymer film thickness and 60 min reduction time in 0.1 M $N_2H_4 \cdot H_2SO_4$ solution at ambient temperature. As seen in Figure 7.33, maximum oxidation peak current of methanol was observed for 50 cycles.

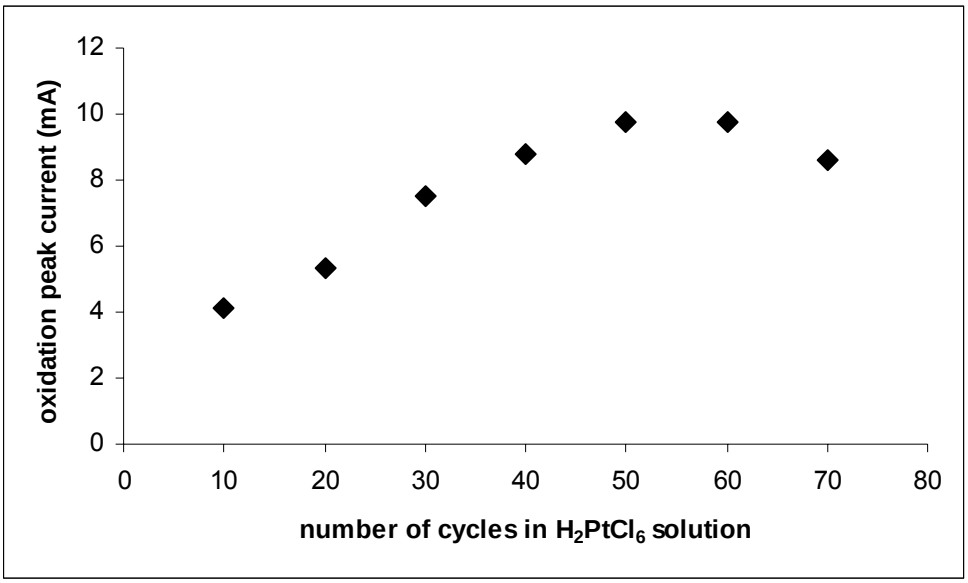

Figure 7.33. Effect of number of cyclic voltammetric scans on oxidation peak current of methanol (70 mC polymer film thickness, 60 min chemical reduction time, ambient reduction temperature).

Chemical reduction time

Chemical reduction of Pt particles was studied using 0.1 M $N_2H_4 \cdot H_2SO_4$ solution for 15 to 90 min. The other experimental conditions were 70 mC polymer film thickness, 50 cyclic voltammetric scans in K_2PtCl_4 solution and ambient reduction temperature. Unlike the case in K_2PtCl_4, Pt particles were able to catalyze electrooxidation of methanol before reduction; meaning that some of the particles were in the reduced state. However, when these particles were further reduced, oxidation peak current of methanol increased. This is attributed to existence of Pt species in the complex form. So, reduction step should be included in the preparation procedure of the Pt/PVF^+ catalyst from H_2PtCl_6 in order to obtain better performance from the catalyst. It can be concluded that 60 min reduction time was enough for chemical reduction of Pt particles obtained from H_2PtCl_6 (Figure 7.34).

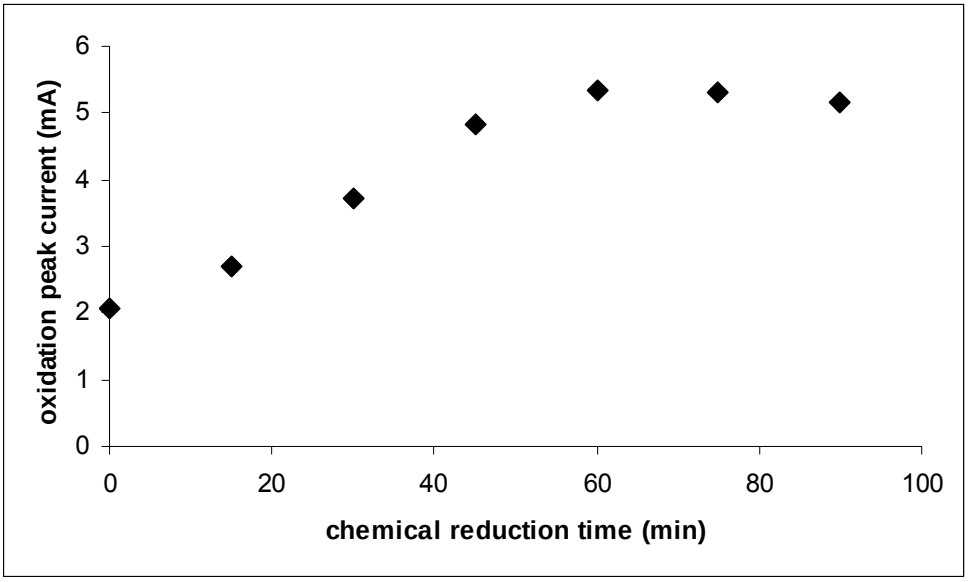

Figure 7.34. Effect of chemical reduction time in 0.1 M $N_2H_4 \cdot H_2SO_4$ solution on oxidation peak current of methanol (70 mC polymer film thickness, 50 cyclic voltammetric scans, ambient reduction temperature).

Chemical reduction temperature

Chemical reduction temperature was also studied; however, increasing reduction temperature did not have any positive contribution to the oxidation peak current of methanol.

Electrochemical reduction potential

In order to investigate the effect of electrochemical reduction potential on oxidation peak current of methanol, Pt particles were reduced in 0.5 M H_2SO_4 solution which was stirred continuously. Experimental conditions were 70 mC polymer film thickness, 50 cyclic voltammetric scans in 3 mM H_2PtCl_6 solution containing 0.5 M H_2SO_4, 15 min electrochemical reduction at ambient temperature. As presented in Figure 7.35 as reduction potential vs. oxidation peak current, maximum oxidation peak current was obtained at -0.40 V vs. SCE.

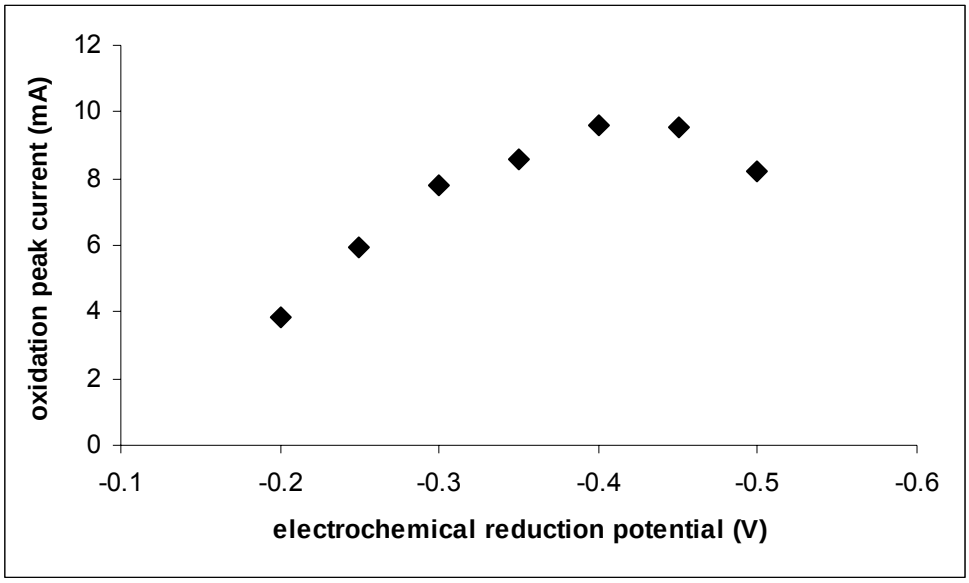

Figure 7.35. Effect of electrochemical reduction potential on oxidation peak current of methanol (70 mC polymer film thickness, 50 cyclic voltammetric scans, 15 min electrochemical reduction at ambient temperature).

Electrochemical reduction time

Figure 7.36 shows electrochemical reduction time vs. oxidation peak current of methanol between 5 and 30 min. Experimental conditions were 70 mC polymer film thickness, 50 cyclic voltammetric scans, -0.40 V vs. SCE electrochemical reduction potential at ambient temperature. Maximum oxidation peak current was obtained for 20 min.

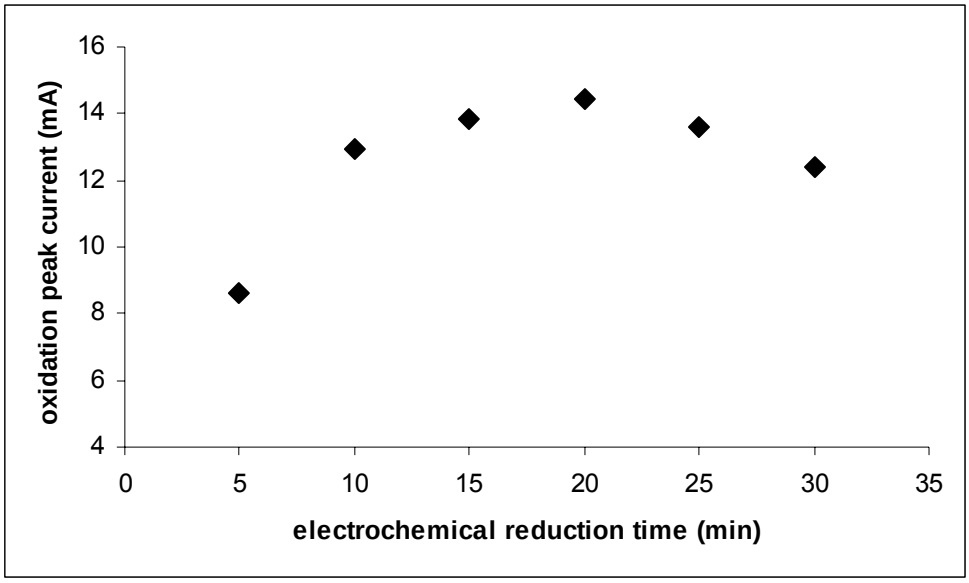

Figure 7.36. Effect of electrochemical reduction time on oxidation peak current of methanol (70 mC polymer film thickness, 50 cyclic voltammetric scans, -0.40 V electrochemical reduction potential at ambient temperature).

When chemical and electrochemical reduction methods were compared, oxidation peak current values were more or less the same for both methods.

7.2.2.2. Immobilization of Pt particles by constant potential electrolysis

Optimization of experimental parameters

Electrolysis potential

Effect of electrolysis potential was studied between -0.25 V and -1.15 V vs. SCE for immobilization of Pt particles by constant potential electrolysis. Oxidation peak current of methanol increased up to -0.85 V and decreased at -1.0 V and -1.15 V. This potential is consistent with the cathodic potential limit during immobilization of Pt particles by cyclic voltammetric scans. Electrolysis potential vs. oxidation peak current is represented in Figure 7.37.

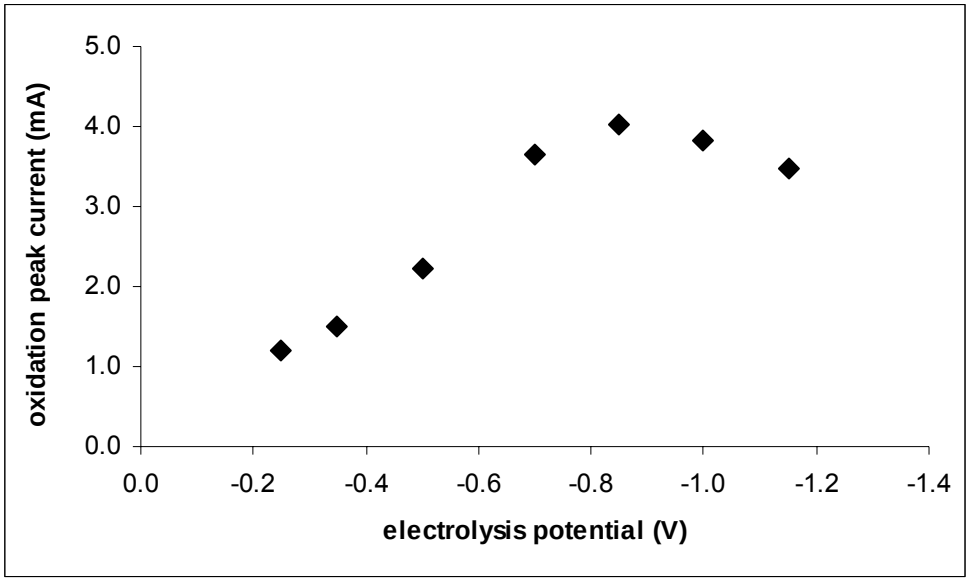

Figure 7.37. Effect of electrolysis potential on oxidation peak current of methanol (70 mC polymer film thickness, 15 min electrolysis time, 60 min chemical reduction at ambient temperature).

Electrolysis time

Effect of electrolysis time on oxidation peak current of methanol was investigated between 5 and 30 min. Maximum oxidation peak current was obtained using an electrolysis time of 20 min (Figure 7.38).

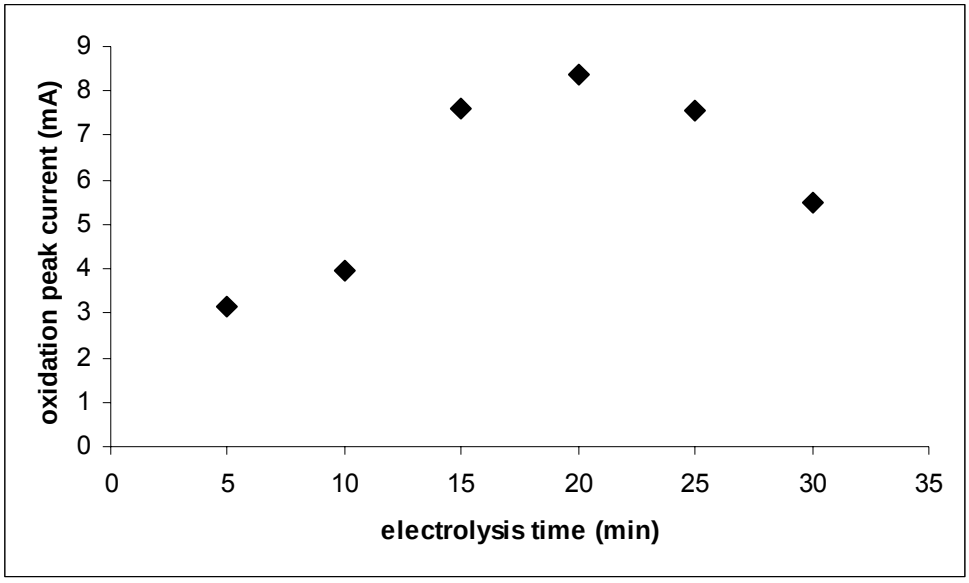

Figure 7.38. Effect of electrolysis time on oxidation peak current of methanol (70 mC polymer film thickness, -0.85 V vs. SCE electrolysis potential, 60 min chemical reduction at ambient temperature).

Comparison of two immobilization methods

Figure 7.39 compares two immobilization methods for obtaining Pt particles in the polymer matrix for 0.5 M CH_3OH solution containing 0.5 M H_2SO_4. Methanol oxidation peaks were observed at approximately at +0.81 V and +0.77 V vs. SCE. Shapes of the CVs are not as regular as the CVs obtained by $PtCl_4^{2-}$ complexes. Oxidation peak current of methanol recorded with the catalysts prepared by constant potential electrolysis is somewhat more than the one prepared by cyclic voltammetric scans.

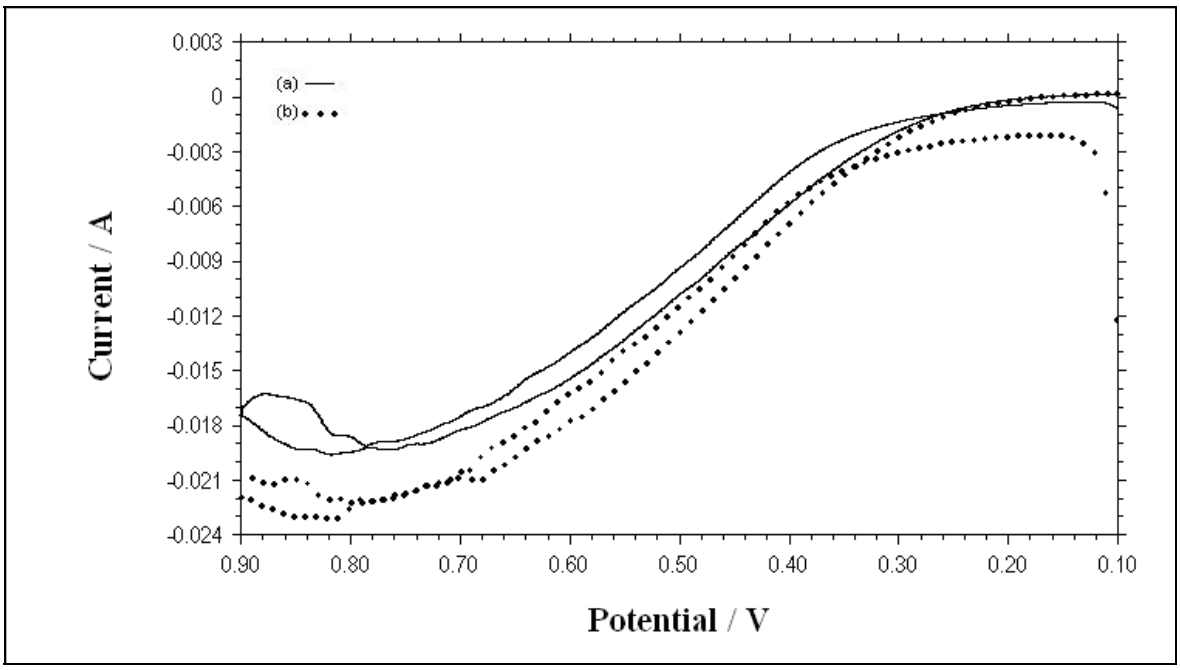

Figure 7.39. CVs of 0.5 M CH_3OH solution containing 0.5 M H_2SO_4 recorded with Pt/PVF^+ catalysts prepared using H_2PtCl_6 by (a) cyclic voltammetric scans, (b) constant potential electrolysis. Scan rate: 5 mV s^{-1}.

Electrochemical characterization of the catalyst

Cyclic voltammetric behavior of Pt/PVF^+ system prepared from H_2PtCl_6 was recorded in 0.5 M H_2SO_4 solution. Similar to Pt/PVF^+ system prepared from K_2PtCl_4 on GCE, the expected oxidation and reduction peaks of weakly and strongly adsorbed hydrogen between 0.00 V and -0.25 V vs. SCE were not observed. A representative CV is given in Figure 7.40 recorded with the catalyst prepared by cyclic voltammetric scans.

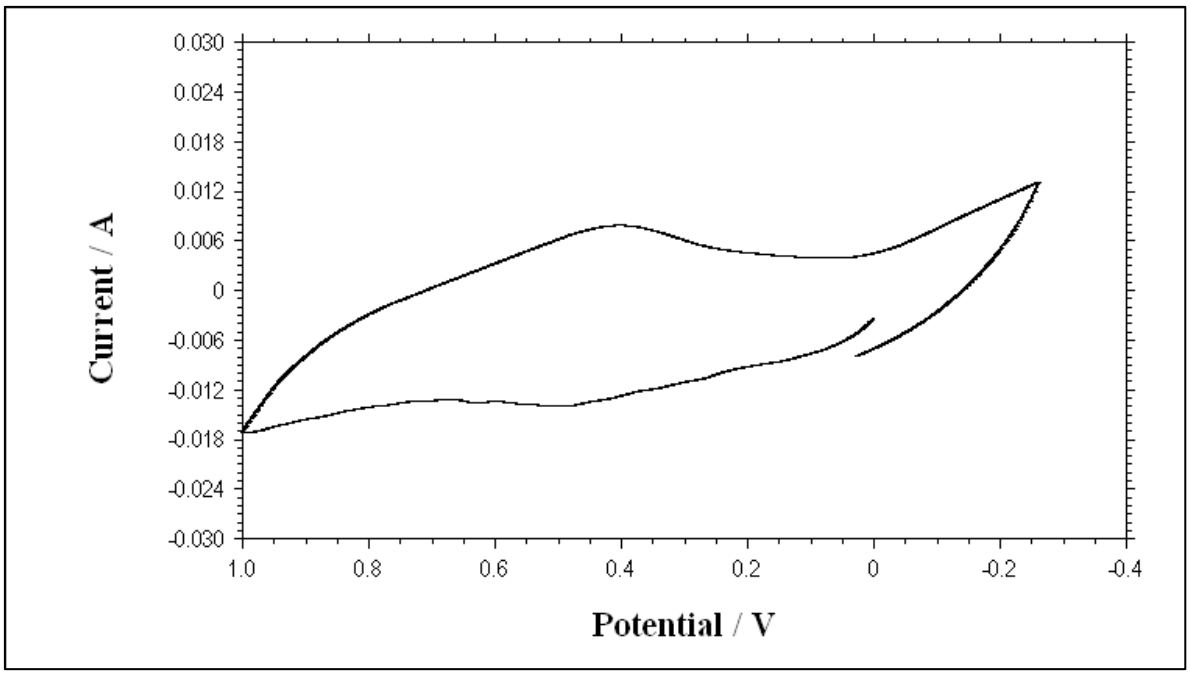

Figure 7.40. CV of 0.5 M H_2SO_4 recorded with Pt/PVF^+ catalysts prepared using H_2PtCl_6. Scan rate: 5 mV s^{-1}.

7.2.2.3. SEM images of Pt/PVF^+ catalysts prepared using H_2PtCl_6

SEM images of Pt/PVF^+ catalysts prepared using H_2PtCl_6 are represented in Figures 7.41. Experimental conditions are 70 mC polymer film, 50 cyclic voltammetric scans in 3 mM H_2PtCl_6 solution containing 0.5 M H_2SO_4 and 60 min chemical reduction at ambient temperature. It was observed that the Pt particles were dispersed over the polymer matrix, however their shapes were not spherical. This observation is also consistent with the cyclic voltammetric behavior of the system in 0.5 M H_2SO_4 solution.

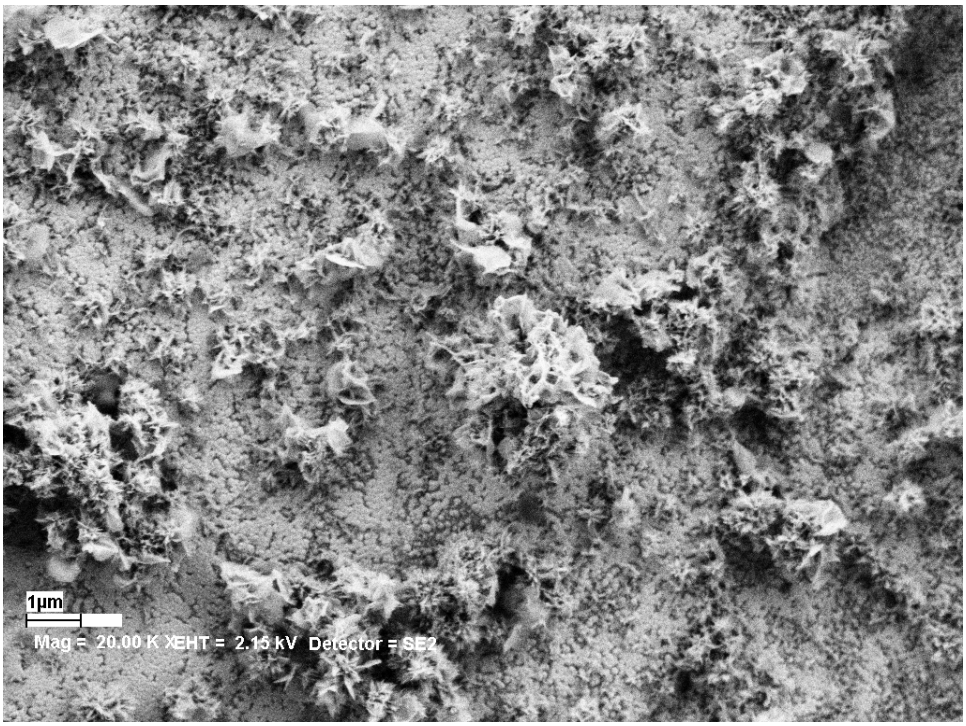

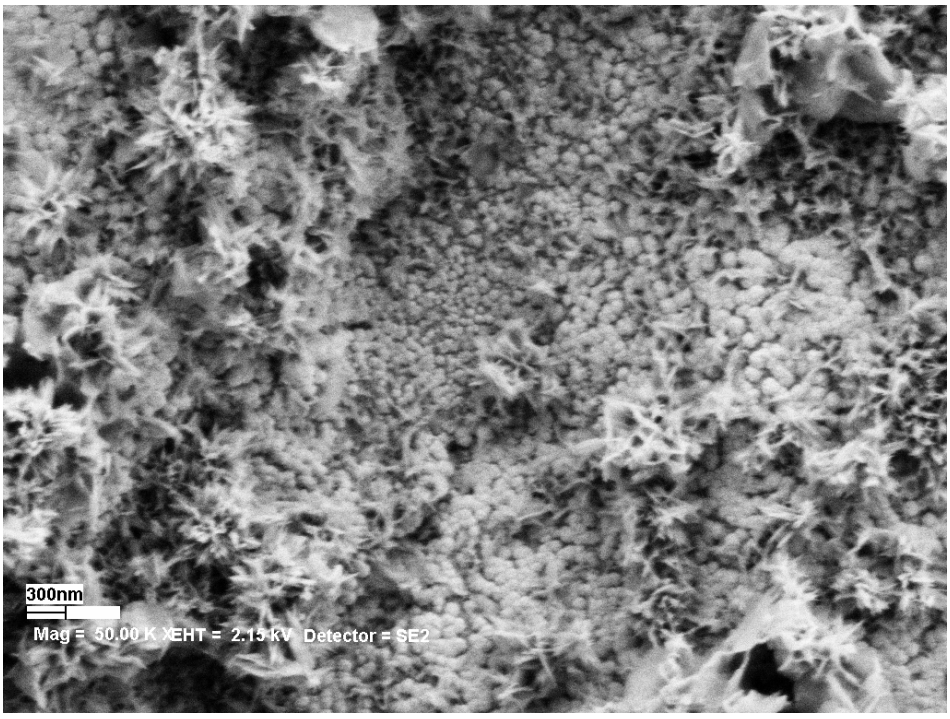

Figure 7.41. SEM images of Pt/PVF$^+$ catalyst prepared using H_2PtCl_6 (70 mC polymer film, 50 cyclic voltammetric scans in 3 mM H_2PtCl_6 solution containing 0.5 M H_2SO_4 and 60 min chemical reduction at ambient temperature).

7.2.2.4. Fuel cell performances of Pt/PVF^+ catalysts prepared using H_2PtCl_6

DMFC mode

Pt/PVF^+ catalyst system prepared using H_2PtCl_6 was first tested in a single fuel cell configuration in DMFC mode at ambient temperature and atmospheric pressure. Experimental conditions during preparation of the catalyst were 100 mC polymer film thickness, 70 cyclic voltammetric scans in 3 mM H_2PtCl_6 solution containing 0.5 M H_2SO_4, 60 min chemical reduction time at ambient temperature. 2 M CH_3OH solution containing 0.5 M H_2SO_4 was used as the fuel and 0.5 M H_2SO_4 solution saturated with pure O_2 was used as the oxidant. The OCV was 457 mV for the system and the maximum power density was 0.1424 mW cm^{-2} at 1.6 mA cm^{-2}. Current/voltage diagram for the fuel cell is given in Figure 7.42.

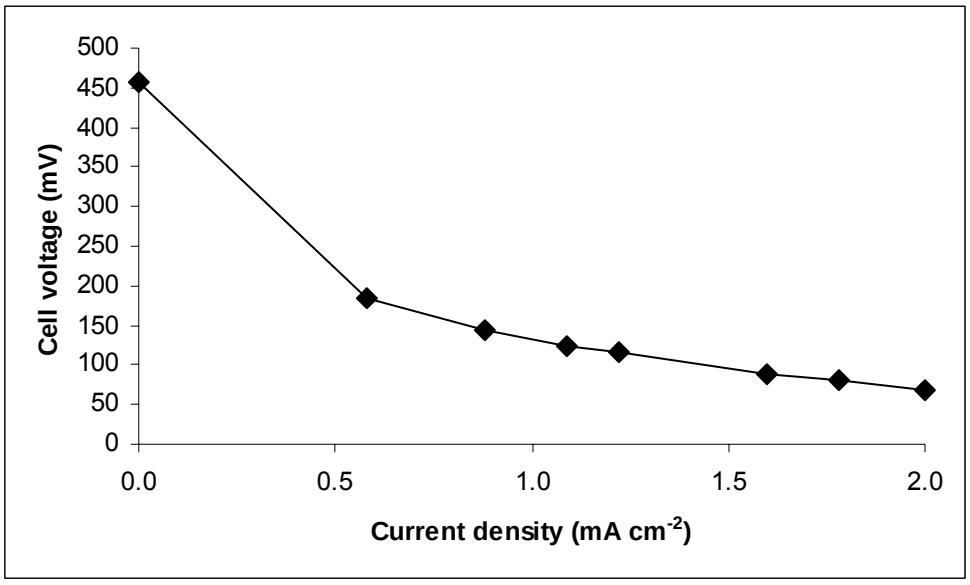

Figure 7.42. Current/voltage diagram for single DMFC using Pt/PVF^+ catalyst as anode and Pt black as cathode at ambient temperature and atmospheric pressure.

DHFC mode

Pt/PVF^+ catalyst system was also tested in a single DHFC configuration at ambient temperature and atmospheric pressure using the same preparation conditions. Saturated aqueous solution of $N_2H_4 \cdot H_2SO_4$ containing 0.1 M K_2SO_4 was used as the fuel and 0.1 M K_2SO_4 solution saturated with pure O_2 was used as the oxidant. An OCV of 285 mV was obtained for the system and the maximum power density was 0.3996 mW cm^{-2} at 3.7 mA cm^{-2}. Current/voltage diagram for the cell is given in Figure 7.43.

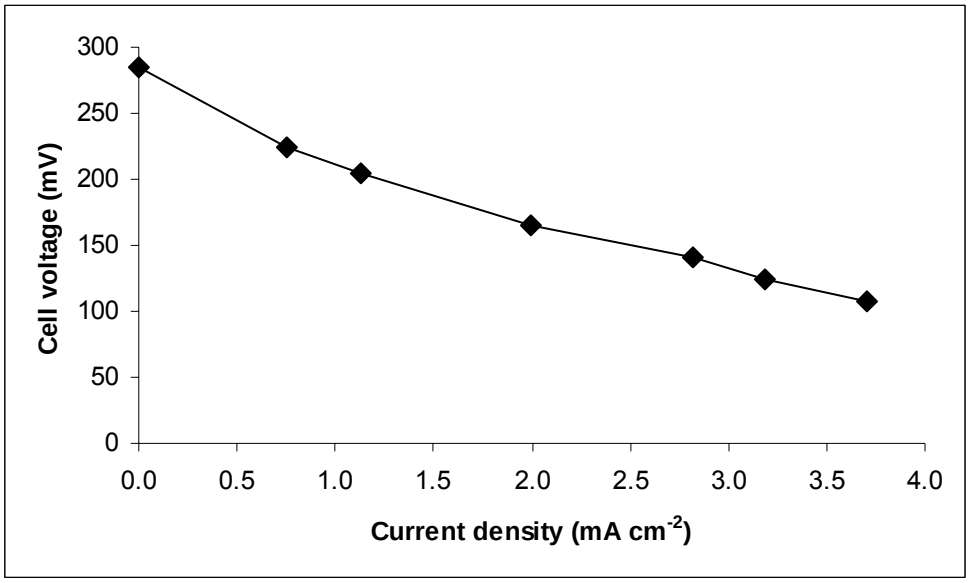

Figure 7.43. Current/voltage diagram for single DHFC using Pt/PVF^+ catalyst as anode and Pt black as cathode at ambient temperature and atmospheric pressure.

7.3. Pd/PVF$^+$ Electrocatalyst System

In the second part of the thesis, Pd/PVF$^+$ catalysts were prepared using K_2PdCl_4 as the Pd precursor. As the catalyst system showed catalytic activity towards hydrazine oxidation, optimization of experimental parameters for the preparation of the catalyst was done according to the oxidation peak current of hydrazine. Because of the practical difficulties concerning with the use of liquid hydrazine, aqueous solution of $N_2H_4 \cdot H_2SO_4$ was used in the experiments.

Figure 7.44 represents the cyclic voltammetric behavior of 10 mM $N_2H_4 \cdot H_2SO_4$ solution containing 0.1 M K_2SO_4 recorded with uncoated Pt disc electrode. As bulk Pt itself showed catalytic activity towards oxidation of $N_2H_4 \cdot H_2SO_4$, an oxidation peak can be observed at +0.36 V vs. SCE. For this reason, Pt disc was not studied as the electrode material.

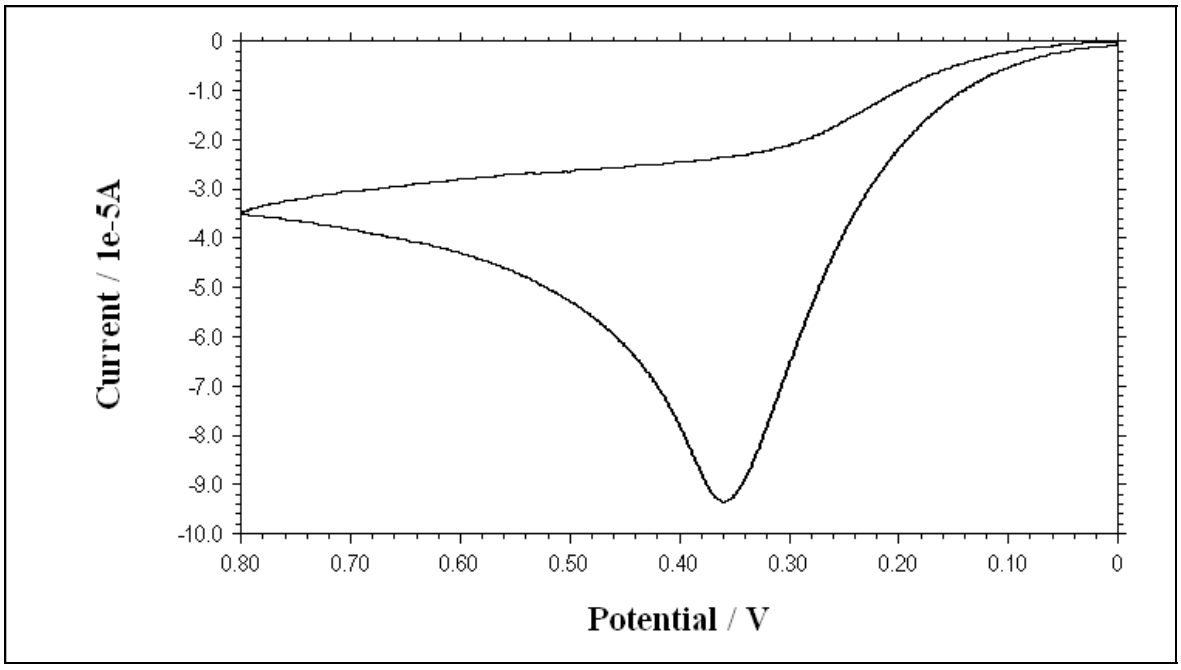

Figure 7.44. CV of 10 mM $N_2H_4 \cdot H_2SO_4$ solution containing 0.1 M K_2SO_4 recorded with uncoated Pt disc electrode. Scan rate: 100 mV s^{-1}.

GCE was used as the electrode material for preparation of Pd/PVF^+ catalysts. CV of 10 mM $N_2H_4 \cdot H_2SO_4$ solution containing 0.1 M K_2SO_4 recorded with uncoated GCE is given in Figure 7.45. As can be seen from the figure, no oxidation peaks were observed in the CV.

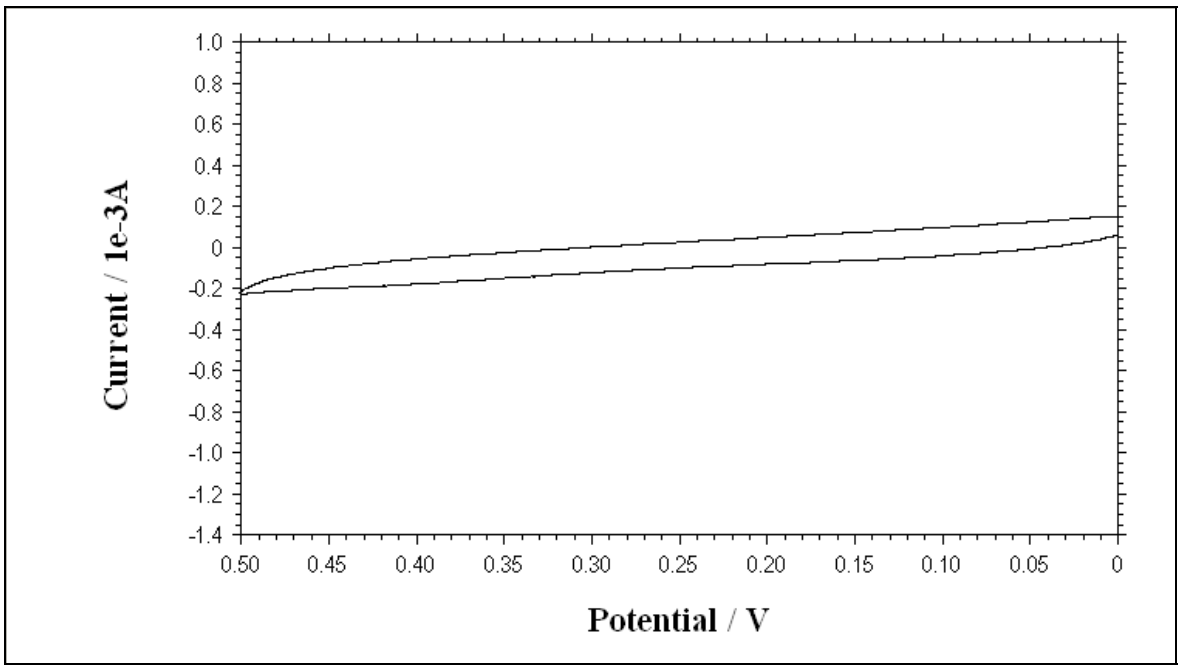

Figure 7.45. CV of 10 mM $N_2H_4 \cdot H_2SO_4$ solution containing 0.1 M K_2SO_4 recorded with uncoated GCE. Scan rate: 100 mV s^{-1}.

Polycyclic voltammogram of 2 mM K_2PdCl_4 solution was recorded with PVF^+ coated GCE for 50 cycles (Figure 7.46). In the CV, oxidation and reduction peaks of PVF are observed at potentials +0.63 V and +0.15 V vs. SCE respectively. Oxidation and reduction peaks observed at -0.10 V, -0.23 V, -0.35 V and -0.60 V belong to the $PdCl_4^{2-}$ complex.

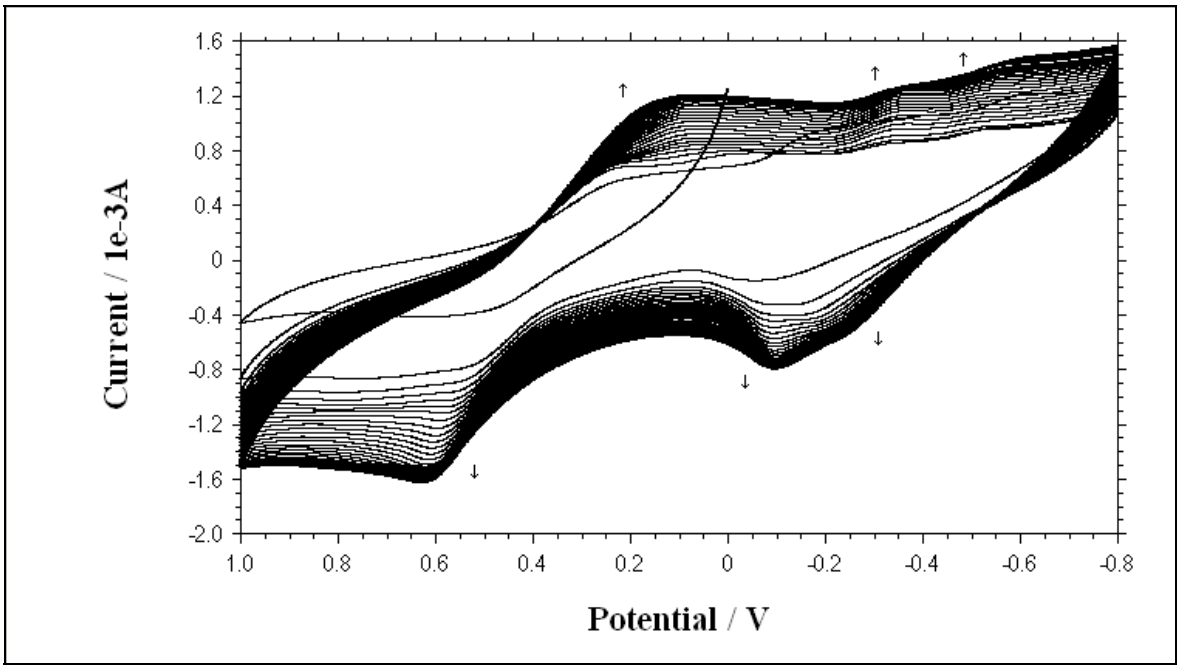

Figure 7.46. Polycyclic voltammogram of 2 mM K_2PdCl_4 solution recorded with PVF^+ coated GCE. Scan rate: 100 mV s^{-1}.

Steps for preparation of Pd/PVF^+ catalyst are schematically represented in Scheme 7.3. Two separate methods were used for immobilization of Pd particles into the polymer matrix; cyclic voltammetric scans and constant potential electrolysis in aqueous solution of K_2PdCl_4. After this step, Pd particles were already in the reduced form and the catalyst system was active towards hydrazine oxidation.

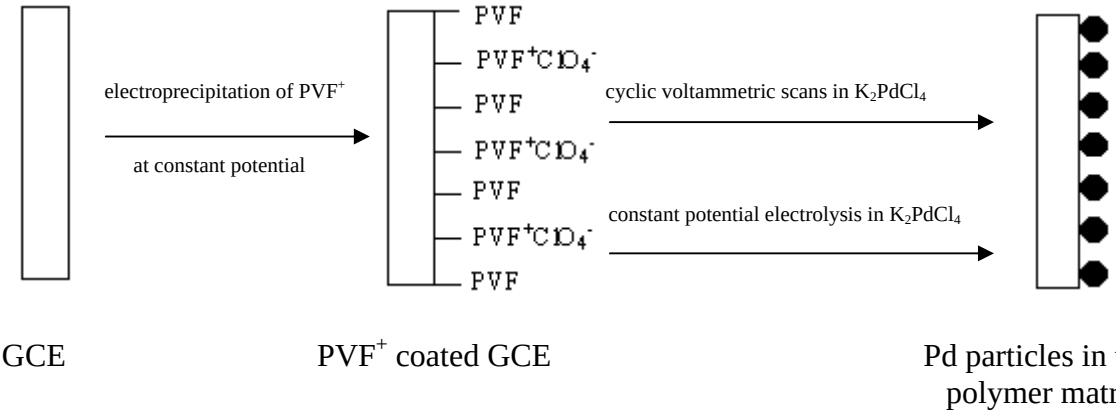

Scheme 7.3. A schematic diagram showing the procedure for the preparation of PVF^+ supported Pd particles.

When CV of the Pd/PVF^+ system was recorded after cyclic voltammetric scans in K_2PdCl_4 solution, oxidation and reduction of Pd particles were observed at -0.10 V and -0.40 V vs. SCE respectively. According to the CV, we can conclude that Pd particles were stable and immobilized into the polymer matrix (Figure 7.47).

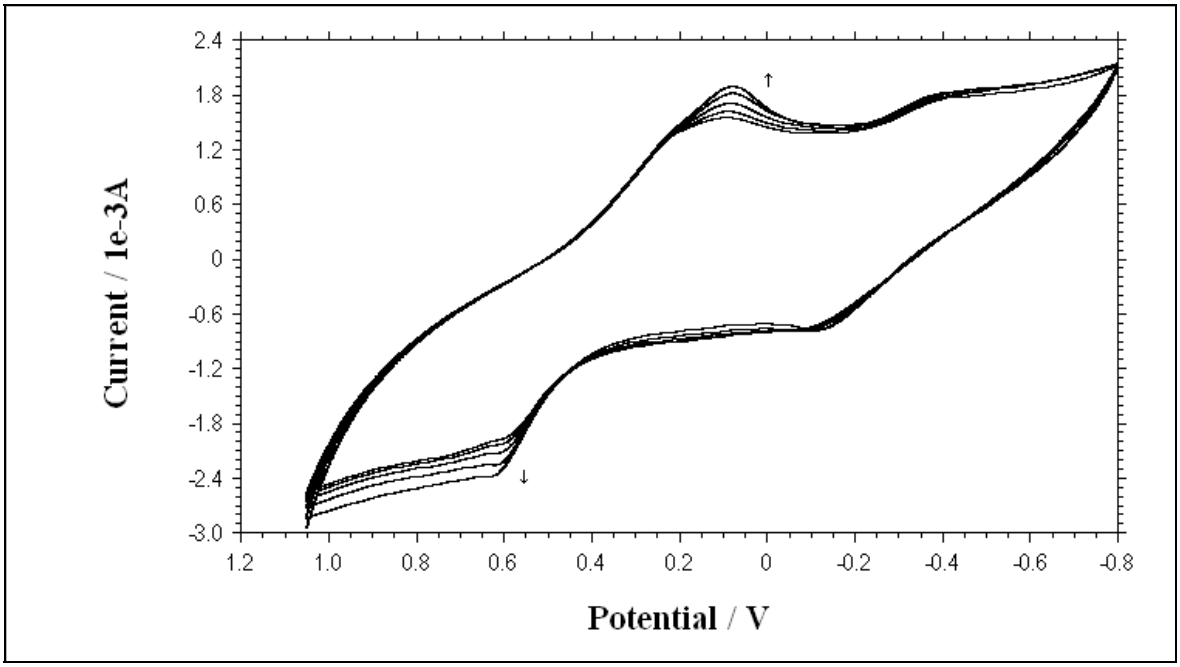

Figure 7.47. Polycyclic voltammogram of Pd/PVF^+ catalyst system on GCE recorded after cyclic voltammetric scans in K_2PdCl_4 solution in 0.1 M NaCl solution. Scan rate: 100 mV s^{-1}.

CV of 10 mM $N_2H_4 \cdot H_2SO_4$ solution containing 0.1 M K_2SO_4 recorded with Pd/PVF^+ system on GCE is given in Figure 7.48. In the CV, hydrazine was irreversibly oxidized at +0.25 V vs. SCE which is consistent with the literature (Li et al., 1997; Guo and Li, 2004; Guo and Li, 2005; Dong et al, 2008).

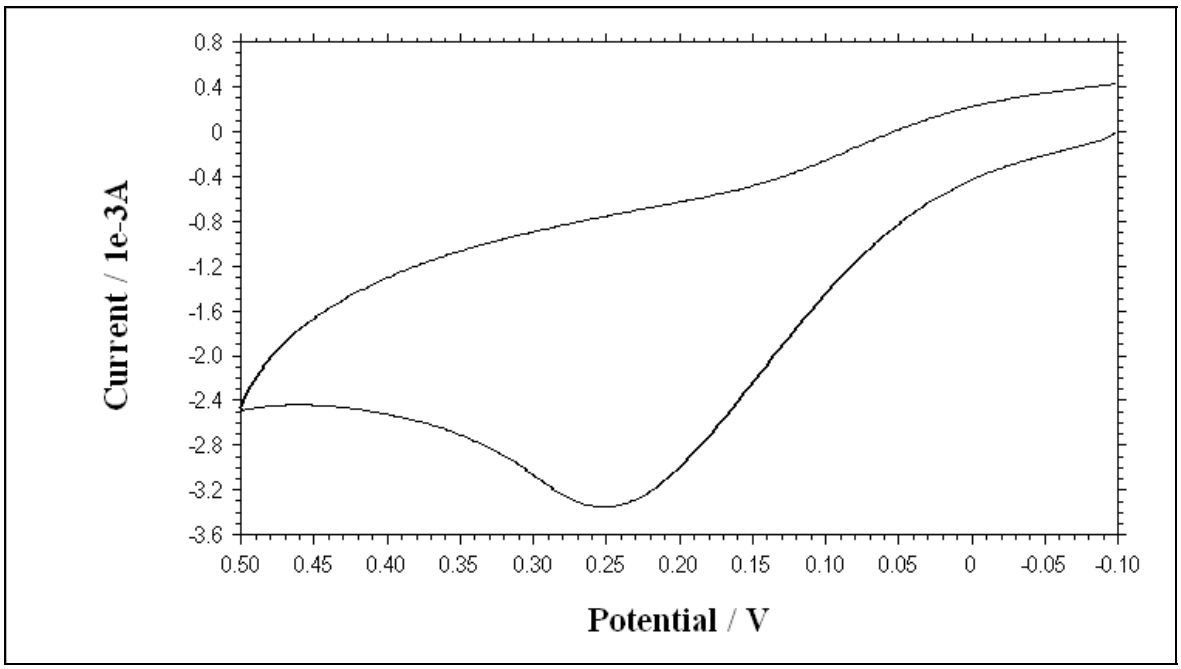

Figure 7.48. CV of 10 mM $N_2H_4 \cdot H_2SO_4$ solution containing 0.1 M K_2SO_4 recorded with Pd/PVF^+ system on GCE. Scan rate: 100 mV s^{-1}.

The effect of PVF^+ support on the performance of the catalyst was evaluated in Figure 7.49. In Figure 7.49.a, CV of 10 mM $N_2H_4 \cdot H_2SO_4$ solution containing 0.1 M K_2SO_4 was recorded with Pd particles directly immobilized on uncoated GCE by applying 50 cyclic voltammetric scans in 2 mM K_2PdCl_4 solution. When the same CV was recorded with the Pd/PVF^+ system (30 mC polymer film, 50 cyclic voltammetric scans), oxidation potential of hydrazine shifted towards a less positive potential (Figure 7.49.b).

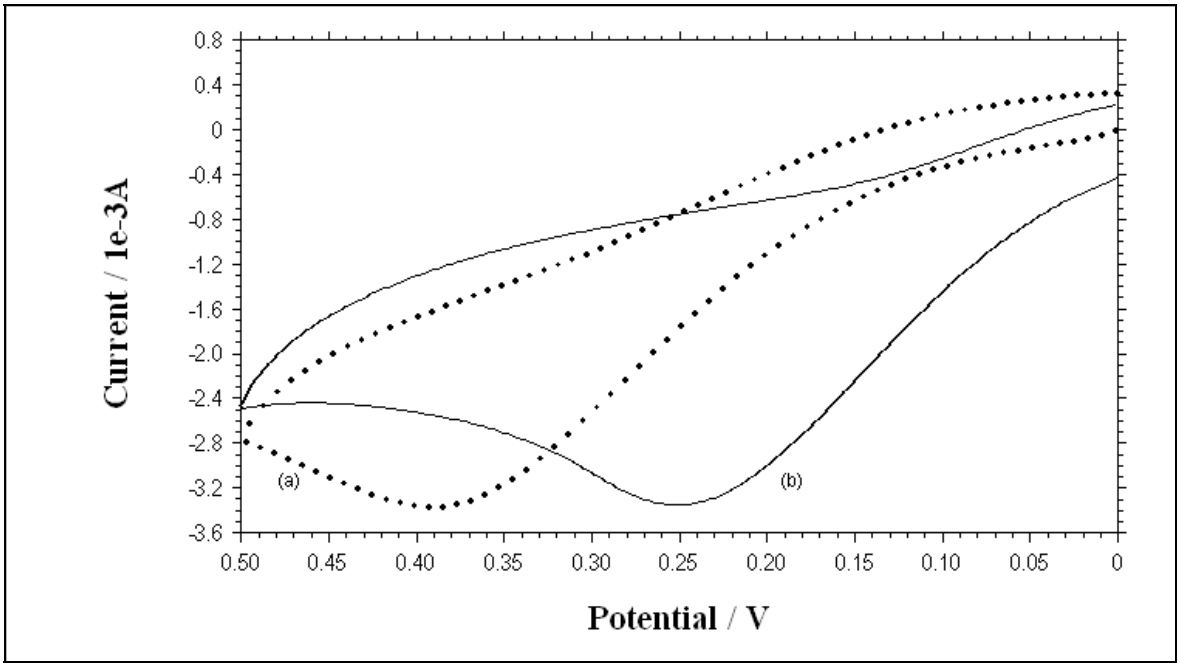

Figure 7.49. CV of 10 mM $N_2H_4 \cdot H_2SO_4$ solution containing 0.1 M K_2SO_4 recorded with (a) unsupported Pd particles, (b) PVF^+ supported Pd particles. Scan rate: 100 mV s^{-1}.

Optimization of experimental parameters

Experimental parameters for preparation of Pd/PVF^+ catalyst system were optimized according to the oxidation peak current values at +0.25 V vs. SCE recorded with 10 mM $N_2H_4 \cdot H_2SO_4$ solution containing 0.1 M K_2SO_4 as the supporting electrolyte while keeping the other parameters constant. All experiments were carried out at ambient temperature.

Polymer film thickness

Polymer film thickness vs. oxidation peak current of hydrazine was examined in order to determine the optimum film thickness (Figure 7.50). Immobilization of Pd particles was done by 50 cyclic voltammetric scans in 2 mM K_2PdCl_4 solution. 30 mC was found as the optimum polymer film thickness.

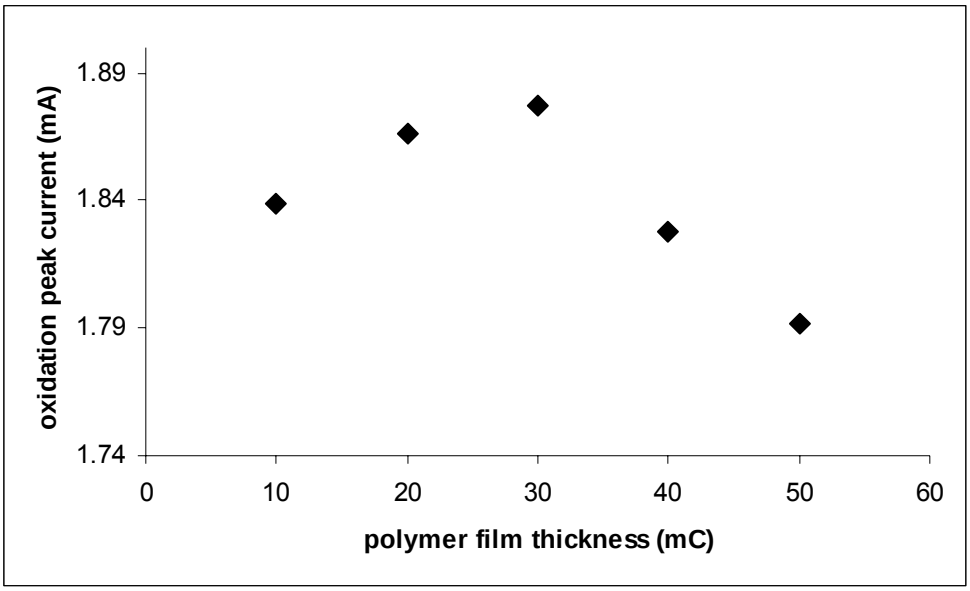

Figure 7.50. Effect of polymer film thickness on oxidation peak current of $N_2H_4 \cdot H_2SO_4$ (50 cyclic voltammetric scans).

Cathodic potential limit during cyclic voltammetric scans

Optimum cathodic potential limit was studied by increasing the limiting potential from 0.0 V to -0.8 V vs. SCE gradually. Maximum oxidation peak current of $N_2H_4 \cdot H_2SO_4$ was obtained when the cathodic limit was -0.8 V vs. SCE (Figure 7.51).

Number of cyclic voltammetric scans in K_2PdCl_4 solution

Number of cyclic voltammetric scans was the parameter which determined the quantity of Pd particles in the catalyst system. Effect of number of cyclic voltammetric scans on oxidation peak current of hydrazine was studied up to 80 cycles at the potential interval +1.0 V and -0.8 V vs. SCE. Polymer film thickness was kept constant as 30 mC. Maximum oxidation peak current was obtained for 50 cycles (Figure 7.52).

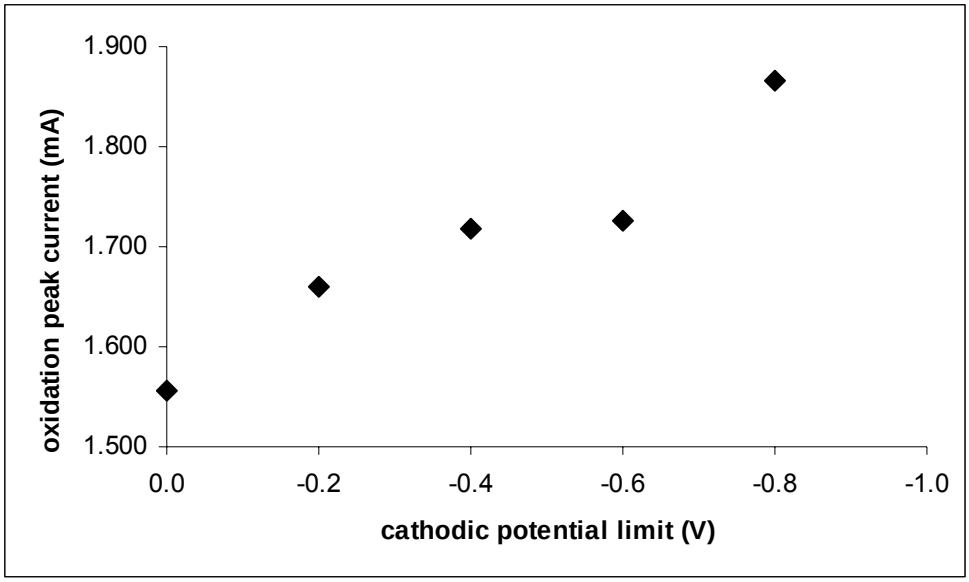

Figure 7.51. Effect of cathodic potential limit on oxidation peak current of $N_2H_4 \cdot H_2SO_4$ (30 mC polymer film thickness, 50 cyclic voltammetric scans).

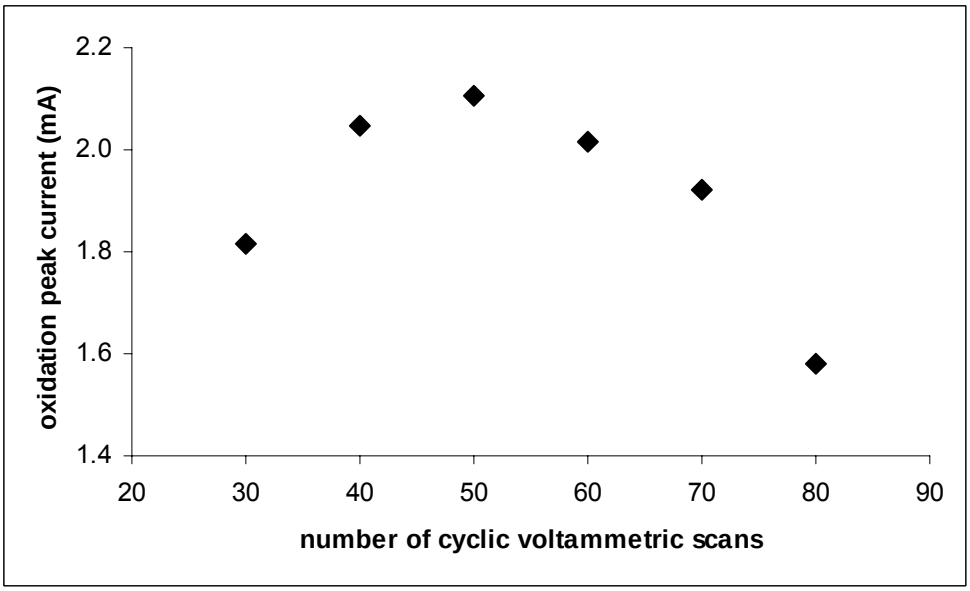

Figure 7.52. Effect of number of cyclic voltammetric scans on oxidation peak current of $N_2H_4 \cdot H_2SO_4$ (30 mC polymer film thickness).

Electrolysis potential during constant potential electrolysis

Optimum electrolysis potential was determined for immobilization of Pd particles by constant potential electrolysis from 2 mM K_2PdCl_4 solution. Consistent with the cathodic potential limit during cyclic voltammetric scans, a potential of -0.8 V vs. SCE gave the maximum oxidation peak current for $N_2H_4 \cdot H_2SO_4$ (Figure 7.53).

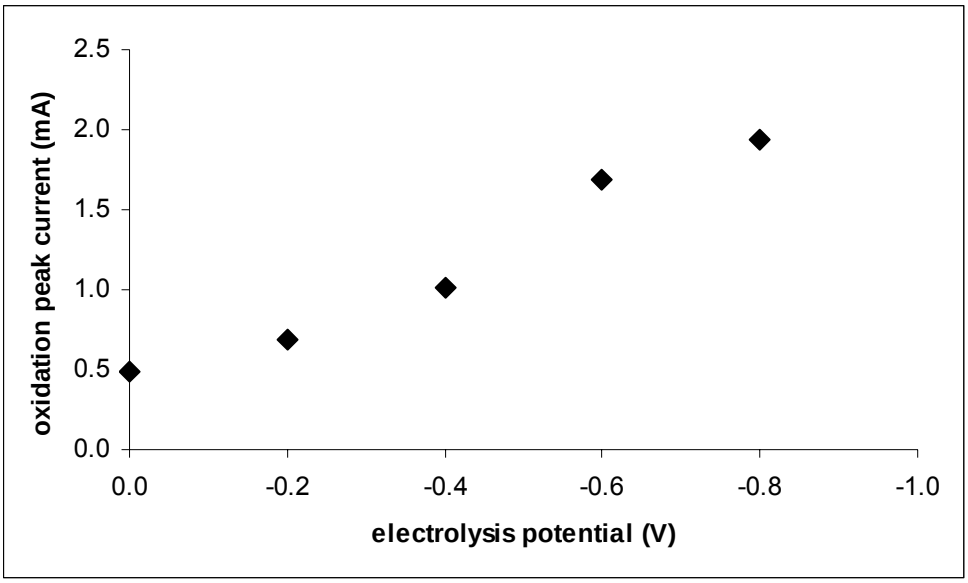

Figure 7.53. Effect of electrolysis potential on oxidation peak current of $N_2H_4 \cdot H_2SO_4$ (30 mC polymer film thickness, 20 min electrolysis time).

Electrolysis time during constant potential electrolysis

During immobilization of Pd particles from K_2PdCl_4 solution by constant potential electrolysis, the amount of Pd particles were determined by the time passed. Electrolysis time vs. oxidation peak current of hydrazine is presented in Figure 7.54. It was observed that when electrolysis was kept more than 30 min, the Pd particles formed on the electrode surface were stripped off from the polymer film which caused the oxidation peak current to decrease. For this reason, 30 min was the optimum electrolysis time for preparation of the Pd/PVF^+ catalyst system by constant potential electrolysis.

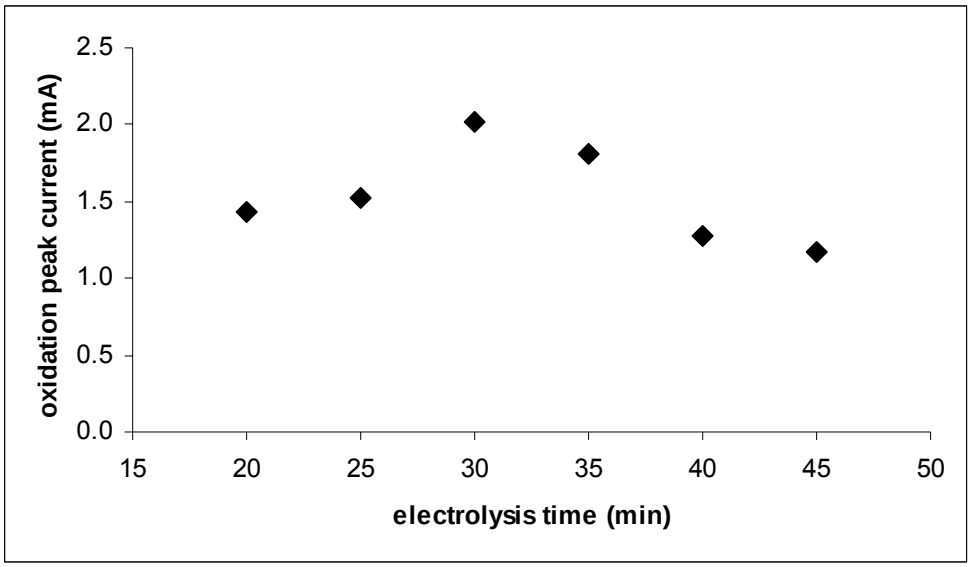

Figure 7.54. Effect of electrolysis time on oxidation peak current of $N_2H_4 \cdot H_2SO_4$ (30 mC polymer film thickness, -0.8 V vs. SCE electrolysis potential).

Comparison of two immobilization methods

In order to compare the two immobilization method, CV of $N_2H_4 \cdot H_2SO_4$ was recorded with Pd/PVF^+ catalysts prepared using the optimum conditions for both methods. Experimental conditions were 30 mC polymer film thickness and 50 cyclic voltammetric scans for cyclic voltammetric method; and 30 mC polymer film thickness, -0.8 V vs. SCE electrolysis potential and 30 min electrolysis time for constant potential electrolysis method. It was observed that the two methods showed very similar catalytic activities towards hydrazine oxidation (Figure 7.55).

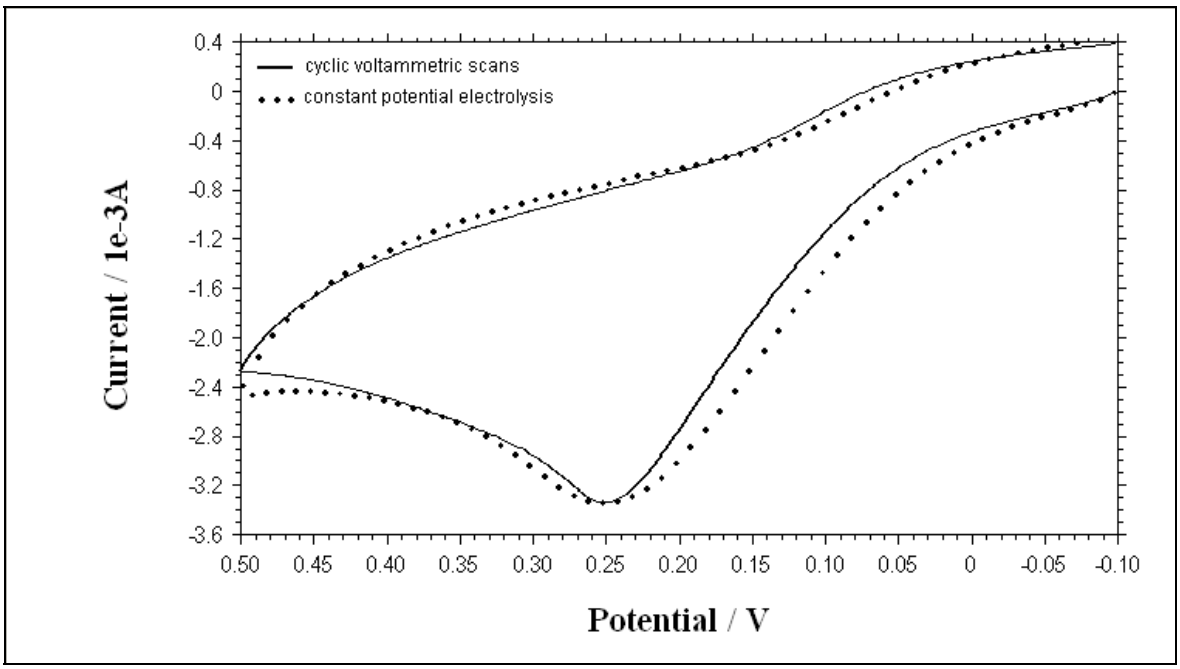

Figure 7.55. CVs of $N_2H_4 \cdot H_2SO_4$ recorded with Pd/PVF^+ catalysts prepared using the optimum conditions for both methods. Scan rate: 100 mV s^{-1}.

7.3.1. SEM images of Pd/PVF^+ catalysts

SEM images of Pd/PVF^+ catalysts prepared by cyclic voltammetric scans and constant potential electrolysis on Pt foil electrode (3mmx3mm) are represented in Figures 7.56 and 7.57 respectively. It was observed that Pd particles were well dispersed over the polymer matrix and shapes of the particles were significantly different in shape for the two preparation methods.

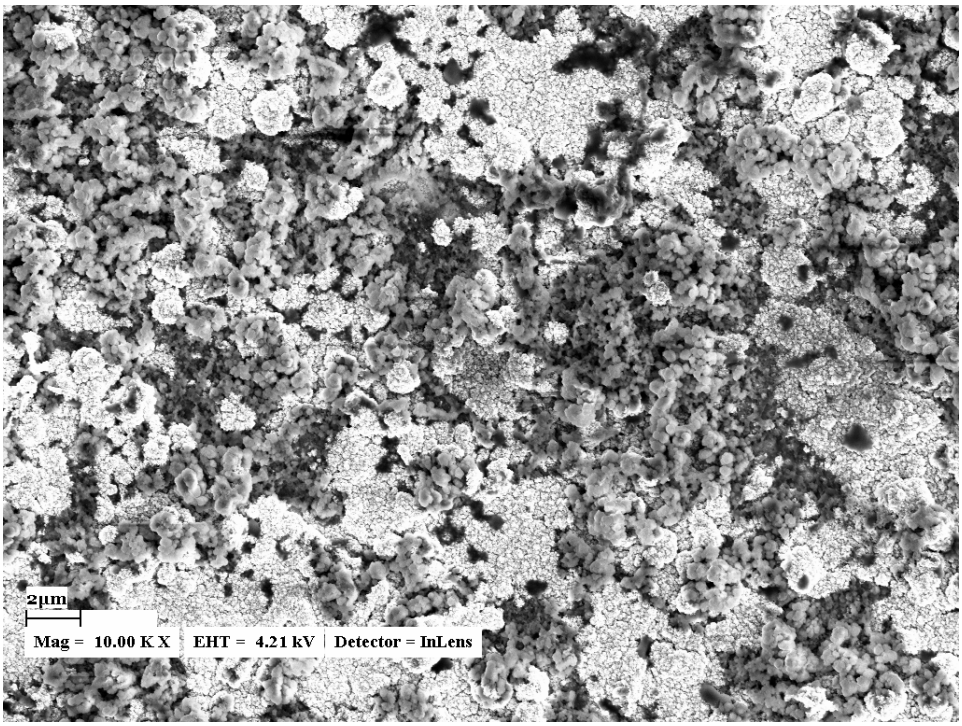

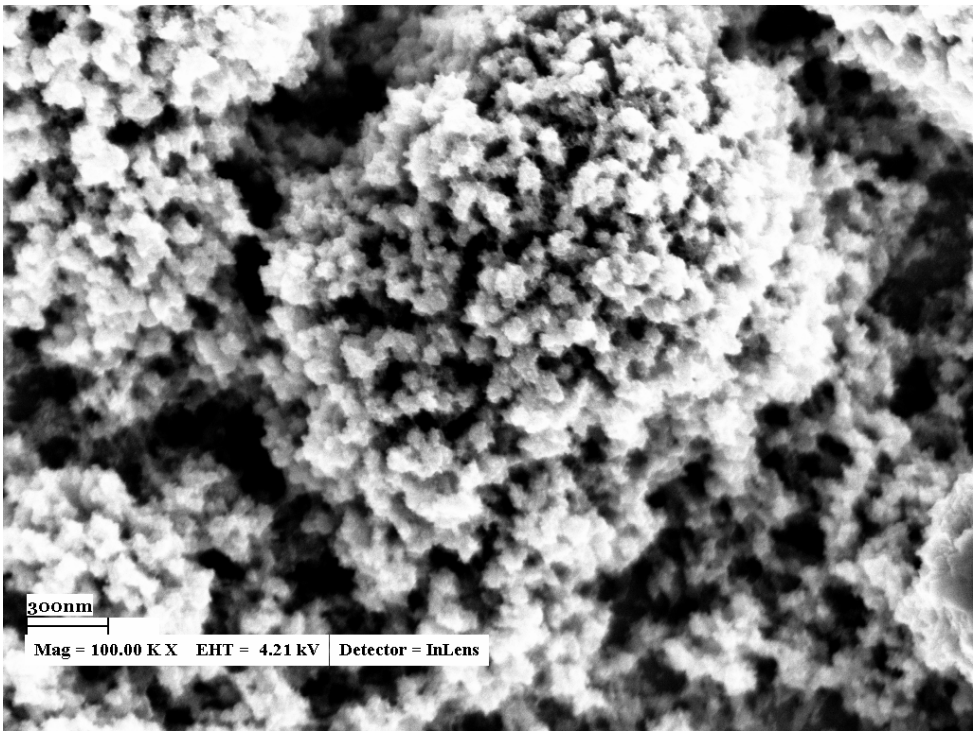

Figure 7.56. SEM images of Pd/PVF$^+$ catalyst prepared by cyclic voltammetric scans (100 mC polymer film thickness, 70 cyclic voltammetric scans in 2 mM K_2PdCl_4).

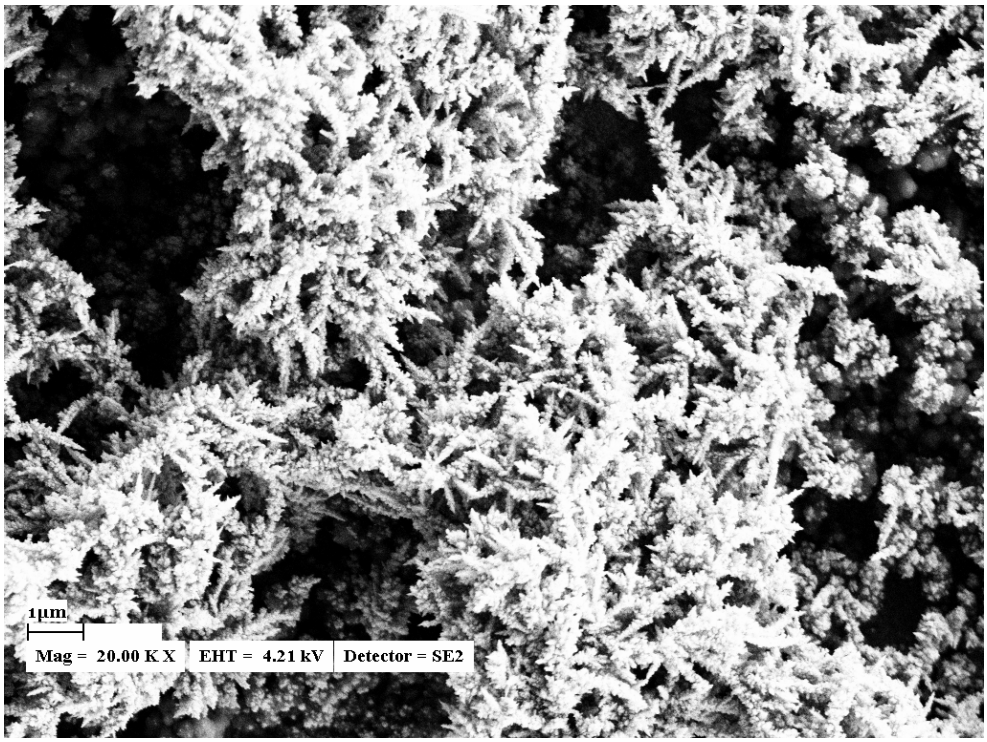

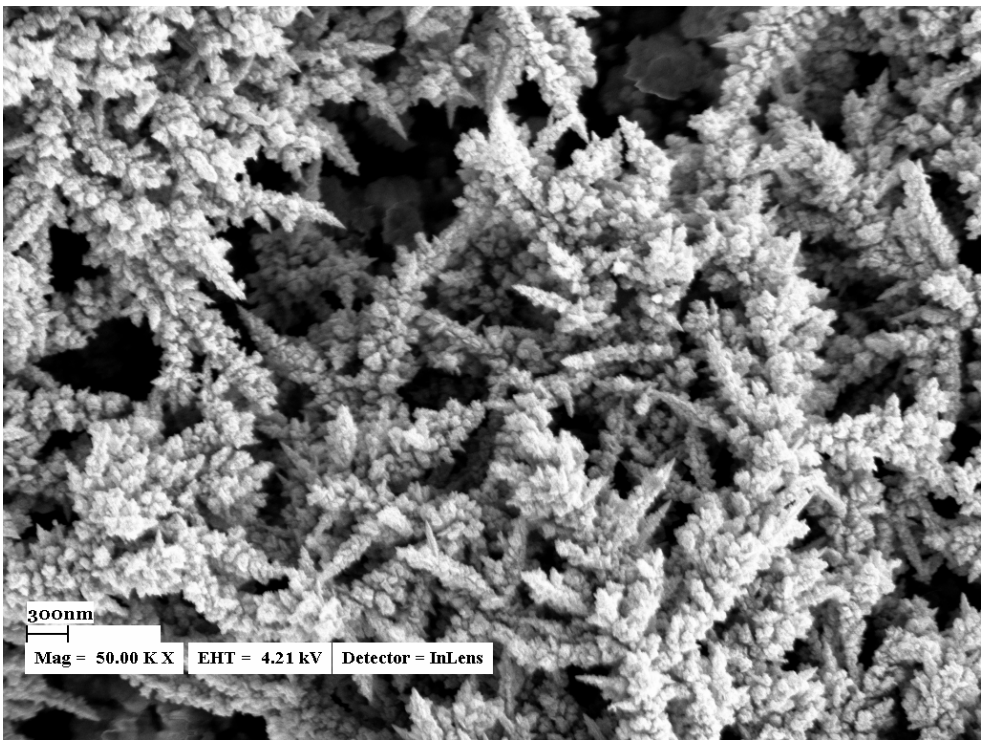

Figure 7.57. SEM images of Pd/ PVF^{+} catalyst prepared by constant potential electrolysis (100 mC polymer film thickness, -0.8 V vs. SCE electrolysis potential, 30 min electrolysis time).

7.3.2. Fuel cell performances of Pd/PVF$^+$ catalysts in DHFC mode

Pd/PVF$^+$ catalyst system prepared by cyclic voltammetric scans

Pd/PVF$^+$ catalyst system prepared by cyclic voltammetric scans in K_2PdCl_4 solution was tested in a single fuel cell configuration in DHFC mode at ambient temperature and atmospheric pressure. Experimental conditions during preparation of the catalyst were 100 mC polymer film thickness and 70 cyclic voltammetric scans in 2 mM K_2PdCl_4. Saturated aqueous solution of $N_2H_4 \cdot H_2SO_4$ containing 0.1 M K_2SO_4 was used as the fuel and 0.1 M K_2SO_4 solution saturated with pure O_2 was used as the oxidant. The OCV of the system was measured as 130 mV and the maximum power density was calculated as 0.009 mW cm^{-2} at 0.17 mA cm^{-2}. Current/voltage diagram for the cell is given in Figure 7.58.

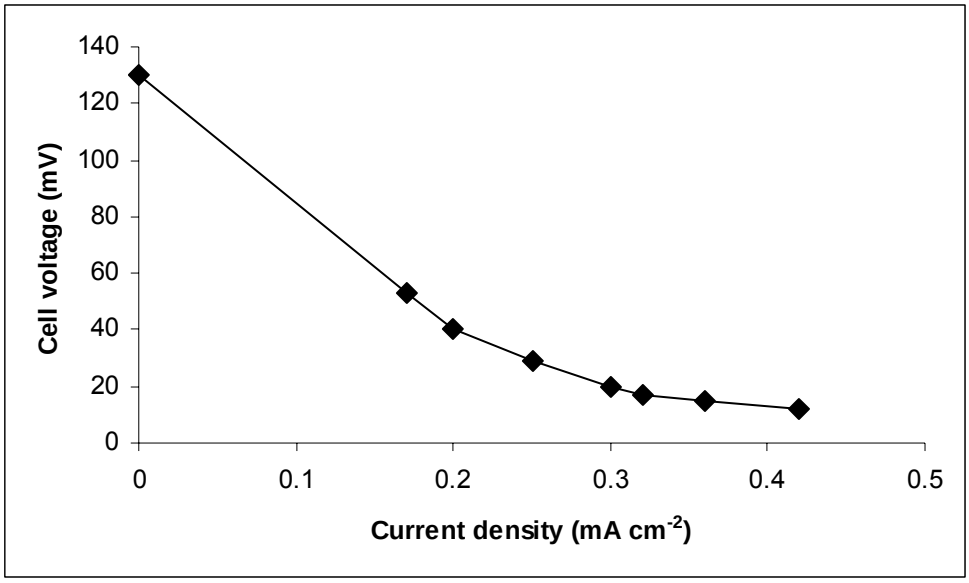

Figure 7.58. Current/voltage diagram for single DHFC using Pd/PVF$^+$ catalyst prepared by cyclic voltammetric scans as anode and Pt black as cathode at ambient temperature and atmospheric pressure.

Pd/PVF$^+$ catalyst system prepared by constant potential electrolysis

Pd/PVF$^+$ catalyst system prepared by constant potential electrolysis in K_2PdCl_4 solution was also tested in a single fuel cell configuration in DHFC mode at ambient temperature and atmospheric pressure. Experimental conditions during preparation of the catalyst were 100 mC polymer film thickness, -0.8 V vs. SCE electrolysis potential and 30 min electrolysis time. Saturated aqueous solution of $N_2H_4 \cdot H_2SO_4$ containing 0.1 M K_2SO_4 was used as the fuel and 0.1 M K_2SO_4 solution saturated with pure O_2 was used as the oxidant. The OCV of the system was 255 mV and the maximum power density was calculated as 0.200 mW cm^{-2} at 1.14 mA cm^{-2}. Current/voltage diagram for the cell is given in Figure 7.59.

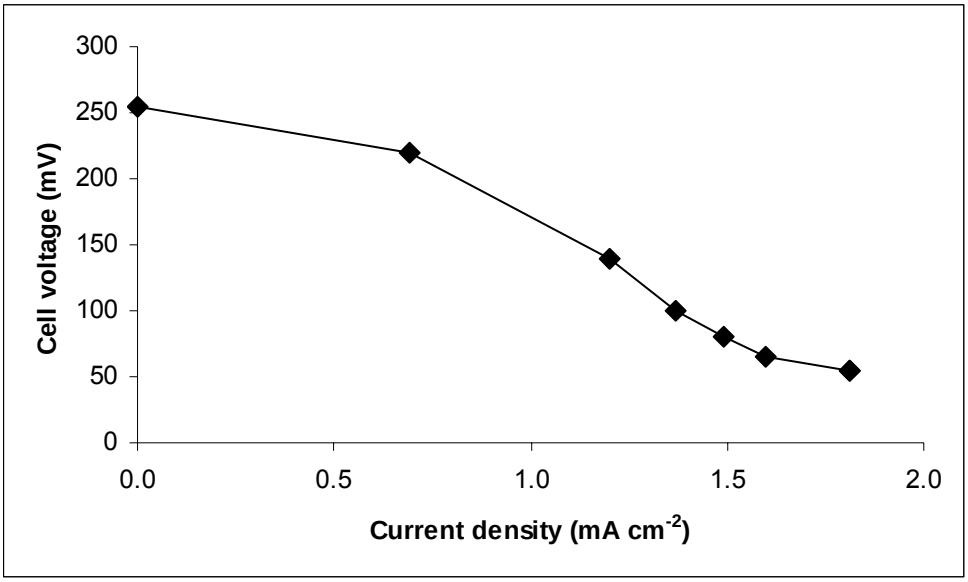

Figure 7.59. Current/voltage diagram for single DHFC using Pd/PVF$^+$ catalyst prepared by constant potential electrolysis as anode and Pt black as cathode at ambient temperature and atmospheric pressure.

8. CONCLUSIONS

Preparation, characterization and fuel cell performances of two distinct electrocatalyst systems utilizing Pt and Pd particles supported on PVF^+ redox polymer system was discussed in the present work. PVF^+ was electrodeposited onto the working electrode by the electrooxidation of methylene chloride solution of PVF containing TBAP at +0.7 V vs. Ag/AgCl. The thicknesses of the polymer films were controlled by the charge passed during the electroprecipitation of oxidized form of the polymer onto the electrode surface.

In the first part of the work, K_2PtCl_4 was used as the first Pt precursor for the preparation of Pt/PVF^+ electrocatalyst system. Pt particles in the complex form were incorporated into the polymer matrix from aqueous K_2PtCl_4 solution via cyclic voltammetric scans in aqueous K_2PtCl_4 solution without supporting electrolyte. Two separate methods were used for reduction of Pt complexes: (i) chemical reduction in hydrazinium sulfate solution, (ii) electrochemical reduction in H_2SO_4 solution.

The Pt/PVF^+ system showed catalytic activity towards methanol oxidation. Each experimental parameter for the preparation of the electrocatalysts was optimized according to the oxidation peak current values recorded during electrooxidation of methanol.

Two peaks of methanol oxidation were observed at the potentials +0.56 V and +0.52 V vs. SCE, respectively, using Pt/PVF^+ electrocatalyst on Pt disc electrode. The onset potential of methanol oxidation was observed at +0.30 V.

When Pt disc electrode was used as the working electrode, the following optimum experimental parameters were determined: polymer film thickness corresponding to 0.8 mC charge; 30 cyclic voltammetric scans in K_2PtCl_4 solution; 60 min chemical reduction time; 40 ^oC chemical reduction temperature; -0.30 V vs. SCE electrochemical reduction potential; 15 min electrochemical reduction time.

Electrochemical characterization of the electrocatalyst systems was done according to the hydrogen adsorption/desorption peaks in H_2SO_4 solution. As expected, the oxidation and reduction peak current values of hydrogen recorded with the catalyst having optimum amount of Pt (corresponding to 30 cycles in K_2PtCl_4) were considerably high with respect to the others.

When GCE was used as the working electrode for the preparation of Pt/PVF^+ electrocatalysts from K_2PtCl_4, two peaks of methanol oxidation were observed at the potentials +0.61 V and +0.57 V vs. SCE respectively. The onset potential of methanol oxidation was observed at +0.40 V. When the two electrode materials were compared, it was concluded that Pt disc electrode gave better results by means of oxidation potentials.

On GCE, optimum experimental conditions were as follows: polymer film thickness corresponding to 50 mC charge; 70 cyclic voltammetric scans in K_2PtCl_4 solution; 60 min chemical reduction time; 40 ^oC chemical reduction temperature; -0.30 V vs. SCE electrochemical reduction potential; 15 min electrochemical reduction time.

Chemical and electrochemical reduction methods were compared at the optimum conditions for the two electrode materials. According to the oxidation peak current values of methanol, chemical reduction was determined as more convenient with both electrodes.

Cyclic voltemmetric behavior of Pt/PVF^+ system on GCE in H_2SO_4 solution was recorded with (a) electrochemically reduced Pt particles in the polymer matrix and (b) chemically reduced Pt particles in the polymer matrix for the characterization of the electrocatalysts. However, oxidation and reduction behavior of weakly and strongly adsorbed hydrogen between 0.00 V and -0.25 V vs. SCE was not observed. According to the data, it was concluded that using Pt disc electrode instead of GCE was better for preparation of Pt/PVF^+ catalysts.

SEM images of Pt/ PVF^+ catalysts prepared on Pt foil compared for different preparation methods. Pt particles that were obtained by chemical reduction were at the nanoscale and well dispersed over the polymer film. However, the particles obtained by electrochemical reduction were not regularly dispersed and spherical.

EDS was also used for the physical characterization of the Pt/PVF^+ system. When the electrocatalyst was prepared on GCE to avoid Pt peaks coming from the electrode material, the spectrum indicated that C, Fe and Pt were the major elements. Quantitative analysis indicated a ratio of 10:1 for Fe and Pt atoms.

Pt/PVF^+ catalyst system prepared using K_2PtCl_4 was first tested in a single fuel cell configuration in DMFC mode at ambient temperature and atmospheric pressure. The open circuit voltage (OCV) was 680 mV for the system and the maximum power density was 0.310 mW cm^{-2} at 0.63 mA cm^{-2}. When the same system was tested in a single DHFC configuration at ambient temperature and atmospheric pressure, the OCV was 190 mV and the maximum power density was 0.224 mW cm^{-2} at 2.8 mA cm^{-2}.

H_2PtCl_6 was used as the second Pt precursor for the preparation of Pt/PVF^+ electrocatalysts. GCE was used as the working electrode. Immobilization of Pt particles from H_2PtCl_6 was performed by both cyclic voltammetric scans and constant potential electrolysis and Pt particles were obtained by chemical and electrochemical reduction methods. Optimum experimental conditions were determined as follows: -0.8 V vs. SCE cathodic potential limit during cyclic voltammetric scans; polymer film thickness corresponding to 70 mC charge; 50 cyclic voltammetric scans in H_2PtCl_6 solution; 60 min chemical reduction time; -0.40 V vs. SCE electrochemical reduction potential; 20 min electrochemical reduction time, -0.85 V vs. SCE electrolysis potential; 20 min electrolysis time.

Chemical and electrochemical reduction methods were compared and oxidation peak current values were approximately the same for both methods. When the two methods for immobilization of Pt complexes (CV and constant potential electrolysis) were compared, oxidation peak current of methanol recorded with the catalysts prepared by constant potential electrolysis was somewhat more than the one prepared by cyclic voltammetric scans.

When the catalysts were characterized by cyclic voltammetry, the expected oxidation and reduction peaks of weakly and strongly adsorbed hydrogen between 0.00 V and -0.25 V vs. SCE were not observed. This result was also consistent with SEM results that the Pt particles were dispersed over the polymer matrix; however their shapes were not spherical.

When fuel cell performances of the Pt/PVF^+ system prepared using H_2PtCl_6 were evaluated at DMFC mode, the OCV was 457 mV for the system and the maximum power density was 0.1424 mW cm^{-2} at 1.6 mA cm^{-2}. In DHFC mode, An OCV of 285 mV was obtained for the system and the maximum power density was 0.3996 mW cm^{-2} at 3.7 mA cm^{-2}.

In the second part of the work, Pd/PVF^+ catalysts were prepared using K_2PdCl_4 as the Pd precursor. GCE which showed no response for hydrazine oxidation was used as the working electrode. Two separate methods were used for immobilization of Pd particles into the polymer matrix; cyclic voltammetric scans and constant potential electrolysis in aqueous solution of K_2PdCl_4. After this step, Pd particles were already in the reduced form and the catalyst system was active towards hydrazine oxidation.

Optimization of experimental parameters for the preparation of the catalyst was done according to the oxidation peak current of $N_2H_4 \cdot H_2SO_4$. The following experimental conditions were found as the optimum preparation conditions: polymer film thickness corresponding to 30 mC charge; -0.8 V vs. SCE cathodic potential limit during cyclic voltammetric scans; 50 cyclic voltammetric scans; -0.8 V vs. SCE electrolysis potential; 30 min electrolysis time.

When the two immobilization methods were compared by oxidation peak current of $N_2H_4 \cdot H_2SO_4$, it was observed that the two methods showed very similar catalytic activities towards hydrazine oxidation.

When SEM images of Pd/PVF^+ catalysts prepared by cyclic voltammetric scans and constant potential electrolysis on Pt foil electrode were compared, Pd particles were well dispersed over the polymer matrix and shapes of the particles were significantly different in shape for the two preparation methods.

Pd/PVF^+ catalyst system prepared by cyclic voltammetric scans in K_2PdCl_4 was tested in a single fuel cell configuration in DHFC mode at ambient temperature and atmospheric pressure. The OCV of the system was measured as 130 mV and the maximum power density was calculated as 0.009 mW cm^{-2} at 0.17 mA cm^{-2}. For the Pd/PVF^+ catalyst system prepared by constant potential electrolysis, DHFC performance results gave an OCV of the system of 255 mV and a maximum power density of 0.200 mW cm^{-2} at 1.14 mA cm^{-2}.

In order to evaluate the effect of PVF^+ support on the catalytic activities of the catalysts, cyclic voltammograms of methanol and $N_2H_4 \cdot H_2SO_4$ were recorded with the unsupported catalysts prepared at the same experimental conditions. For Pt/PVF^+ system, presence of the polymer support greatly enhanced the oxidation peak current of methanol. In the case of Pd/PVF^+ system, oxidation potential of hydrazine shifted towards a less positive potential in the presence of the polymer support. The enhancement at the catalytic activities in the presence of polymer support can be attributed to three effects of PVF^+: (1) as being a positively charged polymer matrix, the negatively charged Pt and Pd complexes can be more easily immobilized into the polymer, (2) as being a redox polymer, PVF acts as a mediator and increases the catalytic activity of the catalysts, and, (3) as being in a porous structure, the polymer supplies an appropriate matrix for the metal particles.

REFERENCES

Abruna, H.D., 1988, Coordination chemistry in two dimensions: Chemically modified electrodes, Coordination Chemistry Reviews, 86, 135-189.

Adlim, M., Bakar, M.A., Liew, K.Y., Ismail, J., 2004, Synthesis of chitosan-stabilized platinum and palladium nanoparticles and their hydrogenation activity, J. Molecular Catalysis: A Chemical, 212, 141-149.

Aokoi, K., Zhao, Y., Chen, J., 2007, Colloidal submicron-palladium particles stabilized with acetate, Electrochimica Acta, 52, 2485-2491.

Arrigan, D.W.M., 1994, Voltammetric determination of trace metals and organics after accumulation at modified electrodes, Analyst, 119, 1953-1966.

Aso, C., Kunitake, T., Nakashima, T., 1969, Cationic polymerization and copolymerization of vinylferrocene, Macromolecular Chemistry, 124, 232-239.

Aydın, G., Çelebi, S.S., Özyörük, H., Yıldız, A., 2002, Amperometric enzyme electrode for L(+)-lactate determination using immobilized L(+)-lactate oxidase in poly(vinylferrocenium) film", Sensors and Actuators B, 87, 8-12.

Calvillo, L., Lazaro, M.J., Garcia-Bordeje, E., Moliner, R., Cabot, P.L., Esparbe, I., Pastor, E., Quintana, J.J., 2007, Platinum supported on functionalized ordered mesoporous carbon as electrocatalyst for direct methanol fuel cells, J. Power Sources, 169, 59-64.

Cao, J., Du, J., Wang, S.J., Mercier, P., Zhang, X., Yang, H., Akins, D.L., 2007, The production of a high loading of almost monodispersed Pt nanoparticles on single-walled carbon nanotubes for methanol oxidation, Electrochemistry Communications, 9, 735-740.

Chang, G., Oyama, M., Hirao, K., 2007, Platinum nano-cluster thin film formed on glassy carbon and the application for methanol oxidation, Thin Solid Films, 515, 3311-3314.

Choi, J.H., Park, K.W., Lee, H.K., Kim, Y.M., Lee, J.S., Sung, Y.E., 2003, Nano-composite of PtRu alloy electrocatalyst and electronically conducting polymer for use as the anode in a direct methanol fuel cell, Electrochimica Acta, 48, 2781-2789.

Cotton, F.A. and Wilkinson, G., 1972, Advanced Inorganic Chemistry, 4th Edition, Wiley-Interscience, New York, 951-952.

Dong, B., He, B.L., Huang, J., Gao, G.Y., Yang, Z., Li, H.L., 2008, High dispersion and electrocatalytic activity of Pd/titanium dioxide nanotubes catalysts for hydrazine oxidation, J. Power Sources, 175, 266-271.

Fıçıcıoğlu, F. and Kadırgan, F., 1997, Electrooxidation of methanol on platinum doped polyaniline electrodes: deposition potential and temperature effect, J. Electroanalytical Chemistry, 430, 179-182.

Gautron, E., Garron, A., Bost, E., Epron, F., 2003, Synthesis, characterization and catalytic properties of polypyrrole-supported catalysts, Catalysis Communications, 4, 435-439.

Guo, D.J. and Li, H.L., 2004, High dispersion and electrocatalytic properties of Pt nanoparticles on SWNT bundles, J. Electroanalytical Chemistry, 573, 197-202.

Guo, D.J. and Li, H.L., 2004, Electrochemical synthesis of Pd nanoparticles on functional MWNT surfaces, Electrochemistry Communications, 6, 999-1003.

Guo, D.J. and Li, H.L., 2005, Highly dispersed Ag nanoparticles on functional MWNT surfacesfor methanol oxidation in alkaline solution, Carbon, 43, 1259-1264.

Guo, D.J. and Li, H.L., 2005, High dispersion and electrocatalytic properties of Pd nanoparticles on single-walled carbon nanotubes, J. Colloid and Interface Science, 286, 274-279.

Gülce, H., Özyörük, H., Yıldız, A., 1994, Electrochemical reduction of anthracenes on poly(vinylferrocenium) coated Pt electrodes in acetonitrile, Ber. Bunsen. Phys. Chem., 98, 228–233.

Gülce, H., Özyörük, H., Yıldız, A., 1994, Electrochemical Oxidation of Anthracenes on Poly(vinylferrocenium) Coated Pt Electrodes in Acetonitrile, Ber. Bunsen. Phys. Chem., 98, 828–832.

Gülce, H., Özyörük, H., Yıldız, A., 1995, Electrochemical response of poly(vinylferrocenium)-coated Pt electrodes to some anions in aqueous media, Electroanalysis, 7,178–183.

Gülce, H., Özyörük, H., Çelebi, S.S., Yıldız, A., 1995, Amperometric enzyme electrode for aerobic glucose monitoring prepared by glucose oxidase immobilized in poly(vinylferrocenium), J. Electroanalytical Chemistry, 394, 63-70.

Gülce, H., Çelebi, S.S., Özyörük, H., Yıldız, A., 1995, Amperometric enzyme electrode for sucrose determination prepared from glucose oxidase and invertase co-immobilized in poly(vinylferrocenium), J. Electroanalytical Chemistry, 397, 217-223.

Gülce, H., Çelebi, S.S., Özyörük, H., Yıldız, A., 1997, Electroanalysis and electrocatalysis using poly(vinylferrocenium) perchlorate coated electrodes, Pure Appl. Chem., 69, 173–177.

Gündoğan-Paul, M., Özyörük, H., Çelebi, S.S., Yıldız,, A., 2002, Amperometric enzyme electrode for hydrogen peroxide determination prepared with horseradish peroxidase immobilized in polyvinylferrocenium (PVF^+), Electroanalysis, 14, 505-511.

Gündoğan-Paul, M., Çelebi, S.S., Özyörük, H., Yıldız,, A., 2002, Amperometric enzyme electrode for organic peroxides determination prepared from horseradish peroxidase immobilized in poly(vinylferrocenium) film, Biosensors and Bioelectronics, 17, 875-881.

Hamnett, A., 1997, Mechanism and electrocatalysis in the direct methanol fuel cell, Catalysis Today, 38, 445-457.

Hasik, M., Drelinkiewicz, A., Choczynski, M., Quillard, S., Pron, A., 1997, Polyaniline containing palladium – new conjugated polymer supported catalysts, Synthetic Metals, 84, 93-94.

Hasik, M., Bernasik, A., Adamczyk, A., Malata, G., Kowalski, K., Camra, J., 2003, Polypyrrole-palladium systems prepared in $PdCl_2$ aqueous solutions, European Polymer Journal, 39, 1669-1678.

http://en.wikipedia.org/wiki/Image:Cyclovoltammogram.jpg

http://techon.nikkeibp.co.jp

http:// www.asi.org

http://www.dtienergy.com

http://www.fctec.com

http://www.fuelcells.org

http://www.fuelcellknowledge.org

http://www.mee-inc.com/eds.html

Ioroi, T., Fujiwara, N., Siroma, Z., Yasuda, K., Miyazaki, Y., 2002, Platinum and molybdenum oxide deposited carbon electrocatalyst for oxidation of hydrogen containing carbon monoxide, Electrochemistry Communications, 4, 442-446.

Iwasita, T., 2002, Electrocatalysis of methanol oxidation, Electrochimica Acta, 47, 3663-3674.

Jung, D.H., Lee, C.H., Kim, C.S., Shin, D.R., 1998, Performance of a direct methanol polymer electrolyte fuel cell, J. Power Sources, 71, 169, 173.

Kaufman, F.B. and Engler, E.M., 1979, Solid-State Spectroelectrochemistry of. Cross-Linked Donor Bound Polymer Films, J. American Chemical Society, 101, 547-549.

Kralik, M. and Biffis, A., 2001, Catalysis by metal nanoparticles supported on functional organic polymers, J. Molecular Catalysis: A Chemical, 177, 113-138.

Kuralay, F., Özyörük, H., Yıldız, A., 2005, Potentiometric enzyme electrode for urea determination using immobilized urease in poly(vinylferrocenium) film", Sensors and Actuators B, 109, 194-199.

Kuralay, F., Özyörük, H., Yıldız, A., 2006, Amperometric enzyme electrode for urea determination using immobilized urease in poly(vinylferrocenium) film, Sensors and Actuators B, 114, 500-506.

Kuralay, F., Özyörük, H., Yıldız, A., 2007, Inhibitive determination of Hg^{2+} ion by an amperometric urea biosensor using poly(vinylferrocenium) film, Enzyme and Microbial Technology, 40, 1156–1159.

Lederer, M. and Leipzig-Pagani, E., 1997, Studies of platinum (II) compounds in aqueous solution. Part 1. K_2PtCl_4, Analytica Chimica Acta, 350, 203-208.

Li, F., Zhang, B., Wang, E., Dong, S., 1997, In situ scanning tunneling microscopy studies of nanometer size palladium particles on highly orientated pyrolytic graphite, J. Electroanalytical Chemistry, 422, 27-33.

Li, F., Zhang, B., Dong, S., Wang, E., 1997, A novel method of electrodepositing highly dispersed nano palladium particles on glassy carbon electrode, Electrochimica Acta, 42, 2563-2568.

Lin, C., Wang, T., Feng, Y., Fang, Y., Wang, X., 2008, Effects of microporous layer preparation on the performance of a direct methanol fuel cell, Electrochemistry Communications, 10, 255-258.

Lizcano-Valbuena, W.H., de Azevedo, D.C., Gonzalez, E.R., 2004, Supported metal nanoparticles as electrocatalysts for low-temperature fuel cells, Electrochimica Acta, 49, 1289-1295.

Michalska, Z.M., Rogalski, L., Rozga-Wijas, K., Chojnowski, J., Fortuniak, W., Scibiorek, M., 2004, Synthesis and catalytic activity of the transition metal complex catalysts supported on branched functionalized polysiloxanes grafted on silica, J. Molecular Catalysis A: Chemical, 208, 187-194.

Motokawa, S., Mohamedi, M., Momma, T., Shoji, S., Osaka, T., 2004, MEMS-based design and fabrication of a new concept micro d,rect methanol fuel cell (μ-DMFC), Electrochemistry Communications, 6, 562-565.

Murray, R.W., 1984, Chemically modified electrodes, Electroanalytic Chemistry, ed. Bard, A.J., Marcel Dekker, New York, 13, 191-368.

Nassef, H.M., Radi, A.E., O'Sullivan, C.K., 2006, Electrocatalytic oxidation of hydrazine at *o*-aminophenol grafted modified glassy carbon electrode: Reusable hydrazine amperometric sensor, J. Electroanalytical Chemistry, 592, 139-146.

Niu, L., Li, Q., Wei, F., Wu, S., Liu, P., Cao, X., 2005, Electrocatalytic behavior of Pt-modified polyaniline electrode for methanol oxidation: Effect of Pt deposition modes, J. Electroanalytical Chemistry, 578, 331-337.

Özer, B.C., Özyörük, H., Çelebi S.S., Yıldız, A., 2007, Amperometric enzyme electrode for free cholesterol determination prepared with cholesterol oxidase immobilized in poly(vinylferrocenium) film", Enzyme and Microbial Technology, 40, 262-265.

Pang, H.L., Zhang, X.H., Zhong, X.X., Liu, B., Wei, X.G., Kuang, Y.F., Chen, J.H., 2008, Preparation of Ru-doped SnO2-supported Pt catalysts and their electrocatalytic properties for methanol oxidation, J. Colloid and Interface Science, 319, 193-198.

Peerce, P.J. and Bard, A.J., 1980, Polymer films on electrodes: Part II. Film structure and mechanism of electron transfer with electrodeposited poly(vinylferrocene), J Electroanalytical Chemistry, 112, 97-115.

Perez, J., Gonzalez, E.R., Ticianelli, E.A., 1998, Oxygen electrocatalysis on thin porous coating rotating platinum electrodes, Electrochimica Acta, 44, 1329-1339.

Pozio, A., De Francesco, M., Cemmi, A., Cardellini, F., Giorgi, L., 2002, Comparison of high surface Pt/C catalysts by cyclic voltammetyry, J. Power Sources, 105, 13-19.

Rao, C.R.K. and Trivedi, D.C., 2005, Chemical and electrochemical depositions of platinum group metals and their applications, Coordination Chemistry Reviews, 249, 613-631.

Rao, C.R.K. and Trivedi, D.C., 2006, A novel one-pot synthesis of free standing Pd-Ppy films: Observation of enhanced catalytic effect by Pd-Ppy layers, Catalysis Communications, 7, 662-668.

Ren, X. and Pickup, P.G., 1994, Strong dependence of the electron-hopping rate in poly-tris(5-amino-1,10-phenanthroline)iron(III/II) on the nature of the counter-anion, J. Electroanalytical Chemistry, 365, 289-292.

Saha, M.S., Li, R., Sun, X., 2008, High loading and monodispersed Pt nanoparticles on multiwalled carbon nanotubes for high performance proton exchange membrane fuel cells, J. Power Sources, 177, 314-322.

Selvaraj, V.and Alagar, M., 2007, Pt and Pt–Ru nanoparticles decorated polypyrrole/multiwalled carbon nanotubes and their catalytic activity towards methanol oxidation, Electrochemistry Communications, 9, 1145-1153.

Serov, A.A., Min, M., Chai, G., Han, S., Kang, S., Kwak, C., 2008, Preparation, characterization, and high performance of RuSe/C for direct methanol fuel cells, J. Power Sources, 175, 175-182.

Shan, J. and Pickup, P.G., 2000, Characterization of polymer supported catalysts by cyclic voltammetry and rotating disk voltammetry, Electrochimica Acta, 46, 119-125.

Shirota, Y., Kakuta, T., Mikawa, H., 1984, Electrochemical oxidation of poly(vinylferrocene) with concurrent precipitation on the electrode: Preparation of an electronically conducting polymer, Macromolecular Chemistry, 5, 337-340.

Sivakumar, C., 2007, Finely dispersed Pt nanoparticles in conducting poly(*o*-anisidine) nanofibrillar matrix as electrocatalytic material, Electrochimica Acta, 52, 4182-4190.

Skoog, D.A., Leary, J.J., 1992, Principles of Instrumental Analysis, 4th Edition, Saunders College Publishing.

Solla-Gullon, J., Rodes, A., Montiel, V., Aldaz, A., Clavilier, J., 2003, Electrochemical characterization of platinum-palladium nanoparticles prepared in a water-in-oil microemulsion, J. Electroanalytical Chemistry, 554-555, 273-284.

Sönmez, M., 2002, Voltammetric behaviors of mercury (II) and silver (I) ions on poly(vinylferrocenium) modified platinum electrode, 2002, MSc thesis, Hacettepe University, Institute of Sciences.

Tang, Z., Geng, D., Lu, G., 2005, Size-controlled synthesis of colloidal platinum particles and their activity for the electrocatalytic oxidation of carbon monoxide, J. Colloid and Interface Science, 287, 159-166.

Urban, P.M., Funke, A., Müller, J.T., Himmen, M., Docter, A., 2001, Catalytic processes in solid polymer electrolyte fuel cell systems, Applied Catalysis A: General, 221, 459-470.

Wang, X. and Hsing, I.M., 2002, Surfactant stabilized Pt and Pt alloy electrocatalyst for polymer electrolyte fuel cells, Electrochimica Acta, 47, 2981-2987.

Wang, J.T., Wasmus, S., Savinell, R., 143, Real-time mass spectrometric study of the methanol crossover in a direct methanol fuel cell, J. Electrochemical Society, 143, 1233-1239.

Wasmus, S. and Küver, A., 1999, Methanol oxidation and direct methanol fuel cells: a selective review, J. Electroanalytical Chemistry, 461, 14-31.

Yamada, K., Asazawa, K., Yasuda, K., Ioroi, T., Tanaka, H., Miyazaki, Y., Kobayashi, T., 2003, Investigation of PEM type direct hydrazine fuel cell, J. Power sources, 115, 236-242.

Yamada, K., Yasuda, K., Fujiwara, N., Siroma, Z., Tanaka, H., Miyazaki, Y., Kobayashi, T., 2003, Potential application of anion-exchange membrane for hydrazine fuel cell electrolyte, Electrochemistry Communications, 5, 892-896.

Yamada, K., Yasuda, K., Tanaka, H., Z., Miyazaki, Y., Kobayashi, T., 2003, Effect of anode electrocatalyst for direct hydrazine fuel cell using proton exchange membrane, J. Power Sources, 122, 132-137.

Yang, C.C., Chiu, S.J., Lin, C.T., 2008, Electrochemical performance of an air-breathing direct methanol fuel cell using poly(vinyl alcohol)/hydroxapatite composite polymer membrane, J. Power Sources, 177, 40-49.

Yu, L., Sathe, M., Zeng, X., 2005, EQCM study of the redox processes of polyvinylferrocene film in L-glutamine Solution, J. Electrochemical Society, 152, E357-E363.

CURRICULUM VITAE

Name Surname	:	Mutlu Sönmez Çelebi
Place of Birth	:	Ordu
Date of Birth	:	1976
Marital Status	:	Married

Education and Academic Position

High School	1991-1992	Ordu Anatolian High School	Ordu
	1992-1994	Bornova Anatolian High Schooll	İzmir
BSc	1994-1999	Hacettepe University, Department of Chemistry	Ankara
MSc	1999-2002	Institute of Sciences of Hacettepe University	Ankara

Job Experience

2000 - onwards	Research Assistant at Hacettepe University, Department of Chemistry